ความเป็นพิษและการเหนี่ยวนำการตายแบบอะพอพโตซิสต่อเซลล์มะเร็งโดยฮ่วนง็อก (*Pseuderanthemum palatiferum* (Nees) Radlk.)

นางสาวเบญจวรรณ ดุนขุนทด

วิทยานิพนธ์นี้เป็นส่วนหนึ่งของการศึกษาตามหลักสูตรปริญญาวิทยาศาสตรมหาบัณฑิต
สาขาวิชาชีวเวชศาสตร์
มหาวิทยาลัยเทคโนโลยีสุรนารี
ปีการศึกษา 2557

CYTOTOXICITY AND APOPTOSIS INDUCTION BY LEAF EXTRACT OF HOAN-NGOC *PSEUDERANTHEMUM PALATIFERUM* (NEES) RADLK. ON HUMAN CANCER CELLS

Benjawan Dunkhunthod

A Thesis Submitted in Partial Fulfillment of the Requirements

for the Degree of Master in Biomedical Sciences

Suranaree University of Technology

Academic Year 2014

CYTOTOXICITY AND APOPTOSIS INDUCTION BY LEAF EXTRACT OF HOAN-NGOC *PSEUDERANTHEMUM PALATIFERUM* (NEES) RADLK. ON HUMAN CANCER CELLS

Suranaree University of Technology has approved this thesis submitted in partial fulfillment of the requirements for a Master's Degree.

Thesis Examining Committee

_____

(Asst. Prof. Dr. Rungrudee Srisawat)

Chairperson

_____

(Asst. Prof. Dr. Benjamart Chitsomboon)

Member (Thesis Advisor)

_____

(Asst. Prof. Dr. Panida Khunkaewla)

Member

_____

(Dr. Kanjana Thumanu)

Member

_____

(Prof. Dr. Sukit Limpijumnong)

Vice Rector for Academic Affairs and Innovation

_____

(Assoc. Prof. Dr. Prapun Manyum)

Dean of Institute of Science

เบญจวรรณ ดุนขุนทด : ความเป็นพิษและการเหนี่ยวนำการตายแบบอะพอพโตซิสต่อเซลล์มะเร็งโดยฮว่านง็อก (*Pseuderanthemum palatiferum* (Nees) Radlk.) (CYTOTOXICITY AND APOPTOSIS INDUCTION BY LEAF EXTRACT OF HOAN-NGOC *PSEUDERANTHEMUM PALATIFERUM* (NEES) RADLK. ON HUMAN CANCER CELLS) อาจารย์ที่ปรึกษา : ผู้ช่วยศาสตราจารย์ ดร.เบ็ญจมาศ จิตรสมบูรณ์, 121 หน้า.

สมุนไพรฮว่านง็อกเป็นพืชที่นิยมใช้กันอย่างแพร่หลายในคนเวียดนามและคนไทยสำหรับทั้งเป็นพืชสมุนไพรและไม้ประดับ การศึกษานี้มีวัตถุประสงค์เพื่อตรวจสอบฤทธิ์ความเป็นพิษของสารสกัดใบฮว่านง็อกที่สกัดด้วยเอทานอลและน้ำต่อเซลล์มะเร็งสายพันธุ์ในคน 4 ชนิด (เซลล์มะเร็งเม็ดเลือดขาวสายพันธุ์ Jurkat เซลล์มะเร็งตับสายพันธุ์ HepG2 เซลล์มะเร็งเต้านมสายพันธุ์ MCF-7 และเซลล์มะเร็งต่อมลูกหมากสายพันธุ์ PC-3) เทียบกับเซลล์เม็ดเลือดขาวชนิดนิวเคลียสเดี่ยวของคน และประเมินฤทธิ์การเหนี่ยวนำการตายแบบอะพอพโตซิสของสารสกัดใบฮว่านง็อกต่อเซลล์มะเร็งเม็ดเลือดขาวสายพันธุ์ Jurkat ฤทธิ์ก่อกลายพันธุ์ของสารสกัดประเมินด้วยเทคนิคเอมส์ ผลการทดลองพบว่าทั้งสารสกัดใบฮว่านง็อกที่สกัดด้วยเอทานอลและน้ำมีปริมาณสารฟีนอลิกใกล้เคียงกัน อย่างไรก็ตามสารสกัดใบฮว่านง็อกที่สกัดด้วยน้ำมีปริมาณสารฟลาโวนอยด์สูงกว่าสารสกัดใบฮว่านง็อกที่สกัดด้วยเอทานอล ซึ่งสอดคล้องกับความสามารถในการต้านอนุมูลอิสระ DPPH ของสารสกัดทั้งสอง

การศึกษาความเป็นพิษต่อเซลล์พบว่าเซลล์มะเร็งสายพันธุ์ต่างชนิดมีความไวต่อฤทธิ์ความเป็นพิษของสารสกัดใบฮว่านง็อกที่สกัดด้วยเอทานอลและน้ำแตกต่างกันขึ้นกับความเข้มข้นของสารสกัด ความเป็นพิษของสารสกัดใบฮว่านง็อกที่สกัดด้วยเอทานอลและน้ำต่อเซลล์มะเร็งสายพันธุ์เรียงลำดับจากมากไปน้อยได้ดังนี้ เซลล์ Jurkat > เซลล์ HepG2 > เซลล์ MCF-7 > เซลล์ PC-3 ดังนั้นเซลล์ Jurkat มีความไวต่อความเป็นพิษของสารสกัดทั้งสองมากที่สุด ที่สำคัญสารสกัดใบฮว่านง็อกที่สกัดด้วยเอทานอลและน้ำแสดงความเป็นพิษต่อเซลล์เม็ดเลือดขาวชนิดนิวเคลียสเดี่ยวของคนต่ำกว่าเซลล์ Jurkat ที่ระดับของความเข้มข้นเดียวกัน

การเหนี่ยวนำให้เกิดการตายแบบอะพอพโตซิสในเซลล์ Jurkat โดยสารสกัดใบฮว่านง็อกที่สกัดด้วยเอทานอลและน้ำขึ้นกับทั้งความเข้มข้นของสารสกัดและระยะเวลาของการบ่ม ทั้งนี้สามารถบ่งชี้การตายแบบอะพอพโตซิสได้จากหลักฐานทางสัญฐานวิทยาของเซลล์ เอกลักษณ์การแตกหักของดีเอ็นเอแบบขั้นบันได การย้อมติดแอนเน็กซินไฟว์-เอฟไอทีซี และการหลั่งของไซโทโครมซีจากไมโทคอนเดรียสู่ไซโตพลาสซึม นอกจากนั้นข้อมูลจากเอฟทีไออาร์ ไมโครสเปกโตรส

โกปี แสดงให้เห็นการเปลี่ยนแปลงของแมคโครโมเลกุล (ไขมัน กรดนิวคลีอิค และโครงสร้างลำดับที่สองของโปรตีน) ในเซลล์ที่ได้รับสารสกัดใบฮว่านง็อกที่สกัดด้วยเอทานอลและน้ำ ซึ่งการเปลี่ยนแปลงดังกล่าวมีความสัมพันธ์กับการเปลี่ยนแปลงของเยื่อหุ้มเซลล์ โปรตีนที่เกี่ยวข้องกับกระบวนการอะพอพโตซิส และการแตกหักของนิวคลีโอโซมระหว่างกระบวนการอะพอพโตซิสมากไปกว่านั้น สารสกัดใบฮว่านง็อกที่สกัดด้วยเอทานอลและน้ำในช่วงความเข้มข้น 150-600 ไมโครกรัมต่อเพลท ไม่มีฤทธิ์ก่อการกลายพันธุ์เมื่อทดสอบด้วยเทคนิคเอมส์ โดยภาพรวมการศึกษาครั้งนี้บ่งชี้ว่าทั้งสารสกัดใบฮว่านง็อกที่สกัดด้วยเอทานอลและน้ำมีฤทธิ์ยับยั้งการเจริญของเซลล์มะเร็งเม็ดเลือดขาวสายพันธุ์ Jurkat โดยการเหนี่ยวนำให้เกิดการตายแบบอะพอพโตซิสผ่านวิถีไมโทคอนเดรียและในช่วงความเข้มข้นที่ทดสอบสารสกัดทั้งสองไม่มีฤทธิ์ก่อกลายพันธุ์ในวิธีทดสอบเอมส์

สาขาวิชาเภสัชวิทยา ลายมือชื่อนักศึกษา_____

ปีการศึกษา 2557 ลายมือชื่ออาจารย์ที่ปรึกษา_____

BENJAWAN DUNKHUNTHOD : CYTOTOXICITY AND APOPTOSIS INDUCTION BY LEAF EXTRACT OF HOAN-NGOC *PSEUDERANTHEMUM PALATIFERUM* (NEES) RADLK. ON HUMAN CANCER CELLS. THESIS ADVISOR : ASST. PROF. BENJAMART CHITSOMBOON, Ph.D. 121 PP.

HOAN-NGOC/ *PSEUDERANTHEMUM PALATIFERUM* (NEES) RADLK./CYTOTOXICITY/MUTAGENICITY/APOPTOSIS/HUMAN CANCER CELL LINE

Pseuderanthemum palatiferum (Nees) Radlk. (*P. palatiferum*) or Hoan-Ngoc is a medicinal plant that widely used in both Vietnamese and Thais as a medicinal and ornamental plant. This study aimed to investigate *in vitro* cytotoxic effects of *P. palatiferum* extracted by 95% ethanol (EEP) and water (WEP) on various human cancer cell lines (leukemia Jurkat, hepatoma HepG2, breast cancer MCF-7, and prostate cancer PC-3) compared to normal peripheral blood mononuclear cells (PBMCs) and assessed apoptosis induction of the extracts on Jurkat cells. The mutagenicity of the extracts was also evaluated by the Ames assay. The results showed that both EEP and WEP contained comparable levels of total phenolic contents. However, WEP contained higher total flavonoid contents than EEP ($p < 0.05$). Likewise, WEP possessed higher DPPH radical scavenging activity than EEP ($p < 0.05$).

In vitro cytotoxicity studies showed that various types of cancer cells exhibited different susceptibilities to EEP and WEP in a dose dependent manner. The

sensitivity of cancer cells to EEP and WEP extracts were ranged in the descending order of Jurkat > HepG2 > MCF-7 > PC-3. Therefore, Jurkat cell was the most sensitive to the lethal effect of both EEP and WEP. Importantly, both extracts exhibited the preferential cytotoxicity towards Jurkat cells but had less toxicity in normal PBMCs cells exposed to the same concentrations of both extracts.

EEP and WEP induced apoptotic cell death on Jurkat cells in both dose- and time-dependent manners as evidenced by the morphological changes, DNA ladder formation, annexinV-PI binding and the distribution of cytochrome C from mitochondria to cytosol. In addition, FTIR microspectroscopy also showed the changing of macromolecules (lipid, nucleic acid, and secondary structure of proteins) in EEP- or WEP-treated cells which can be related to changes of plasma membrane, apoptotic proteins, and internucleosomal DNA cleavage during apoptosis process. Moreover, the extracts in the range of 150 to 600 µg/plate had no mutagenicity in the Ames assay. This study suggested that both EEP and WEP exhibits antiproliferative effect on Jurkat cells by apoptosis induction through the mitochondrial pathway, and the extracts possesses at the range of study no mutagenic activity in the Ames assay.

School of Pharmacology Student's Signature_____

Academic Year 2014 Advisor's Signature_____

ACKNOWLEDGEMENTS

I would like to express my deepest sincere and gratitude to my kind advisor, Asst. Prof. Dr. Benjamart Chitsomboon for her guidance, valuable advice, endless kindness and support for my work.

I would like to thank all my thesis committees for their suggestions and criticisms. I also would like to thank Asst. Prof. Dr. Panida Khunkaewla for her valuable suggestions on improving flow cytometry analysis. I also appreciate Dr. Kanjana Thumanu for her help in the FTIR analysis, especially the use of FTIR facility at Synchrotron Light Research Institute, Nakhon Ratchasima.

I would like to thank Assoc. Prof. Dr. Kaew Kangsadalampai and Dr. Kalyarat Kruawan for demonstrating the technique of Ames test.

I would like to thank Dr. Kongkanda Chayamarit of forest Herbarium, Royal Forest Department, Bangkok, for plant identification.

I am very grateful to Suranaree University of Technology for providing me with the financial means and the laboratory facilities for conducting my research.

Finally, I wish to thank my parents and all my friends for their being with me and for their support, understanding, inspiration, and encouragement throughout my study.

Benjawan Dunkhunthod

CONTENTS

Page

CONTENTS (Continued)

Page

CONTENTS (Continued)

Page

CONTENTS (Continued)

Page

LIST OF TABLES

LIST OF FIGURES

LIST OF FIGURES (Continued)

Figure **Page**

LIST OF FIGURES (Continued)

Figure **Page**

LIST OF FIGURES (Continued)

Figure **Page**

LIST OF ABBREVIATIONS

µg/ml	=	Microgram per milliliter
µl	=	Microliter
µM	=	Micromolar
g	=	Gravitational acceleration
ANOVA	=	Analysis of variance
ATP	=	Adenosine triphosphate
BSA	=	Bovine serum albumin
CAE	=	Catechin equivalent
CLS	=	Cell line services
DI water	=	Distilled water
DMEM	=	Dulbecco's Modified Eagle Medium
DMSO	=	Dimethylsulfoxide
DNA	=	Deoxyribonucleic acid
DPPH	=	2,2-diphenyl-1-picrylhydrazyl
EDTA	=	Ethylenediaminetetraacetic acid
EEP	=	Ethanol extract of fresh leaves of PP
FBS	=	Fetal bovine serum
FRAP	=	Ferric reducing antioxidant power
g	=	Gram

LIST OF ABBREVIATIONS (Continued)

GAE	=	Gallic acid equivalent
h	=	Hour
HEPES	=	4-(2-hydroxylethyl)-1-piperazineethanesulfonic acid
IC_{50}	=	Median inhibition concentration
kDa	=	Kilodalton
kg	=	Kilogram
L	=	Liter
LD_{50}	=	Median lethal dose
M	=	Molar
min	=	Minute
mg	=	Milligram
mg/ml	=	Milligram per milliliter
ml	=	Milliliter
mM	=	Millimolar
MTT	=	3-(4,5-dimethythiazol-2-yl)-2,5-diphenyltetrazolium bromide
nm	=	Nanometer
OD	=	Optical density
PBS	=	Phosphate buffered saline
PI	=	Propidium iodide

LIST OF ABBREVIATIONS (Continued)

PP	=	*Pseuderanthemum palatiferum*
RNase A	=	Ribonuclease A
ROSs	=	Reactive oxygen species
rpm	=	Revolution per minute
RPMI 1640	=	Roswell Park Memorial Institute number 1640
RT	=	Room temperature
SD	=	Standard deviation
SDS-PAGE	=	Sodium dodecyl sulfate polyacrylamide gel electrophoresis
TFC	=	Total flavonoid contents
TPC	=	Total phenolic contents
VH	=	Vehicle
v/v	=	volume by volume
WEP	=	Water extract of fresh leaves of *P. palatiferum*
w/v	=	weight by volume

CHAPTER I

INTRODUCTION

1.1 Introduction

The global burden of cancer continues to increase largely because of the aging and growth of the world population along with an increasing adoption of cancer-causing behaviors, particularly smoking. According to GLOBOCAN 2012 estimates, there are about 8.2 million cancer deaths and 14.1 million new diagnosed cancer cases (Ferlay et al., 2015).

Cancers are diverse and heterogeneous, but all share the ability to deregulate cell proliferation together with apoptosis suppression. These properties constitute the common requirements upon which neoplastic, transformation, progression, and metastasis of cancer will subsequently develop (Evan and Vousden, 2001). In terms of cancer chemoprevention, there are considerable emphasis on identifying novel natural products that selectively induce apoptosis and growth arrest in cancer cells without cytotoxic effects on normal cells (Tsao et al., 2004).

Several studies have described the beneficial effects of dietary polyphenols (flavonoids) on the risk reduction of chronic diseases, including cancer. It has been shown that diets rich in phenolic compounds had cytotoxic effect toward several cancer cell lines via apoptotic induction (Granado-Serrano et al., 2006; Peng et al., 2006; Das et al., 2009; Li et al., 2008).

In Vietnam, *Pseuderanthemum palatiferum* (Nees) Radlk. or *P. palatiferum* is considered as a new medicinal plant in folk medicine for both treatment and prevention of many diseases such as blood pressure, diarrhea, arthritis, pharyngitis, hemorrhoids, tumors, colitis, bleeding, wounds, cancer, and so on (Dieu et al., 2005). A few years ago, *P. palatiferum* has become popular among Thai people. According to folkloric medicine, its fresh leaves are claimed to cure various diseases. *P. palatiferum* leaves have been reported to contain many important compounds such as flavanoids, apigenin, stigmasterol, β-sitosterol, β-sitosterol-3-0-β-glucoside, and apigenin-7-0-β-glucoside (Dieu et al., 2008). Several studies have described the beneficial effects of *P. palatiferum* such as antioxidant activity, antidiabetic activity, anti-inflammatory activity, hypotensive activity, and antiproliferative activity (Chayarop et al., 2011; Khonsung et al., 2011; Pamok et al., 2012; Sittisart and Chitsomboon, 2014). Moreover, several studies have been reported the cytotoxic effects of *P. palatiferum* crude extracts against different cancer cell lines such as colon cancer cell lines; HCT15, SW48, SW480 (Pamok et al., 2012), Caco2, and breast cancer cell lines (Phasuk and Meeratana, 2014).

β-sitosterol is the most abundant phytosterol. Phytosterols are enriched in legumes, oil seeds, and unrefined plant oils as found in foods such as peanut butter, pistachios, and sunflower seeds (Awad et al., 2007). β-sitosterol has been reported to have antibacterial, anti-inflammatory, antihypercholesterolemic, antifungal, and anticancer properties (Ling and Jones, 1995). β-sitosterol has also been shown to inhibit the *in vitro* proliferation of human breast MCF-7 and MDA-MB-231 adenocarcinoma cells (Chai et al., 2008; Awad et al., 2007), and induce apoptosis in the murine fibrosarcoma MCA-102 (Moon et al., 2007).

Therefore, *P. palatiferum* leaves containing flavonoids and β-sitosterol as main constituents may possess anticancer activity through apoptosis-mediated pathway. Though the Vietnameses have used *P. palatiferum* leaves as a folk medicine for a long time, the pharmacologic studies of its claimed properties are still limited, and the long-term effects of its use are still largely unknown.

1.2 Research objectives

1. To screen the cytotoxic activity of 95% ethanol extract of *P. palatiferum* (EEP) and the water extract of 95% ethanol extract of *P. palatiferum* (WEP) on four human cancer cell lines (PC-3, HepG2, MCF-7, and Jurkat cell lines) compared with normal peripheral blood mononuclear cells (PBMCs).
2. To investigate whether the EEP- or WEP-induced cytotoxicity, in the most sensitive Jurkat cell line, is mediated through apoptotic mechanism.
3. To investigate cellular changes in both treated and untreated cells using Fourier-transform infrared microspectroscopy (FTIR).
4. To evaluate the *in vitro* mutagenic activity of EEP or WEP.

1.3 Scope and limitation of the study

P. palatiferum leaves were purchased from local area in Yasothon province, June of 2012. This thesis only focused on the study of mutagenicity and anticancer activities of the crude extracts from *P. palatiferum* leaves (EEP or WEP). The anticancer activity was limited to *in vitro* cytotoxicity. Cytotoxicity was investigated

on four human cancer cell lines (PC-3, HepG2, MCF-7, and Jurkat cell line) compared to normal cells (PBMCs). The induction of apoptosis cell death was investigated only on Jurkat cell line. Apoptosis was assessed by DNA fragmentation in chromatin staining, DNA ladders formation in agarose gel, Annexin V-PI staining, and reduction of the intensity of intact cytochrome C in mitochondria. The changing of macromolecules in both EEP- and WEP-treated and untreated cells was evaluated using Fourier-transform infrared microspectroscopy (FTIR). Mutagenic activity was evaluated using the *in vitro* Ames assay.

.

1.4 Expected results

The EEP or WEP could have possessed cytotoxicity towards Jurkat cells through apoptosis induction mechanism. The extracts should not have mutagenicity for long time daily consumption. This information could have been used as a basic pharmacological data for a consideration of their therapeutic potential in the future.

CHAPTER II

LITERATURE REVIEW

2.1 Cancer

Cancer is a class of chronic diseases characterized by out-of-control cell growth. Cancer cells do not experience programmatic death and instead continue to grow and divide. This leads to a mass of abnormal cells that grow out of control, leading to the development of solid lumps (tumors) (Crosta, 2003; Devi, 2005). The causes of cancer development depend on various factors such as family history (genetics), health, nutrition, personal habits, and the environment. The development of cancer takes place in a multi-step process including initiation, promotion/ progression, and metastasis as shown in Figure 2.1 (Brudnak, 2000). The first is the initiation stage. Cells become cancer cells because of DNA damage. The damaged DNA can lead to deregulations of genes (p53, tumor suppressor gene) involved in biochemical signaling pathways associated with control of cell proliferation or disruption of the natural processes of cellular, communication, development, and differentiation (Devi, 2005). Initiation is irreversible and the initiated cells may usually escape the apoptosis process during the development of the neoplasm. The next stage is the promotion/progression of cancer development. The process may be accelerated by repeated exposures to carcinogens. The initiated cells continue to gain more mutations, and the most aggressive selected clone it continues to divide and leading to increases in tumor size. At this stage, tumor cells acquire “wound-healing”

characteristics such as secretion of chemo-attractants to attract inflammatory immune cells, angiogenesis factors, proteases, etc. The tumor cell is now unrestricted in both its life-span and localization. The final stage is metastasis. As the tumor progression advances, the cells lose their adherence properties, detach from the tumor mass, and invade the neighboring tissues. They gain the ability to enter the blood vessels and lymph, and move to a different location in the body, and establish a new site of tumors development. These form the distant metastases, resulting in widely spread cancers.

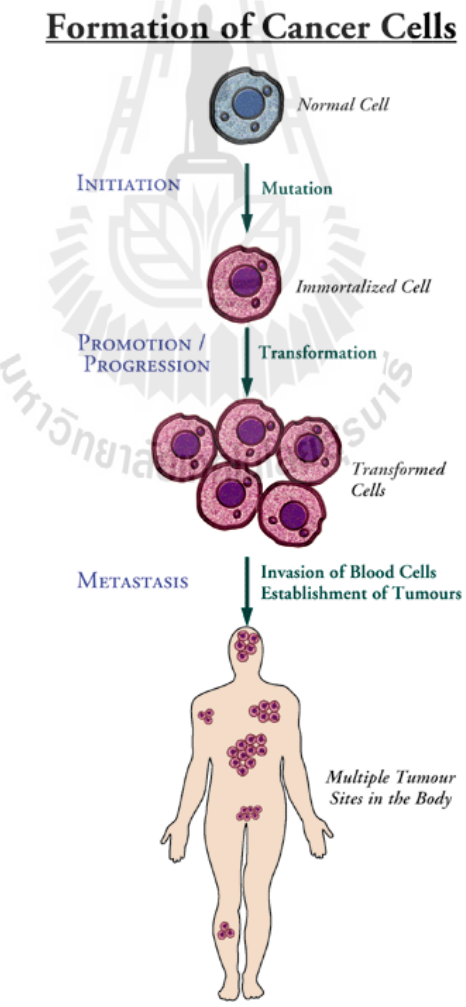

Figure 2.1 Formation of cancer cells (Brudnak, 2000).

2.2 Programmed cell death (PCD)

Programmed cell-death (or PCD) is the death of a cell in any form, mediated by an intracellular program. PCD is carried out in a regulated process, which is fundamental importance for the development of multicellular organisms and homeostasis of their tissues. The programmed cell death can be divided into three types including type I PCD or apoptosis, type II PCD or autophagy, and type III PCD or necrosis (Chaabane et al., 2013). Type I PCD or classic apoptosis, is a mechanism of programmed cell death that affects single cells scattered in a population of healthy cells. Type II PCD or autophagy is the basic catabolic mechanism that involves cell degradation of unnecessary or dysfunctional cellular components through the actions of lysosomes. Type III PCD or necrotic accidental cell death is a form of cell injury that results in the lethal disruption of cell structure and activity. The different types of cell death are often defined by morphological features (Figure 2.2).

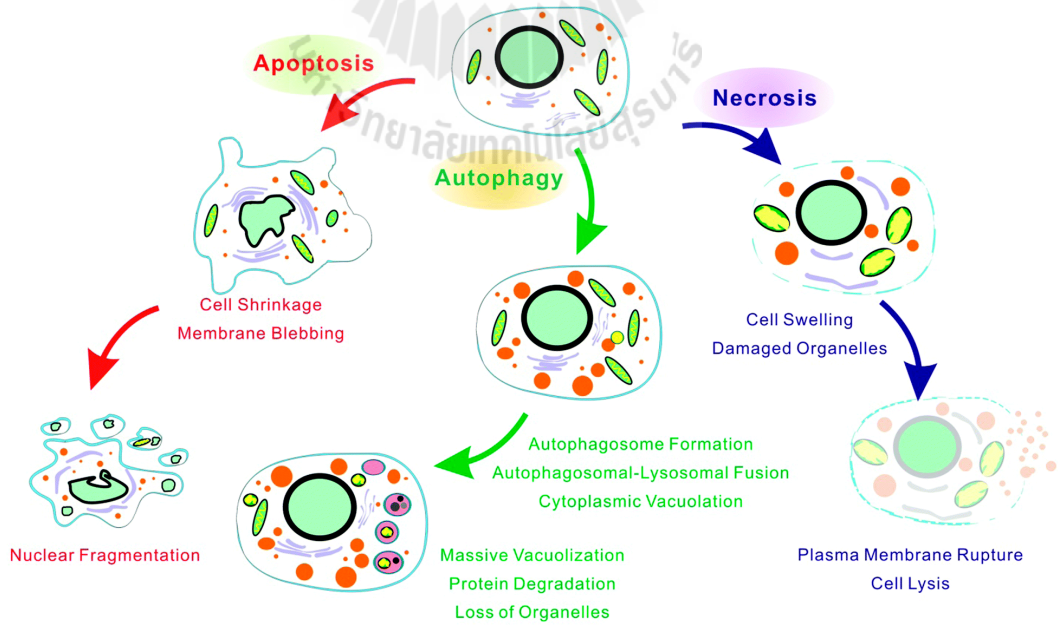

Figure 2.2 Morphological features of apoptosis, autophagy, and necrosis (Tan et al., 2014).

2.2.1 Distinguishing apoptosis from necrosis

The differences between necrotic and apoptotic cell death can be characterized by morphological and biochemical features as shown in Figure 2.3 and Table 2.1. Apoptosis is a mechanism of programmed cell death that affects single cell scattered in a population of healthy cells. Apoptosis is needed for proper embryonic development, maintaining of tissue homeostasis in adults and proper functioning of immune system when cells are damaged by disease, noxious agents, and cancer cells (Norbury and Hickson, 2001; Gavrilescu and Denkers, 2003; Favaloro et al., 2012). However, apoptosis is not perfect and dysregulation in this process can cause a wide spectrum of defects such as neurodegenerative diseases, ischemic damage, autoimmune disorders, and many types of cancer (Bell, 2002). Cells undergoing apoptosis show characteristic morphological features including cell shrinkage, plasma and nuclear membrane blebbing, organelle relocalization and compaction, chromatin condensation, and production of membrane-enclosed particles containing intracellular material known as apoptotic body formation (Lowe and Lin, 2000; Bold et al., 1997). The biochemical hallmarks of apoptosis can be divided into four types: (1) caspase cascade activation by pro-apoptotic signals resulting to initiate and execute the apoptotic degradation phase including DNA degradation and the typical morphologic features, (2) degradation of DNA by endogenous DNases, which cut internucleosomal region into DNA fragments of 180-200 base pairs (ladder of DNA on agarose gel electrophoresis) (Sarastea and Pulkkic, 2000), (3) ATP supplementation, preservation of cellular ATP that is essential for the apoptotic process (Eguchi, Shimizu, and Tsujimoto, 1997), and (4) phosphatidylserine (PS) exposure on the external leaflet of the plasma membrane of

cells and marks apoptotic cells for clearance by macrophages without associated inflammatory response (Lee et al., 2013). Necrosis or accidental cell death is a form of cell injury that results in the lethal disruption of cell structure and activity. Cells that died by necrosis may release harmful chemicals that initiate both inflammatory and damage neighboring cells (Zong and Thompson, 2006).

Necrosis is caused by external factors to the cell or tissue such as reactive oxygen species (ROS), toxins, radiation, heat, trauma, and lacking of oxygen due to the blockage of blood flow, etc. The morphology of necrotic cells is characterized by collapsing plasma membrane, swelling of cell membrane and mitochondria, and ending in cells lysis (Sarastea and Pulkkic, 2000). The biochemical features of necrosis include loss of regulation of ion hemostasis, random digestion of DNA which forms a smear of DNA on agarose gel electrophoresis. Loss of plasma membrane integrity resulting to leakage of intracellular contents can induce local inflammatory reactions with edema and damage to neighboring cells (Proskuryakov, Konoplyannikov, and Gabai, 2003). Also, the process is uncontrolled and passive, and does not require energy (ATP) (Eguchi, Shimizu, and Tsujimoto, 1997).

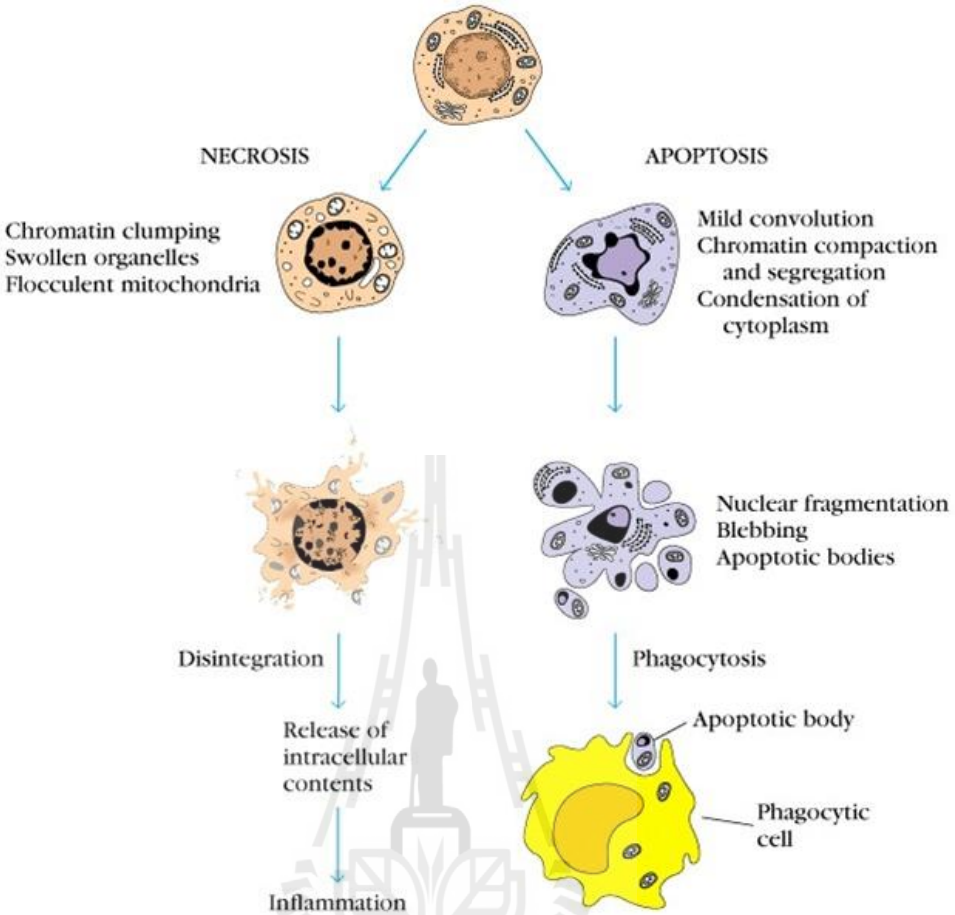

Figure 2.3 Morphological changes of apoptosis and necrosis (Pathology Department of Shantou University Medical College, 2006).

Table 2.1 Differential features and significances of necrosis and apoptosis (Boehringer Mannheim GmbH, 1998).

Necrosis	Apoptosis
Morphological features	
● Loss of membrane integrity	● Membrane blebbing, but no loss of integrity
	● Aggregation of chromatin at the nuclear membrane
● Begins with swelling of cytoplasm and mitochondria	● Begins with shrinking of cytoplasm and condensation of nucleus
● Ends with total cell lysis	● Ends with fragmentation of cell into smaller bodies
● No vesicle formation, complete lysis	● Formation of membrane bound vesicles (apoptotic bodies)
● Disintegration (swelling) of organelles	● Mitochondria become leaky due to pore formation involving proteins of the bcl-2 family.
Biochemical features	
● Loss of regulation of ion homeostasis	● Tightly regulated process involving activation and enzymatic steps
● No energy requirement (passive process, also occurs at 4°C)	● Energy (ATP)-dependent (active process, does not occur at 4°C)
● Random digestion of DNA (smear of DNA after agarose gel electrophoresis)	● Non-random mono- and oligonucleosomal length fragmentation of DNA (Ladder pattern after agarose gel electrophoresis)
● Postlytic DNA fragmentation (= late event of death)	● Prelytic DNA fragmentation
	● Release of various factors (cytochrome C, AIF) into cytoplasm by mitochondria
	● Activation of caspase cascade
	● Alterations in membrane asymmetry (i.e., translocation of phosphatidylserine from the cytoplasmic to the extracellular side of the membrane)
Physiological significance	
● Affects groups of contiguous cells	● Affects individual cells
● Evoked by non-physiological disturbances (complement attack, lytic viruses, hypothermia, hypoxia, ischemica, metabolic poisons)	● Induced by physiological stimuli (lack of growth factors, changes in hormonal environment)
● Phagocytosis by macrophages	● Phagocytosis by adjacent cells or macrophages
● Significant inflammatory response	● No inflammatory response

2.2.2 Mechanisms of apoptosis

Two major apoptosis pathways are distinguished according to whether caspases are involved or not. There are classified as caspase-dependent pathway and caspase-independent pathway.

2.2.2.1 Caspase-dependent pathway

The caspase-dependent apoptotic pathway can be characterized by the involvement of caspase in this type cell death process. Two major types of caspase-dependent apoptotic pathway are mitochondrial (intrinsic) pathway and death receptor (extrinsic) pathway as shown in Figure 2.4.

The extrinsic pathway can be activated by the engagement of TNF receptor superfamily, including TNF-R1, CD95 (Fas), TRAIL-R1 and TRAIL-R2 (MacFarlane and Williams, 2004) by their respective ligands into the death inducing signaling complex (DISC) through Fas-associated death domain (FADD) leading to caspase-8 activation (Calvino-Fernández and Parra-Cid, 2010). Activated caspase-8 stimulates apoptosis via two parallel cascades: it can directly cleave and activate the downstream effectors of caspase-3, -6, and -7, which then cleave multiple substrates within the cells, or it can cleave Bid into its active form, tBid. tBid then translocates to mitochondria, activates Bak or Bax, and leads to release of cytochrome C, apoptosis-inducing factors (AIF), and other molecules from mitochondria, and apoptosis will be induced (Wang et al., 2005).

The intrinsic pathway can be induced by the release of cytochrome C from mitochondria, and various stimuli, including elevations in the levels of pore-forming pro-apoptotic Bcl-2 family proteins such as Bax. In the cytosol, cytochrome C interacts with the adaptor protein apoptotic peptidase

activating factor 1 (Apaf-1), and activates pro-caspase-9 to form the apoptosome. Active caspase-9 directly cleaves and activates the executioner caspase-3 (MacFarlane and Williams, 2004).

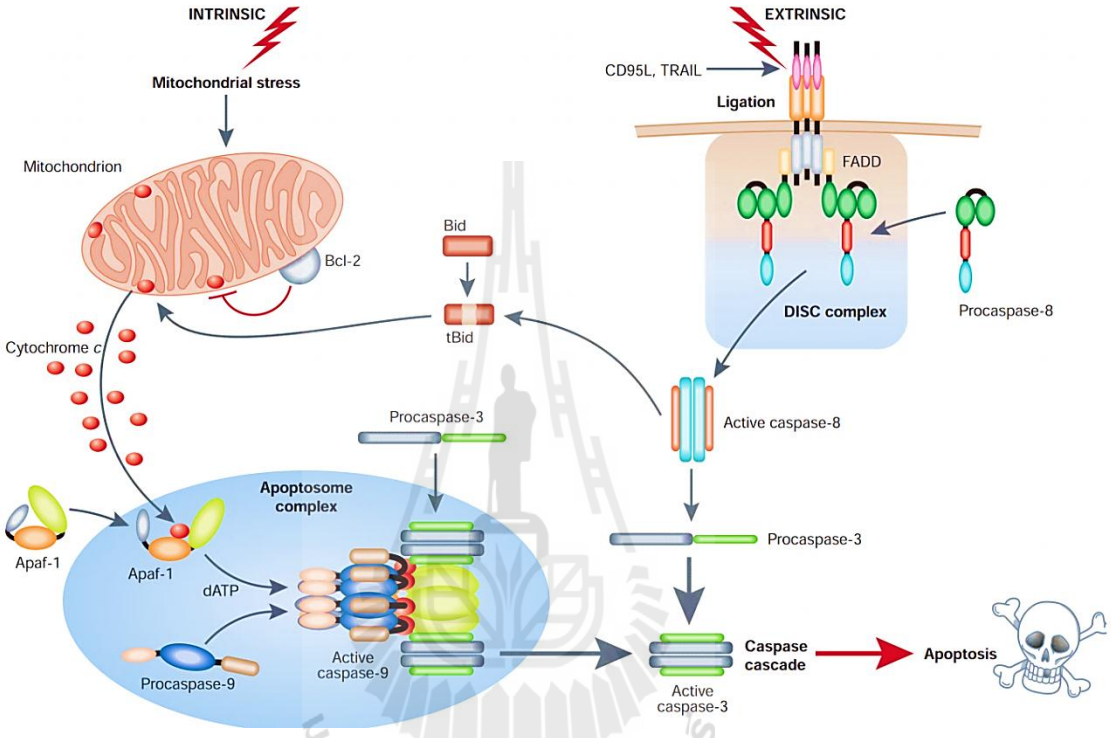

Figure 2.4 Two major types of caspase-dependent apoptotic pathway are mitochondrial (intrinsic) pathway and death receptor (extrinsic) pathway (MacFarlane and Williams, 2004).

2.2.2.2 Caspase-independent pathway

Apoptotic cell death via caspase-independent mechanism (Figure 2.5) or called “apoptosis-like” cell death (Bröker, Kruyt, and Giaccone, 2005) is caused by various factors such as UV radiation, lysosomal membrane permeabilization, virus infection, bacterial infection, drugs, p53 suppression tumor factors, and Granzyme A. Granzyme A is also important in cytotoxic T cell that induces single-stranded DNA damage as well as rapid loss of cell membrane integrity and mitochondrial transmembrane potential, which is initial step of the apoptosis through caspase independent pathways (Candé et al., 2002; Lieberman and Fan, 2003). The mitochondrial membrane damage is caused to release of several factors such as cytochrome C, Smac/Diablo, Omi/HtrA2, AIF, and EndoG from the intermembrane space into the cytosol (Kim, Emi, and Tanabe, 2006). The releases of Omi/HtrA2, AIF, and EndoG have been shown to function as caspase-independent death executors. AIF is one of pro-apoptotic factors which recruit potential partners such as nucleases to degrade DNA and trigger cell death (Lorenzo and Susin 2004). Moreover, mitochondria dysfunction is causing to reactive oxygen species (ROS) production which can mediate poly (ADP-ribose) polymerase-1 (PARP-1) activation, and PARP-1 activation is necessary for AIF release from mitochondria. So ROS also involves in this type of cell death networks (Kang et al., 2004). Moreover, Endo G appears to work in conjugation with both AIF and the caspase-activated DNase CAD/DFF40 in chromatin condensation and nuclear degradation (Bras et al., 2005).

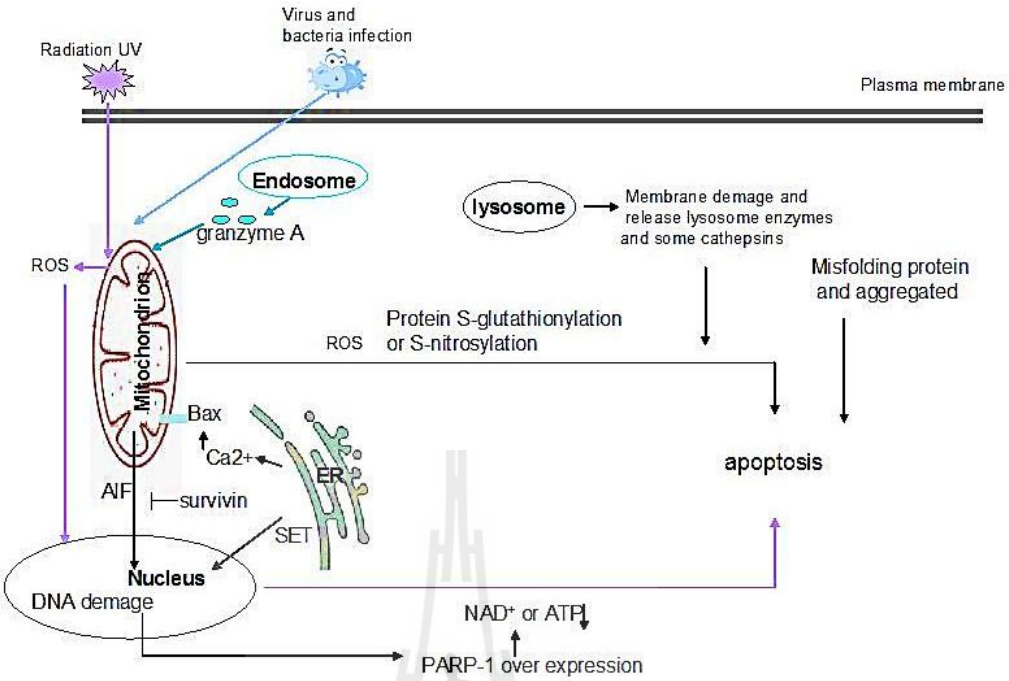

Figure 2.5 Caspase-independent apoptosis pathway (Hongmei, 2012).

2.2.2.3 Caspase cascade

Caspases are a family of genes important for maintaining homeostasis through regulating cell death (caspase-3, -6, -7, -8, and -9 in mammals) and inflammation (caspase-1, -4, -5, -12 in humans and caspase-1, -11, and -12 in mice). The caspase cascade is an important process in both the extrinsic and intrinsic pathways of apoptosis. Activation of apoptotic caspase results in subsequent amplification by the activation and cleavage of other downstream caspases (Li and Sheng, 2012; McIlwain, 2013). Caspases involved in apoptosis have been identified into two subgroups, the initiator caspases, consisting of caspase-2, -8, -9 and -10, and the executioner caspases, consisting of caspase-3, -6 and -7. Activation of initiator caspases is mediated by the binding of adapter molecules to protein interaction motifs in their prodomains. This pro-domain includes caspase recruitment domain

(CARD) (caspases-2 and caspase-9) or death effector domain (DED) (caspases-8 and caspase-10) (Taylor et al., 2008). The clustering of the initiator caspases with other molecules allows to cleave and activate the executioner caspases-3 and -7 (Boatright and Salvesen, 2003). Caspase-3 is an executioner caspase, which cleavages the majority of the substrates, examined the enzyme poly (ADP-ribose) polymerase (PARP), which responds to DNA strand breaks. The activation of caspase-activated DNase can result in DNA degradation (Slee, Adrain, and Martin, 2001). The degradation of lamin by caspases-6 can lead to the chromatin condensation and decomposition of the nuclear membrane. The cleavages of fodrin by caspases result in apoptotic body formation (Fan et al., 2005).

2.2.2.4 Detection of apoptosis

Detection of apoptotic cell death can be performed by several assays that analyse either morphological changes or distinct biochemical events occurring during programmed cell death, including observing nuclear morphology changes by Hoechst staining, analyzing DNA fragmentation by gel electrophoresis, detecting cytochrome C release by flow cytometry, and detecting phosphatidylserine externalization by annexinV-PI staining (Yin et al., 2011; Cohausz et al., 2008; Choi and Kim, 2009; Tsagarakis et al., 2010). Currently, Fourier-transform infrared microspectroscopy (FTIR), the vibrational technique for fast analysis of biological molecules (lipids, proteins, and nucleic acids) in intact cells or tissues, has been applied to study apoptosis and necrotic cell death of human leukaemia U937 and CCRF-CEM cells (Zelig et al., 2009). This technique presents several advantages, such as sensitivity, rapidity, and no requirement for staining or reagents (Gasparri and Muzio, 2003).

2.3 Overview of *Pseuderanthemum palatiferum* (Nees) Radlk.

Pseuderanthemum palatiferum (Nees) Radlk. is a new medicinal plant belonging to the Acanthacea family (Figure 2.6). Its vernacular names are "Hoan-Ngoc" or "Xuan-Hoa". This plant was found in the latter half of the 1990's in Cuc Phuong forest in northern Vietnam (Chayarop et al., 2011). This plant can grow very fast and bloom in southern and northern areas of the country (Dieu et al., 2005). This plant has been used in Vietnam both as medicinal and ornamental plants. Hoan-Ngoc was taken into Thailand about 20 years ago by a vietnam Era veteran and passed to the northeast of Thailand such as Surin, Burirum and Sisaket provinces. Its Thai name is "Payawanorn" or "Wan-Ling". Hoan-Ngoc is a shrub tree of 1-3 m high. Stem is quadrangular, glabrous, and green in color. Leaf arrangement is opposite, simple, and green foliage color. Shape of leaf is lanceolate to elliptic, 3-5×5-15 cm, acuminate at terminal, attenuate at base and entire margin. Flower is inflorescence and irregular. Corolla is white-violet tin color (Chuakul and Arunya, 2008). In Vietnam, Hoan-Ngoc has been used for both treatment and prevention of many diseases such as blood pressure, diarrhea, arthritis, pharyngitis, hemorrhoids, tumors, colitis, bleeding, wounds, cancer, and so on. In addition, Hoan-Ngoc has also been used for treatment and prevention of various diseases in animals (Dieu et al., 2005; Dieu et al., 2008). A few years ago, Hoan-Ngoc has become popular among Thai people. According to folkloric medicine, its fresh leaves are claimed to cure various diseases, including diarrhea, peptic ulcer, hepatitis, nephritis, hypertension, and diabetes. In addition, Hoan-Ngoc has gained its reputation for alleviating or curing cancer, the number one cause of death among Thai people (Health Information System Development Office, 2005). However, Hoan-Ngoc products, including dried powder for decoctions, herbal

tea bags, and capsules have been developed and commercialized without quality control.

Figure 2.6 (A) Leaves and (B) Flowers of *Pseuderanthemum palatiferum* (Nees) Radlk. (Kusherb, www, 2012; AuntieV, www, 2012).

A report on constituents of Hoan-Ngoc leaves has been recently established (Chayarop et al., 2011). The phytochemical screenings revealed that this plant contained flavonoids, phenolic compounds, unsaturated lactone rings, and steroids nuclei. Dieu et al. (2008) reported that the chemical composition of Hoan-Ngoc was a mixture of β-sitosterol, β-sitosterol-3-0-β-glucoside, apigenin-7-0-β-glucoside, 1-triacontanol, and salicylic acid. In addition, the leaves of Hoan-Ngoc contained 30.8% of the dry matters as crude proteins, minerals such as Ca, Mg, Fe and Cu, and amino acids such as lysine, methionine and threonine. Moreover, the plant has been reported to possess antioxidant activity, anti-inflammatory activity (Chayarop et al., 2011; Sittisart and Chitsomboon, 2014), antidiabetic activity (Chayarop et al., 2011), hypotensive activity (Khonsung et al., 2011), hypoglycemic activity (Padee et al.,

2010), and antiproliferative activity (Thi Mai et al., 2011; Pamok et al., 2012; Phasuk and Meeratana, 2015).

2.4 Roles of phytochemicals in apoptosis

Several studies showed that phytochemicals in fruits, vegetables and grains, especially flavonoids and apigenin-7-O-glucoside in polyphenol compounds and β-sitosterol in phytosterol, had antiproliferation or anticancer activities through apoptotic induction (Bennani et al., 2007; Ramos et al., 2007; Janmejai and Gupta, 2009). Five bioactive compounds from *Citrus aurantifolia*, namely limonin, limonexic acid (LNA), isolimonexic acid (ILNA), β-sitosterol glucoside (SG), and limonin glucoside (LG), significantly inhibited human pancreatic cancer Panc-28 cells with IC_{50} values in the range of 18-42 μM. The cytotoxicity induction occurred through p21, p53, and cytochrome C-mediated intrinsic apoptotic pathway (Patil et al. 2010). Chai et al. (2008) reported that β-sitosterol isolated from *Cyrtandra cupulata* Ridl. inhibited the growth of breast cancer MCF-7 cells in a dose-dependent manner. Moon et al. (2007) also reported that β-sitosterol induced apoptosis in the murine fibrosarcoma MCA-102 by increasing caspase activity and poly (ADP-ribose) polymerase (PARP) cleavage, and caspase-3 inhibitor z-DEVD-FMK significantly inhibited β-sitosterol-induced cell death. Awad et al. (2007) demonstrated that β-sitosterol exposure promoted its enrichment in transformed cell membranes and significantly inhibited tumor cell growth in human breast MCF-7 and MDA-MB-231 adenocarcinoma cells.

Das et al. (2009) showed that flavonoids (apigenin, [-]-epigallocatechin, (-) epigallocatechin-3-gallate (EGCG), and genistein) induced apoptosis in T98G and

U87MG cells via multiple mechanisms, including increase ROS production, activation of kinases, down-regulation of survival pathways and inflammatory factors, and activation of death receptors and mitochondrial pathways. Janmejai and Gupta, (2007) found that apigenin-7-O-glucoside, the major constituent of chamomile extract, caused minimal growth inhibitory responses in normal cells, while significantly decreased cell viability in various human cancer cell lines.

2.5 Mutagenicity

Mutagenesis is a process by which the genetic information of an organism is changed in a stable manner, resulting in a mutation. The mutagenesis can lead to cancer and various genetic disorders (Wikipedia, 2015b). Mutations are referred to as spontaneous mutations and environmental agents which cause mutations and are known as mutagens. The spontaneous mutations are thought to arise through chance errors in chromosomal division, DNA replication, and faulty DNA repair. The environmental agents include physical (x-ray, ultraviolet) and chemical mutagen. The mutagens act either directly or indirectly via mutagenic metabolites, on the DNA producing lesions and as a result of the replication or chromosomal partition mechanism, and other cellular processes (Wikipedia, 2015a). Moreover, many chemical mutagens require biological activation to become mutagenic. The important groups of enzymes involved in the production of mutagenic metabolites include cytochrome P450, microsomal epoxide hydrolase, and glutathione S-transferase (Marinković1, Pašalić, and Potočki, 2013). Mutagens that are not mutagenic by themselves but require biological activation are called promutagens (Wikipedia, 2015a). In present, there are *in vitro* cell-culture testing for identifying

mutagenic agents that might cause cancer, such as Ames assay, chromosomal aberrations, unscheduled DNA synthesis, cell transformation assays, and microarray expression analysis (Goldmanand Shields, 2003). Ames assay is wieldy used for detecting the mutagenic potential of new chemicals and drugs. *Salmonella typhimurium* strain was used in the test, which is incapable of synthesizing histidine. *S. typhimurium* strain used in the test have different mutations. Each of these mutations is designed to be responsive to mutagens that act via different mechanisms such as base-pair substitutions or frameshift mutations. (Mortelmans and Zeiger, 2000).

CHAPTER III

MATERIALS AND METHODS

3.1 Materials

3.1.1 Plant

Pseuderanthemum palatiferum (Nees) Radlk or Hoan-Ngoc was purchased from Yasothon province, Thailand. It was harvested in July 2011. Specimen was identified by Dr. Kongkanda Chayamarit of forest Herbarium, Royal Forest Department, Bangkok, Thailand. A voucher specimen (BKF 174009) was deposited at the Forest Herbarium, Royal Forest Department, Bangkok, Thailand (Sittisart and Chitsomboon, 2014).

Figure 3.1 The leaves of *Pseuderanthemum palatiferum* (Nees) Radlk (Kusherb, www, 2012).

3.1.2 Cell lines

MCF7 (human breast adenocarcinoma cell line), HepG2 (human hepatocyte carcinoma cell line), and PC-3 (human prostate adenocarcinoma cell line) were purchased from American Type Culture Collection (ATCC, USA). Jurkat leukemic cell line was purchased from Cell Line Services (CLS), Germany. Human normal peripheral blood mononuclear cells (PBMCs) were obtained from buffy coat, which were kindly provided by Blood Bank of Maharat Nakhon Ratchasima Hospital Nakhon Ratchasima province, Thailand.

HepG2 and MCF-7 cells were cultured in Dulbecco's Modified Eagle's medium (DMEM) with high glucose supplemented with 10% FBS and 100 U/ml penicillin and 100 µg/ml streptomycin.

Jurkat cells, PC-3 and PBMCs cells were cultured in RPMI-1640. All complete media were supplemented with 10% FBS, 100 U/ml penicillin and 100 µg/ml streptomycin.

All cell lines were maintained at 37 ºC in 5% CO_2 and 95% humidity.

3.1.3 Bacterial strains

Salmonella typhimurium strains TA98 and TA100 were used to evaluate mutagenic activity of EEP and WEP. The *S. typhimurium* strains were provided by Dr. B.N. Ames of the University of California, Berkeley, CA, USA.

3.1.4 Chemicals and instruments

The chemicals, materials and instruments employed in the present studies were summarized in Tables 3.1 and 3.2.

Tables 3.1 List of chemicals.

Name	Source
2-aminoanthracene	Sigma
2-Nitrofluorene	Santa Cruz
Absolute ethanol	Carlo erba
Agarose	Gibco
Ammonium sodium phosphate tetrahydrate	Acros organics
Ampicillin	T.P. Drug Laboratory
Apoptosis Assay Kit - FITC	Exbio
Ascorbic acid (Vitamin C)	Fluka
Bacto agar	Difo
Biocoll separating solution	Biochrom AG
Biotin	Acros organics
Boric acid	Fischer
Catechin	Fluka
Citric acid	Fisher Scientific
D-Glucose	Univar
D-glucose-6-phosphate	Univar
Dimethyl sulfoxide (DMSO)	Amresco
DNA Ladder 100 bp	BIOLabs Inc.

Table 3.1 List of chemicals (Continued).

Name	Source
Dulbecco's Modified Eagle's Medium - high glucose	Invitrogen
EDTA (Ethylenediaminetetraacetic acid)	Sigma
Ethidium bromide	Sigma
Etoposide (20 mg/ml)	Fytosid
Folin & Ciocalteu's Phenol Reagent	Sigma
Gallic acid	Riedel-de Haen®
HEPES (N-2-hydroxyethylpiperazine-N-2-ethanesulfonic acid)	Usb
Hexane	Carlo erba
L-Histidine	Acros organics
Magnesium chloride	Analar Normapur
Magnesium sulfate	Carlo erba
Methyl alcohol	Fisher Scientific
Millipore's FlowCellect^{TM} Cytochrome c kit	Millipore
MTT [3(4,5-dimethylthiazol-2-yl) ,5-diphenyltetrazolium bromide]	Invitrogen
Nicotinamide adenine dinucleotide phosphate (NADP)	Sigma
Nutrient broth No.2	Oxoid
Penicillin G	Sigma-Aldrich
Potassium chloride	Carlo erba
Potassium phosphate, dibasic (anhydrous)	Univar
QIAamp DNA Mini and Blood	Qiagen

Table 3.1 List of chemicals (Continued).

Name	Source
RPMI 1640	Invitrogen
S9 fraction	Chiang Mai University
Sodium acetate	Aldrich
Sodium ammonium phosphate	Acros organics
Sodium azide	Sigma
Sodium hydroxide	Carlo erba
Sodium monohydrogen phosphate heptahydrate	Merck
Streptomycin solution sulfate	Sigma-Aldrich
Trisma base	Carlo erba
Triton X-100	Aldrich
Trolox (6-Hydroxy-2,5,7,8-tetramethylchroman-2-carboxylic acid)	Sigma
Trypan blue dye	Fluka
Trypsin	Gibco
Tween-20	Sigma
ρ-formaldehyde	Carlo erba

Tables 3.2 List of instruments.

Name	Source
Bruker Vertex 70 spectrometer coupled with a Bruker-Hyperion 2000 microscope	Bruker Optics
Centrifuge (modelCT15RT)	Techcomp

Tables 3.2 List of instruments (Continued).

Name	Source
Dessicator	Schott
Electrophoresis power supply (EPS 601)	Amersham
Electrophoresis system (model HE33)	Hoefer
FACScalibur cell analyzer	Becton Dickinson
(model FACSCalibur Flowcytometry)	
Inverted fluorescence microscope (model Olympus IX51)	Olympus
Inverted microscope (model CKX41)	Olympus
Laminar flow hood	ESCO
(model CLASS II Biohazard safety cabinet)	
Light microscope (model CX21))	Olympus
Low-e microscope slides (MirrIR)	Kevley Technologies
Lyophilizer(model Freeze-zone 12 plus)	Labconco Corporation
Microcentrifuge	SORVALL
Microplate spectrophotometer	Bio-Rad
Nanodrop(model ND-1000 spectrophotometer)	Bio-Active
pH meter	Selecta
Pump	Millipore
Rotary evaporator with vacuum (model R205)	Buchi
Water bath	Memmert
WEALTEC Dolphin-DOC ultraviolet analyzer	WEALTEC

3.2 Methods

3.2.1 Preparation of crude Hoan-Ngoc leave extracts

The preparation of crude Hoan-Ngoc leave extracts was described by Sittisart and Chitsomboon, 2014. Briefly, fresh leaves (4 kg) were blended in 95% ethanol and filtered through gauze. The extract was centrifuged at 3,500×*g* for 10 min, and then the supernatant was filtered through a Whatman No.1 filter paper. After that, the ethanolic filtrate was concentrated using a vacuum rotary evaporator (Buchi Labortechnik AG, Flawil, Switzerland) and dried by lyophilization (Freeze-Zone 12 plus, Labconco Corporation, Missouri, USA) into powder of 95% ethanol crude extract (EEP; 87.63 g). The EEP (40 g) was partitioned between hexane and water (1:1, v/v). The water fraction was collected, centrifuged at 14,000×*g* for 10 min at 4 ^{o}C, and then the supernatant was filtered through a Whatman No.1 filter paper. After that, the water fraction was evaporated and lyophilized into powder of water fraction of 95% ethanol crude extract (WEP; 21 g). The EEP and WEP were stored in a refrigerator at -20 ^{o}C till use in subsequent experiments. The EEP and WEP were dissolved in dimethyl sulfoxide (DMSO) and water respectively when were used in experiments. For cell culture experiments, the EEP was dissolved in DMSO and diluted to 0.1% (v/v) in cell culture medium. The WEP was dissolved in cell culture medium directly.

3.2.2 Determination of phytochemicals and antioxidant activity

3.2.2.1 Total Phenolic Content (TPC)

The total phenolic content of individual extract was determined colorimetrically using Folin-Ciocalteau method (Singleton, Orthofer, and

Lamuela-Ravent´os, 1998). This method is based on a chemical reduction of the reagent, a mixture of tungsten and molybdenum oxides. Briefly, 0.1 ml of the extracts was added to 2 ml of 2% Na_2CO_3 solution and mixed thoroughly. After 2 min, 0.1 ml of 50% Folin-Ciocalteau reagent was added, mixed and incubated for 30 min at room temperature. Then, the absorbance of the extracts was measured at 750 nm using a Cecil 1000 series spectrophotometer (Cecil Instruments, Cambridge, UK). Gallic acid solutions ranging from 0.05 to 0.3 mg/ml were used to prepare a standard curve. The phenolic contents of the extracts were expressed as milligrams of gallic acid equivalent (GAE) per gram of dried extract.

3.2.2.2 Total Flavonoid Content (TFC)

Total flavonoid content was determined using the aluminium trichloride colorimetric assay (Liu et al., 2002). The reaction is based on formation of acid stable complexes between aluminium chloride with the C-4 keto group and either the C-3 or C-5 hydroxyl group of flavones and flavonols. Aluminium chloride also forms acid labile complexes with the ortho-dihydroxyl groups of flavonoids. The intensity of yellow color of the kelate formed by the flavonoids, when treated with $AlCl_3$ in acetate buffer, was spectrophotometrically determined (Constanta and Rodica, 2010). Briefly, 0.25 ml of the extracts was diluted with 1.25 ml of distilled water. Then, 0.075 ml of 5% $NaNO_2$ solution was added to the mixture. After 6 min, 0.15 ml of 10% $AlCl_3 \cdot 6H_2O$ solution was added, mixed and incubated 5 min. Then, 0.5 ml of 1 M NaOH was added and the total volume was made up to 2.5 ml with distilled water. The absorbance of the extracts was measured immediately at 510 nm using a spectrophotometer. The catechin solution (0.05-0.4 mg/ml) was used as a

standard for the calibration curve. Total flavonoid contents of the extracts were expressed as milligrams of catechin equivalent (CAE) per gram of dried extract.

3.2.2.3 The 2, 2-diphenyl-1-picrylhydrazyl (DPPH) assay

This assay is based on the measurement of the scavenging ability of antioxidants towards the stable radical DPPH, and hence the decreasing absorbance at 515-528 nm. The free radical DPPH (purple) is reduced to the corresponding hydrazine (no color) when it reacts with hydrogen donors from antioxidant compounds as shown in Figure 3.2 (Sánchez-Moreno, Larrauri, and Saura-Calixto, 1999).

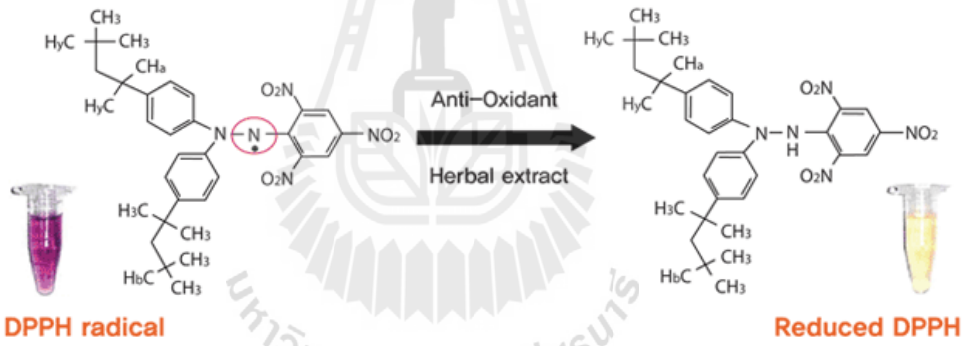

Figure 3.2 Structure of DPPH before and after reaction with antioxidant (Damo, www, 2010).

The DPPH˙ scavenging activity was determined by following the method of Sánchez-Moreno et.al. (1999). Briefly, one milliliter of the extracts at different concentrations was added to 3.9 ml of DPPH solution (63 mM). The mixture was shaken vigorously at room temperature for 45 min in the dark and measured the absorbance at 515 nm using a spectrophotometer. The free radical scavenging activity

was calculated as shown below. The IC_{50} of $DPPH^{\cdot}$ was determined from a dose response curve using linear regression analysis. Decreasing DPPH solution absorption indicates an increase of DPPH radical scavenging activity.

$$DPPH^{\cdot} \text{ inhibition (\%)} = \frac{[(A_{control}-A_{sample})\times 100}{A_{control}}$$

Where $A_{control}$ = The absorbance of control

A_{sample} = The absorbance of different concentrations of sample extracts

3.2.3 *In vitro* Cytotoxic test (MTT assay)

3.2.3.1 Cytotoxic effect against 4 human cancer cell lines

The cytotoxic effect of EEP and WEP on cell proliferation was determined by 3-(4, 5-dimethylthiazol-2-yl)-2, 5-diphenyltetrazolium bromide (MTT) assay (Chun et al., 2007). Briefly, the cells were seeded in a 96-well plate at a density of 2×10^4 cells/well for PC-3 and 2.5×10^4 cells/well for HepG2 and MCF-7. The cells were allowed to adhere overnight, and then treated with various concentrations of EEP or WEP for 24 h. Jurkat cells were seeded at a density of 2.5×10^4 cells/well and treated with various concentrations of EEP or WEP for 24 h. After incubation, the cultured medium was removed and 0.5 mg/ml (final concentration) MTT was added. Then, cells were further incubated for 4 h at 37 °C. Formazan crystal formed by viable cells was dissolved in DMSO, and absorbance was measured at 540 nm with a microplate spectrophotometer (Benchmark Plus, Bio-Rad, Japan).

3.2.3.2 Cytotoxic effect against normal peripheral blood mononuclear cells (PBMCs)

Buffy coat isolated from normal human blood was kindly given from Blood Bank of Maharat Nakhonratchasima Hospital Nakhon Ratchasima province, Thailand). Buffy coat was isolated by Biocoll separating solution, density 1.077 g/ml. Briefly, 7 ml of buffy coat was added to a 15 ml conical tube. The buffy coat was diluted with an equal volume of PBS and then carefully laied onto the Biocoll separating solution. The tube was centrifuged without the brake at 400×*g* for exactly 30 min at 25 °C. The layer of PBMCs between the plasma and Biocoll separating solution was collected and washed twice with PBS (centrifuged at 400×*g* for 5 min). The cells were collected for cytotoxic assay (MTT assay).

3.2.4 Evaluation of apoptosis

3.2.4.1 DNA fragmentation

In apoptotic cells, DNA is cleaved by an endonuclease that fragments the chromatin into nucleosome size of 180-200 base pairs and appears as a DNA ladder or DNA fragments. The DNA fragmentation was analyzed using agarose gel electrophoresis to demonstrate a "ladder" pattern. Briefly, Jurkat cells were seeded at density 1.875×10^6 cells/dish in 100 mm^2 culture dish and were treated with 100, 300, and 600 µg/ml of EEP or WEP at 24 h. For time course study, cells were treated with 300 µg/ml EEP or WEP for 6, 12, and 24 h. 0.1% DMSO and 40 µg/ml of etoposide were used as a vehicle and positive control, respectively. After treatment, Jurkat cells were collected and centrifuged at 400×*g* for 5 min. Cells were washed with PBS and recentrifuged at 400×*g* for 5 min. Cells pellet was resuspended in 200

µl of PBS and extracted using QIAamp DNA Mini Kit (QIAGEN, Germany) (Appendix C). Five microgram of DNA sample in AE buffer was mixed with 100 µg/ml of RNase A (final concentration) and incubated at 37 °C for 30 min. Then, the DNA sample was loaded in 1.5% agarose gel. The gel was run at 70 volts, 1.50 h and then stained with 0.5 µg/ml ethidium bromide. The DNA fragment was visualized under ultraviolet light (WEALTEC, Corp., Sparks, Nevada, USA).

3.2.4.2 Hoechst 33258 staining

Nuclear morphological change as a late marker of apoptosis was observed by staining of DNA with Hoechst 33258. Jurkat cells were seeded at density of 5×10^5 cells/plate in a 6-well plate. After treatment, Jurkat cells were collected and centrifuged at 400×*g* for 5 min. Cells were washed with PBS and recentrifuged at 400×*g* for 5 min. The cells were fixed with 200 µl of ρ-formaldehyde (4%, v/v) for 20 min. Then, the cells were washed with PBS and further stained with 10 µg/ml of Hoechst 33258 for 30 min at room temperature in the dark. The stained cells were washed with PBS and visualized under the inverted fluorescence microscope (Olympus IX51, Olympus Corporation, Japan).

3.2.4.3 Annexin V-PI staining

The Annexin V-PI staining was used to evaluate early and late apoptotic cells induced by EEP or WEP. The Jurkat cells were seeded at density 5×10^5 cells/plate in a 6-well plate. After treatment, Jurkat cells were collected and centrifuged at 400×*g* for 5 min. Cells were washed with PBS and recentrifuged at 400×*g* for 5 min. Then, cells were stained with Annexin V-FITC Apoptosis Detection Kit (EXBIO, Czech Republic). Briefly, after washing, cells were prepared at density 5×10^5 cells in 100 µl of 1X Binding buffer. Then, 5µl of Annexin V-FITC and 5µl of

PI were added and incubated for 15 min in the dark at the room temperature. After incubation, four hundred microliters of 1X Binding buffer were added and analyzed by flow cytometer (Becton Dickinson Biosciences, USA).

3.2.4.4 Cytochrome C release

The release of key mitochondrial proteins such as cytochrome C is an important hallmark in apoptotic pathway and is considered a point of no return in the apoptosis process. The levels of cytochrome C in mitochondria can be detected by directly probed with anti-cytochrome c-FITC and analyzed by a flow cytometer. Jurkat cells were seeded at density 5×10^5 cells/well in a 6-well plate. After treatment, Jurkat cells were collected and centrifuged at 400×*g* for 5 min. Cells were washed with PBS and recentrifuged at 400×*g* for 5 min. Then, cells pellets were prepared at density 1×10^6 cells in 200 µl of PBS and stained using Millipore's FlowCellectTM Cytochrome C kit (Millipore, USA) following the manufacturer's instructions (Appendix C). The stained cells were analyzed by flow cytometry (BD FACS Calibur with Cell Quest Pro software). Three individual experiments were performed.

3.2.4.5 FTIR microspectroscopy

Fourier-transform infrared microspectroscopy (FTIR), the vibrational technique, affords a new technique for analysis of biological molecules (lipids, proteins and nucleic acids). The vibrational changes of macromolecules in cells are related to FTIR spectra changes. Therefore, FTIR technique was used to evaluate cellular and biochemical changes occurring during apoptosis in Jurkat cells.

Jurkat cells were seeded at the density 5×10^5 cells/well in a 6-well plate. After treatment, Jurkat cells were collected and centrifuged at 400×*g* for 5 min. Cells were washed with 0.85% NaCl and recentrifuged at 400×*g* for 5 min. Cells

pellet were dropped onto low-e microscope slides (MirrIR, Kevley Technologies) and vacuum dried for 30 min in a desiccator to eliminate the excess water. The dried cells were kept in a desiccator until analysis with FTIR.

FTIR spectra were recorded using a spectroscopy facility, at the Synchrotron Light Research Institute (Public Organization), Thailand. FTIR spectra were acquired with a Bruker Vertex 70 spectrometer coupled with a Bruker Hyperion 2000 microscope (Bruker Optics Inc., Ettlin-gen, Germany) - equipped with a nitrogen cooled MCT (HgCdTe) detector with a 36 × IR. The spectra were obtained in the reflection mode with the wavenumber range of 4000-600 cm^{-1}, using an aperture size of 50 µm × 50 µm, with a resolution of 6 cm^{-1}. Each spectrum was collected at 64 scans. OPUS 7.2 software (Bruker Optics Ltd, Ettlingen, Germany) was used to acquire FTIR spectral data and control instrument system.

The spectra of non-treated cells and EEP- or WEP-treated cells were identified by Principal Component Analysis (PCA) using variability of the Unscrambler 9.7 software (CAMO Software AS, Oslo, Norway). The spectral range of 3000-2800 cm^{-1} and 1300-850 cm^{-1} were used for EEP-treated cells, and 3000-2800 cm^{-1} and 1800-850 cm^{-1} was used for WEP-treated cells. The preprocessing of the spectra was performed by second derivative transformations using Savitzky-Golay algorithm (nine smoothing points) and normalized with extended multiplicative signal correction (EMSC). This method is used for identifying the overlapping of two or more absorption peaks, reducing variation between replicate spectra, and correcting for baseline shift. Score plots (2D) and loading plots were used to represent the different classes of data and relations among variables of data set, respectively,

The integrated peak areas of sample were analyzed using OPUS 7.2 software (Bruker) with a spectral range of 3000-2800 cm^{-1} and 1750-1730 cm^{-1} (lipid spectra), and 1300-850 cm^{-1} (nucleic acids spectra). The integrated peak areas of amide I spectra (1700-1590 cm^{-1}) were calculated from band curve-fitting of the original spectrum of each sample.

3.2.5 Ames test

The mutagenicity of EEP was evaluated by Ames test in pre-incubation procedure using *Salmonella typhimurium* strains TA98 and TA100, regardless of the absence or presence of S9 mix (Maron and Ames, 1983). Briefly, one hundred microliters of EEP or WEP with various concentrations were mixed with 500 µl of S9 mix or phosphate buffer. Then, 100 µl of bacterial culture was added, mixed, and further pre-incubated in a shaking water bath at 37 °C for 20 min. After incubation, 2 ml of top agar was added and mixed again. The mixture solution was poured onto minimal glucose agar plates and incubated at 37 °C for 48 h. The number of revertant colonies was counted after incubation. Negative control was prepared from the mixture without the extracts in the same manner as the assay to give the number of spontaneous revertants. The positive controls applied were 2-NF and sodium azide for the absence of S9 mix of TA98 and TA100 respectively, and 2-AA for the presence of S9 mix of both TA98 and TA100. The extract was considered as mutagenic if the number of revertants per plate was at least doubled over the spontaneous revertant frequency.

3.2.6 Statistical analysis

All statistical analyses were conducted using SPSS software (Statistics Package for the Social Sciences, version 11). The data from the total phenolic and flavonoid contents results were analyzed by a Student's t-test to determine the statistical significance between two groups. DPPH, flow cytometer (cytochrome C release), and integrated areas of the biological bands of lipids and the nucleic acid bands were analyzed by one-way analysis of variance (ANOVA) with a post hoc Tukey's analysis to determine differences between treatment and control groups (Nascimento et al., 2013). The differences between groups was considered to be statistically significant when $p < 0.05$. The mutagenicity was evaluated according to the 2-fold rule (Hakura et al., 2005).

CHAPTER IV

RESULTS

4.1 Phytochemicals and antioxidant activity

4.1.1 Extraction yield

Pseuderanthemum palatiferum or Hoan-ngoc fresh leave was extracted by 95% ethanol and then partitioned between hexane and water (1:1, v/v), giving the 95% ethanol extract of *P. palatiferum* (EEP) and the water extract of EEP (WEP), respectively. Table 4.1 illustrates the percentages of recovery from fresh leave of *P. palatiferum*. EEP exhibited a percentage of recovery of 2.91%, while WEP had a percentage of recovery of 1.15%. WEP that was prepared from the water fraction of EEP partitioned with hexane and water (1:1, v/v) showed a percentage of 52.5% recovery.

Table 4.1 The percentage yields of crude extracts of *P. palatiferum* leaves extracts.

Extract	Amount and source of preparation	Yield (g)	Percentage of recovery
EEP	1,500 g of fresh leaves	87.63	2.91 (from fresh leaves)
WEP	40 g of EEP	21.00	52.5 (from EEP)
	(1,826 g from fresh leaves)		1.15 (from fresh leaves)

4.1.2 Total phenolic and flavonoid content

Initial studies conducted to investigate and determine the total phenolic and total flavonoid contents from EEP and WEP were shown in Figure 4.1. The total phenolic content (TPC) was analyzed by fitting the calibration curve of gallic acid (R^2 = 0.9928). The total flavonoid content (TFC) was calculated using the calibration curve of catechin (R^2 = 0.9973). The results exhibited that the TPC of EEP and WEP was 331.5±3.24 and 338.12±6.54 mg GAE/g, respectively. The TFC of WEP (310.33±1.56 mg CAE/g) was significantly ($p < 0.05$) higher than that of EEP (291.19±2.42 mg CAE/g).

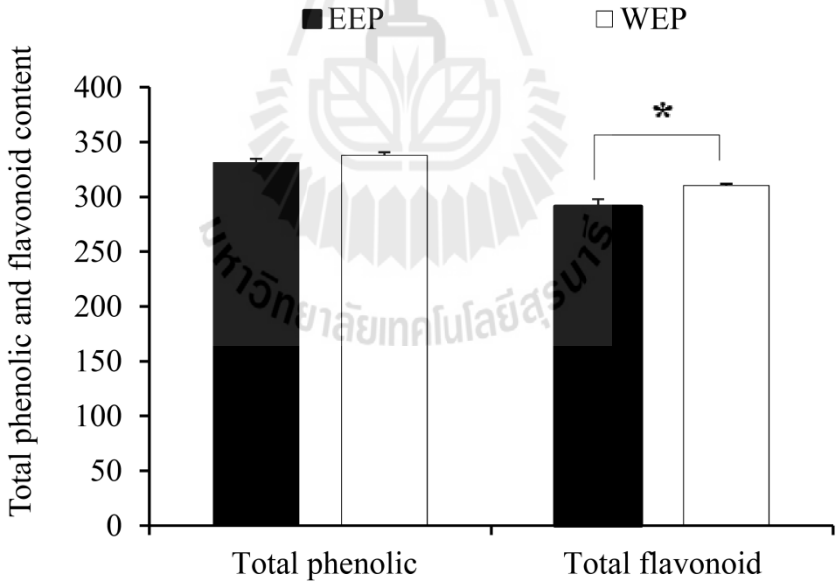

Figure 4.1 Total phenolic and flavonoid contents of EEP and WEP. Values are mean ± SD (n = 3) and are representative of three independent experiments with similar results. Statistical analysis was performed by Student's *t*-test. * means $p < 0.05$.

4.1.3 The 2, 2-diphenyl-1-picrylhydrazyl (DPPH) assay

The free radical-scavenging activity of EEP, WEP, and reference standards (vitamin C and trolox) was evaluated by the DPPH assay, and the results were expressed as IC_{50} values. A lower value of IC_{50} indicates a higher antioxidant activity. As shown in Figure 4.2, the IC_{50} values of DPPH radical scavenging activity of EEP and WEP were 9.87±0.21 and 8.27±0.07 μg/ml, respectively. The positive antioxidant controls, ascorbic acid and trolox showed the scavenging activity with IC_{50} values of 3.41±0.03 and 3.44±0.03 μg/ml, respectively. Therefore, the results suggested that both EEP and WEP demonstrated the ability to scavenge DPPH free radicals. The WEP possessed the higher DPPH radical scavenging activity than that of EEP ($p < 0.05$). However, the radical scavenging activity of both EEP and WEP was not as effective as the other positive antioxidant controls.

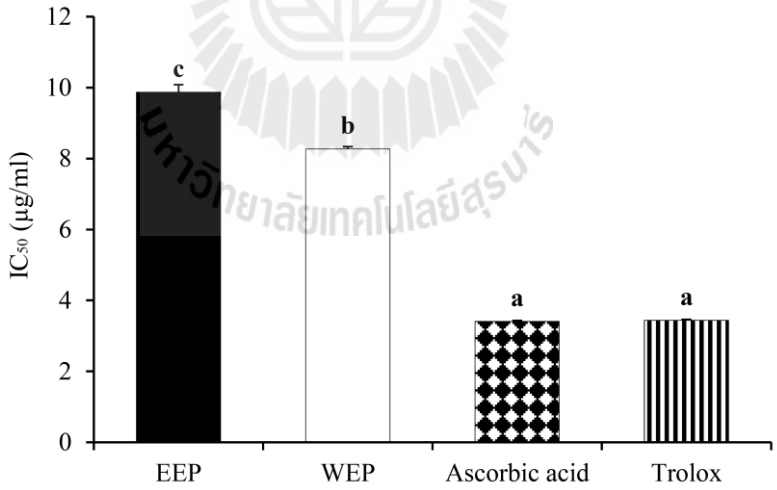

Figure 4.2 DPPH radical scavenging activity of EEP and WEP and positive controls (ascorbic acid and trolox). Values are expressed as means ± SD (n = 3) and are representative of three independent experiments with similar results. Bars marked with different letters are significantly different at $p < 0.05$ as determined by one-way ANOVA.

4.2 *In vitro* cytotoxicity

4.2.1 Cytotoxic effect against 4 human cancer cell lines

MTT assay has been widely used for measuring mammalian cell survival and proliferation. The reduction of tetrazolium dye (MTT) to purple coloured formazan products depends on mitochondrial dehydrogenase activity in the living cells (Mosmann, 1983). Figure 4.3A and 4.3B showed that Jurkat, HepG2, and MCF-7 cell lines exhibited different susceptibility to EEP and WEP in a dose dependent manner. EEP and WEP exerted high antiproliferation only in Jurkat and HepG2 cell lines. The *in vitro* cytotoxic effect of EEP and WEP against various human cancer cell lines, namely Jurkat, HepG2, MCF-7 and PC-3 after 24 h of exposure were expressed as the concentration of the extract causing 50% of cancer cell death (LC_{50}) (Table 4.2). The LC_{50} was calculated from a dose response curve using linear regression analysis. The LC_{50} of antiproliferative effects of EEP against Jurkat and HepG2 cell lines were 476.35±31.51 and 927.01±90.84 µg/ml, respectively. Similarly, the LC_{50} of antiproliferative effects of WEP in Jurkat and HepG2 cell lines were 389.94±13.26 and 794.90 ± 48.78 µg/ml, respectively. Notably, WEP had a higher antiproliferative activity towards Jurkat cells than that of EEP ($p < 0.05$). The breast cancer MCF-7 cells showed less susceptible to EEP and WEP treatments (LC_{50} > 1,500 µg/ml). The prostate cancer cells PC-3 displayed tolerance to the EEP and WEP treatment. Both extracts at the concentration up to 1,500 µg/ml still had no cytotoxicity towards PC-3. Overall, the results suggested that both EEP and WEP at the range of 50-1500 µg/ml exhibited the highest antiproliferative effects against Jurkat cell lines followed by HepG2 and MCF-7 cells, respectively, and had no

cytotoxicity against PC-3. Moreover, WEP possessed higher anti-proliferative effects against Jurkat cells than EEP.

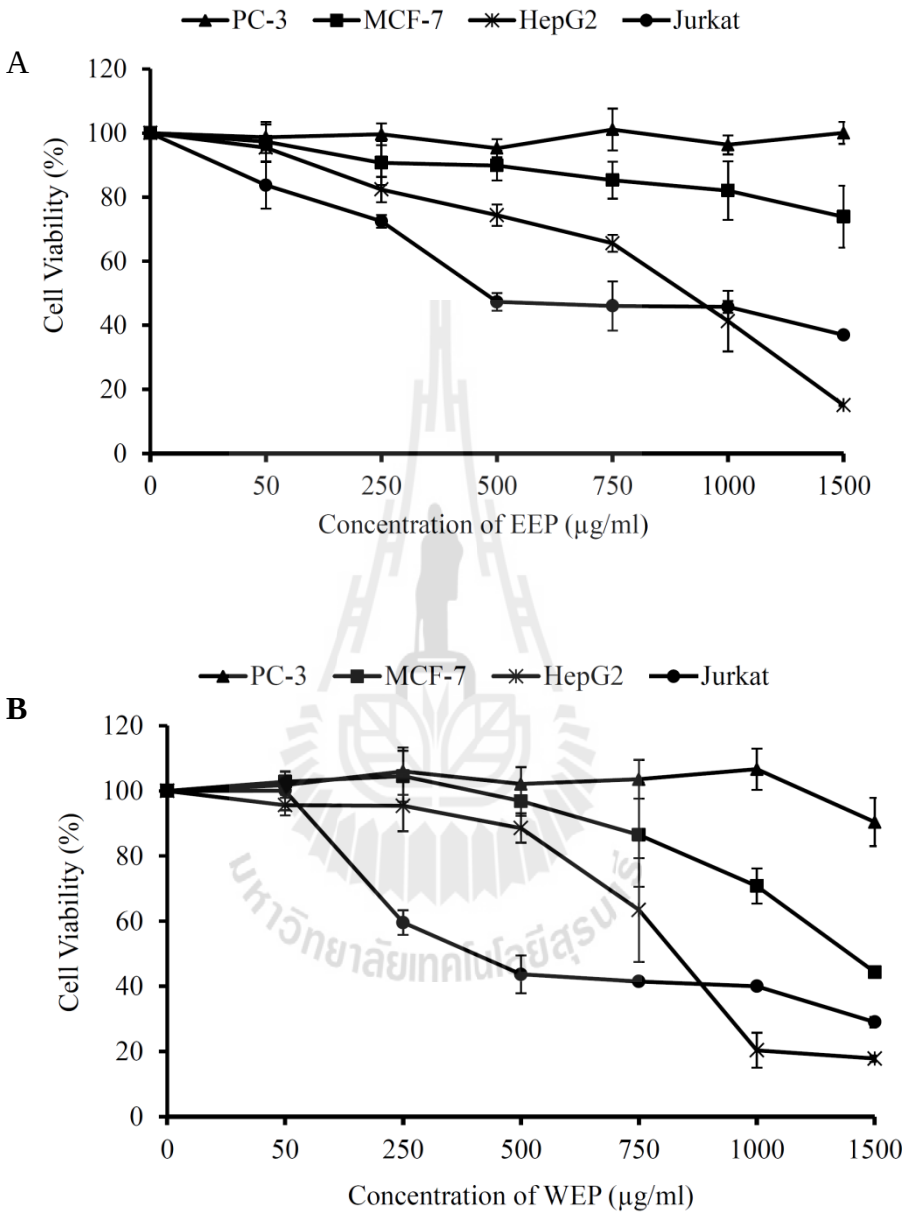

Figure 4.3 Cytotoxic effect of EEP (A) and WEP (B) against different human cancer cell lines, PC-3, MCF-7, HepG2 and Jurkat cells. The cells were exposed to various concentrations of EEP and WEP for 24 h. The cells were assessed for cell viability by MTT assay. Reported means ± SD values (n=4) are from a representative of three independent experiments.

Table 4.2 The LC_{50} values of extracts against different human cancer cell lines.

Cancer cells	LC_{50}(µg/ml)	
	EEP	**WEP**
Jurkat	476.35 ± 31.51[a]	389.94 ± 13.26[b]
HepG2	927.01 ± 90.84[a]	853.16 ± 49.71[a]
MCF-7	>1,500	1,434.45 ± 85.62
PC-3	>1,500	>1,500

Values are mean ± SEM (n = 4) and are representative of three independent experiments with similar results. Different letters within the same row are significantly different at $p < 0.05$ as determined by a Student's *t*-test.

4.2.2 Cytotoxic effect against normal peripheral blood mononuclear cells (PBMCs)

The *in vitro* cytotoxic effect of EEP and WEP against Jurkat cell lines compared to peripheral blood mononuclear cells, PBMCs (normal cells) after 24 h of exposure was shown in Figure 4.4(A) and 4.4(B). The results showed that Jurkat cell lines and PBMCs exhibited different susceptibilities to EEP and WEP in a dose dependent manner. The antiproliferative effects of EEP and WEP (250-1500 µg/ml) towards Jurkat cell lines was significantly greater ($p < 0.05$) than PBMCs. EEP exhibited the antiproliferative effects with the LC_{50} values of 476.35±31.51 µg/ml in Jurkat cell lines and more than 1,500 µg/ml in PBMCs. Similarly, WEP exhibited the antiproliferative effects in Jurkat cell lines and PBMCs with the LC_{50} values of 389.94±13.26 µg/ml and more than 1,500 µg/ml, respectively. These results suggested that both EEP and WEP showed higher antiproliferative activity towards Jurkat cell lines than PBMCs. The greater inhibition of cell viability by the extracts in human T cell leukemia Jurkat in comparison to normal human PBMCs *in vitro* was supported the anticancer properties of Hoan-Ngoc leaves, though in anticancer activity of the extract should be further investigated.

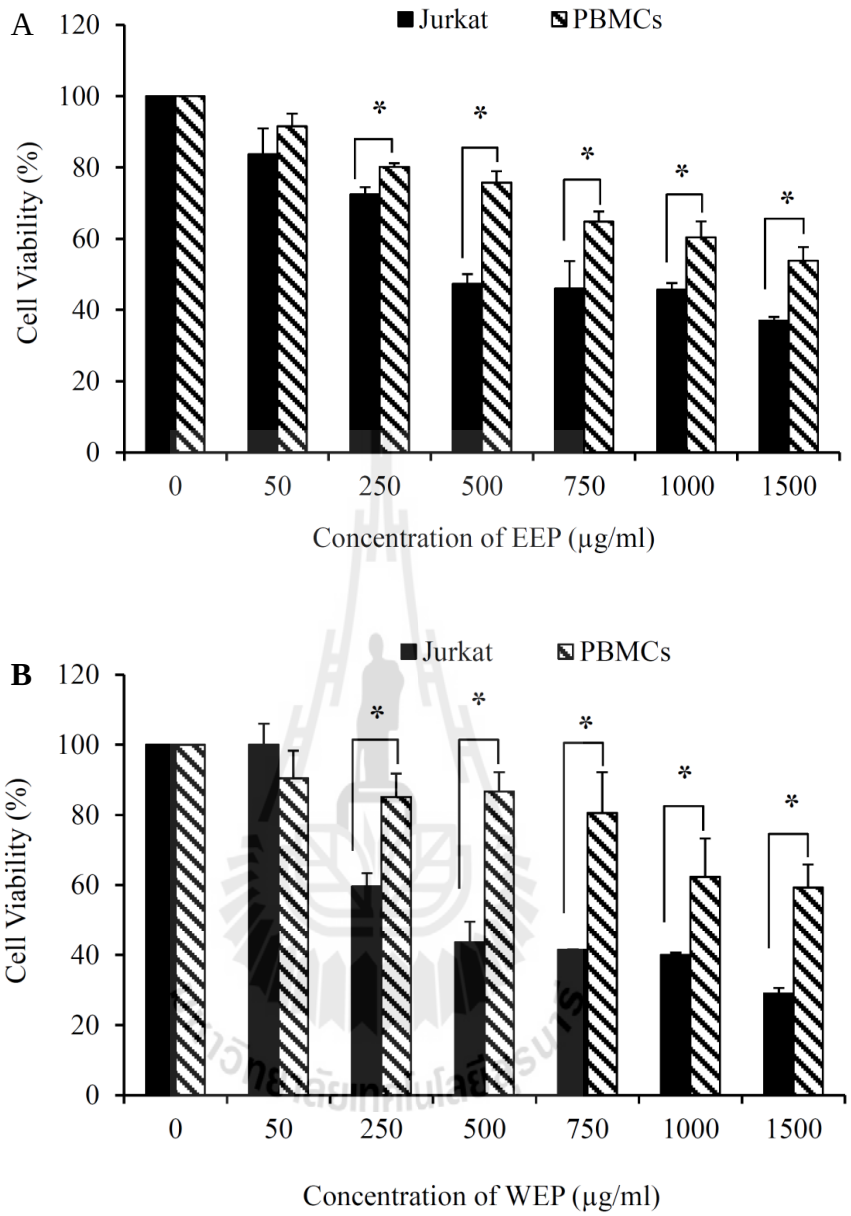

Figure 4.4 Cytotoxic effects of (A) EEP and (B) WEP against normal human peripheral blood mononuclear cells (PBMCs) compared to Jurkat cell lines. Cells were exposed to various concentrations of EEP and WEP for 24 h prior to assessment of cell viability by MTT assay. Values are mean ± SD (n = 4) and are representative of three independent experiments with similar results. Statistical analysis was performed by Student's *t*-test. * indicates significant differences between two groups ($p < 0.05$).

4.3 Evaluation of apoptosis

4.3.1 DNA fragmentation

The DNA fragmentation is used to detect DNA laddering at approximately 180-200 base pairs that is occurring when cells undergo apoptosis. Figure 4.5(A-D) showed that EEP and WEP induced the apoptotic cell death in both concentration- and time-dependent manners. The fragmented DNA was clearly observed in Jurkat cells after exposure to EEP and WEP at 300 and 600 µg/ml for 24 h and at 300 µg/ml for 12 and 24 h. No DNA fragmentation was observed in negative control cells, whereas the DNA ladder formation was clearly observed in the positive control group (40 µg/ml etoposide) at 24 h of exposure.

4.3.2 Hoechst 33258 staining

The nuclear morphological changes of Jurkat cells after EEP and WEP treatment were observed by Hoechst 33258 staining. The extent of apoptotic cell death induced by EEP and WEP was dose- and time- dependent (Figure 4.6 and 4.7). The positive control (40 µg/ml of etoposide) showed the typical apoptotic morphological changes, including membrane blebling, cell shrinkage, condensed and fragmented nuclei (arrow white). Similarly, the Jurkat cells after exposed to EEP and WEP at 300 and 600 µg/ml for 24 h also demonstrated condensed and fragmented nuclei, but both extracts had no effect at 100 µg/ml. The time course study revealed that Jurkat cells exposed to 300 µg/ml of EEP or WEP showed nuclear condensation and DNA fragmentation at 12 and 24 h post exposure, but no alteration of nuclear morphological changes was observed at the earlier time point (6 h). As expected, non-treated cells showed normal nuclear morphology.

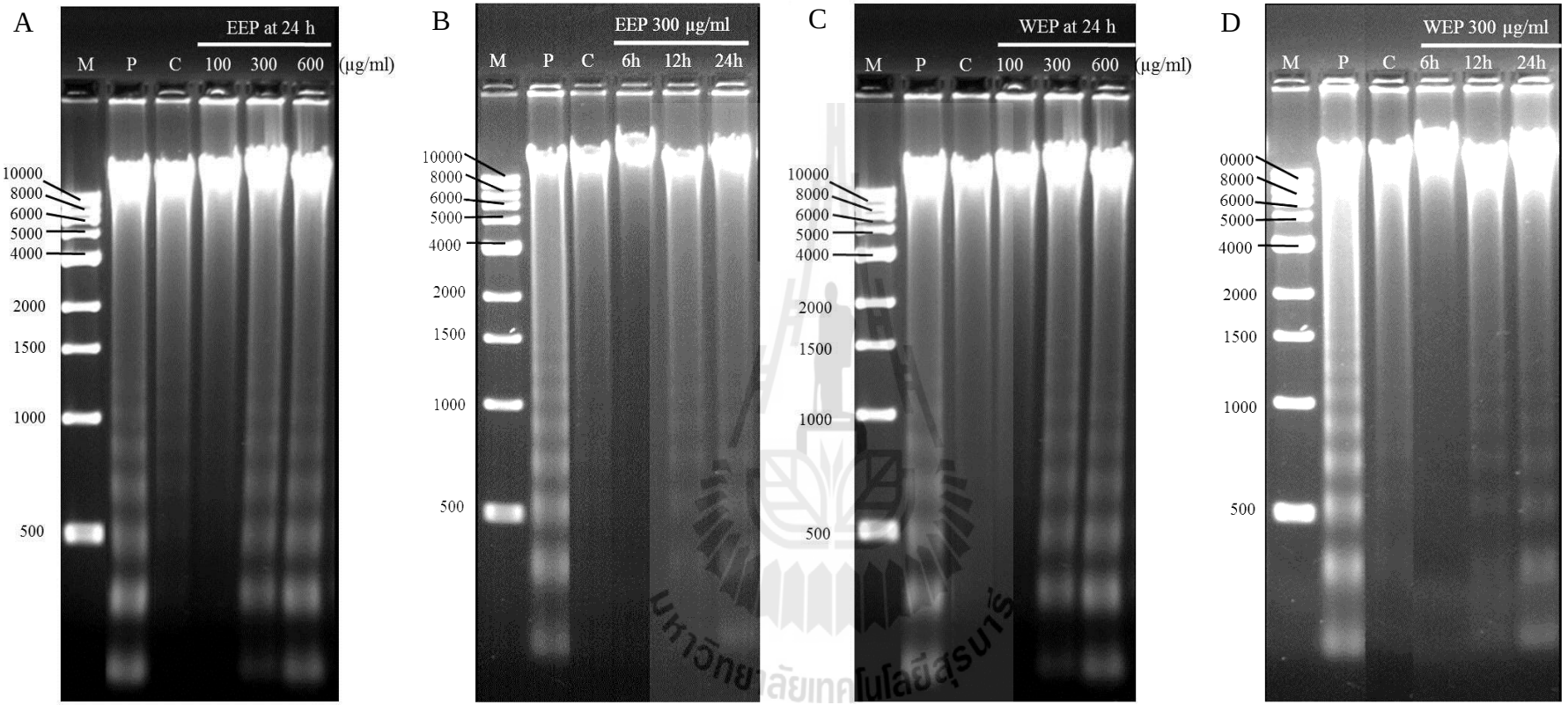

Figure 4.5 DNA fragmentation in Jurkat cells exposed to various concentrations of EEP for 24 h (A) and at 300 µg/ml for 6, 12 and 24 h (B). DNA fragmentation in Jurkat cells exposed to various concentrations of WEP for 24 h (C) and at 300 µg/ml for 6, 12 and 24 h (D). Lane M, 1 kb DNA marker; lane P, positive control (40 µg/ml of etoposide); lane C, control.

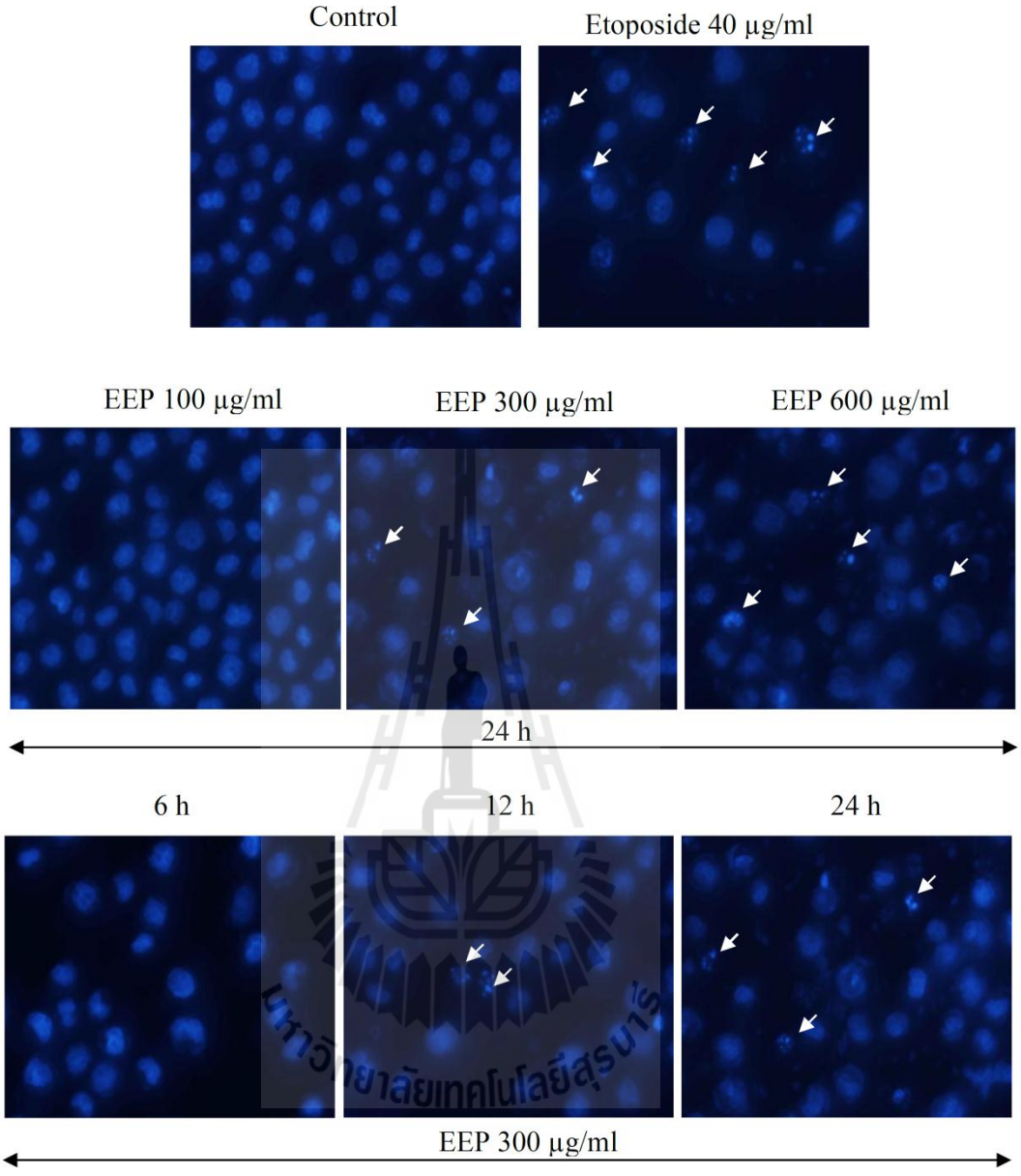

Figure 4.6 Nuclear morphological changes in Jurkat cells exposed to EEP with 100, 300, and 600 µg/ml for 24 h and exposed to EEP with 300 µg/ml for 6, 12, and 24 h. The condensed or fragmented nuclei were indicated by white arrows (Magnified × 400).

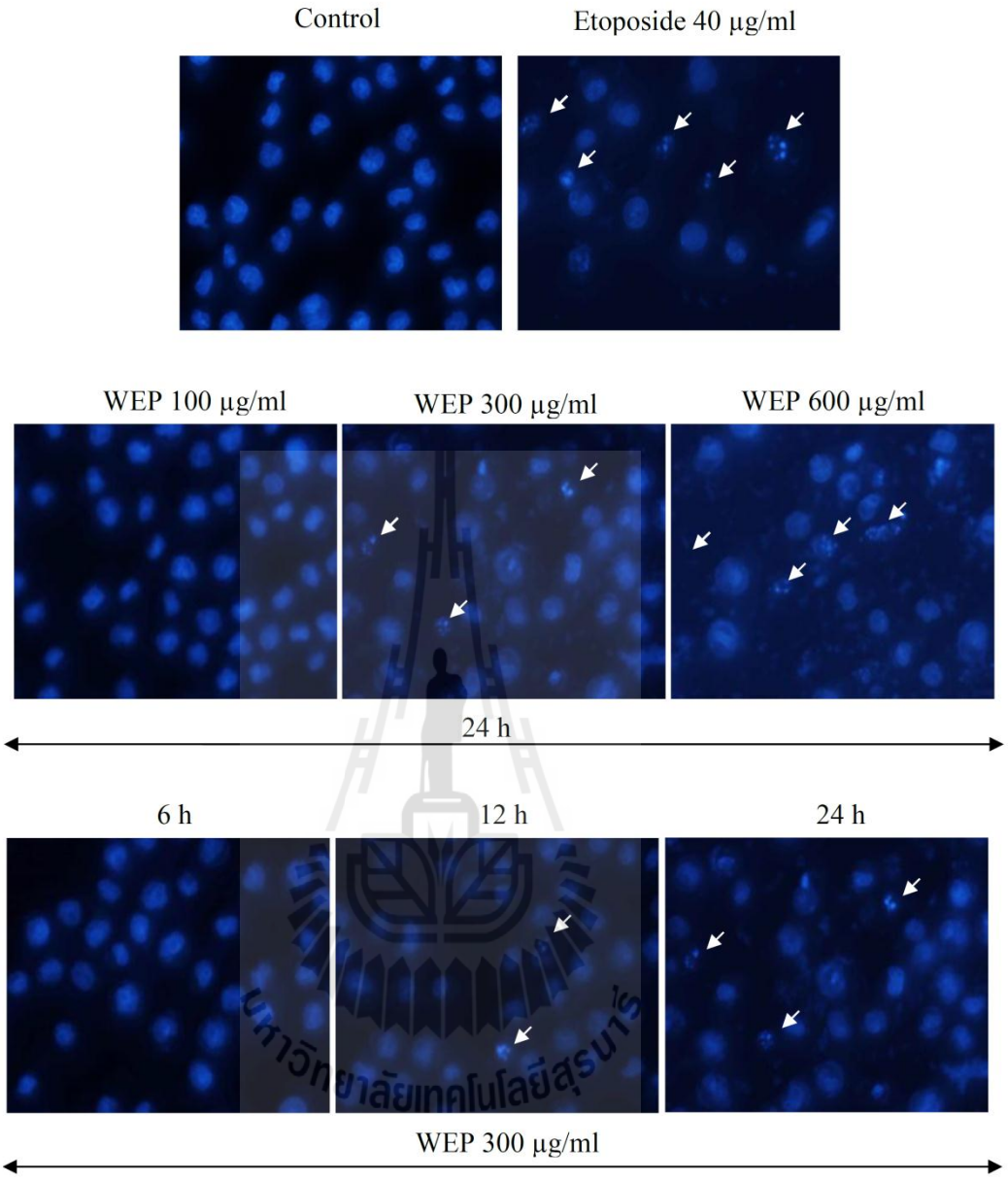

Figure 4.7 Nuclear morphological changes in Jurkat cells exposed to WEP at 100, 300, and 600 µg/ml for 24 h and exposed to 300 µg/ml of WEP for 6, 12, and 24 h. The condensed or fragmented nuclei were indicated as white arrows (Magnified × 400).

4.3.3 Annexin V-PI staining

The Annexin V-PI assay was further performed to confirm the apoptotic cell death induced by EEP or WEP. Annexin V, is a Ca^{2+}-dependent phospholipid-binding protein that has a high affinity for phosphatidylserine (PS) translocating from the inner to the outer leaflet of the plasma membrane, that is occurring in early stage of apoptotic process. PI is a red fluorescence dye, which binds to nucleic acids by intercalating. PI is membrane impermeant and generally excluded from viable cells. Therefore, the annexinV-PI staining was used to evaluate live cells (Annexin V^-/PI^-), early apoptotic cells (Annexin V^+/PI^-), late apoptotic cells (Annexin V^+/PI^+), and necrotic cells (Annexin V^-/PI^+). The percentages of EEP- or WEP-induced apoptotic cells were increased in both dose- and time-dependent manners (Figure 4.8 and 4.9). The percentages of early apoptotic cells increased from 6.90% in control cells to 7.93% and 14.24% after treatment with 300 and 600 µg/ml of EEP for 24 h, respectively. However, the percentages of early apoptotic cells at 100 µg/ml EEP were slightly decreased to 5.21% when compared to control. Likewise, in time course study, the percentages of early apoptotic cells increased from 6.96% in control cells to 8.44% and 11.42% after treatment with 300 µg/ml of EEP for 12 and 24 h, respectively. However, no alteration of percentages of apoptotic cells was observed by the same treatment of EEP at 6 h (6.93%). Furthermore, the percentages of early apoptotic cells increased from 8.62% in control cells to 9.29% and 30.29% in WEP-treated cells at 300 and 600 µg/ml for 24 h, respectively. In contrast, exposure of cells to 100 µg/ml of WEP for 24 h decreased the percentages of early apoptotic cells (0.21%) when compared to control. For time course study, the percentages of early apoptotic cells increased from 4.34% in control cells to 12.26%,

11.93%, and 12.57% after exposed to 300 µg/ml EEP for 6, 12, and 24 h, respectively. As expected, the induction of apoptosis by etoposide increased the percentages of early apoptotic cells to 16.66% when compared to controls (3.46%).

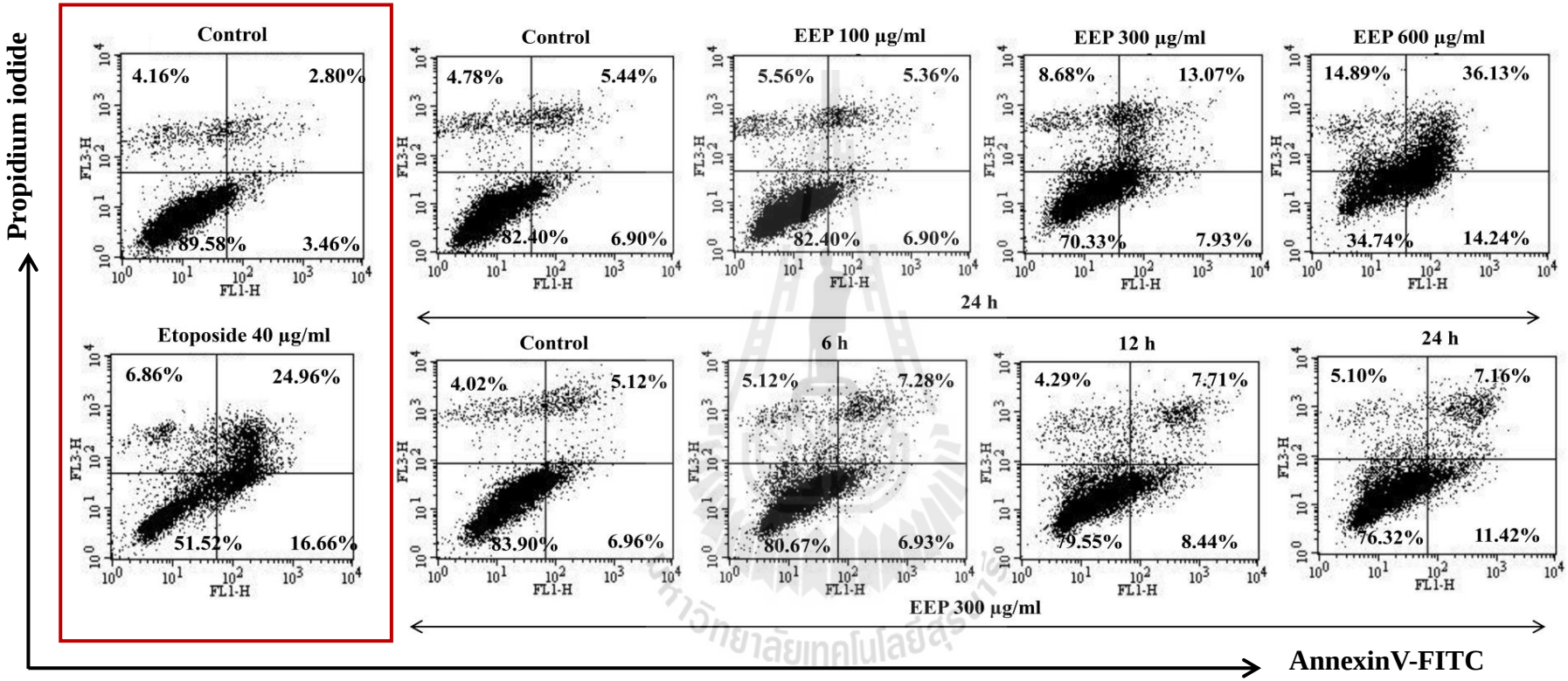

Figure 4.8 Flow cytometric analysis of apoptosis in Jurkat cells exposed to various concentrations of EEP for 24 h and kinetics of apoptosis induction in Jurkat cells exposed to 300 µg/ml of EEP. The apoptosis of Jurkat cells was detected by flow cytometry using AnnexinV-PI staining method. Data are a representative of two independent experiments.

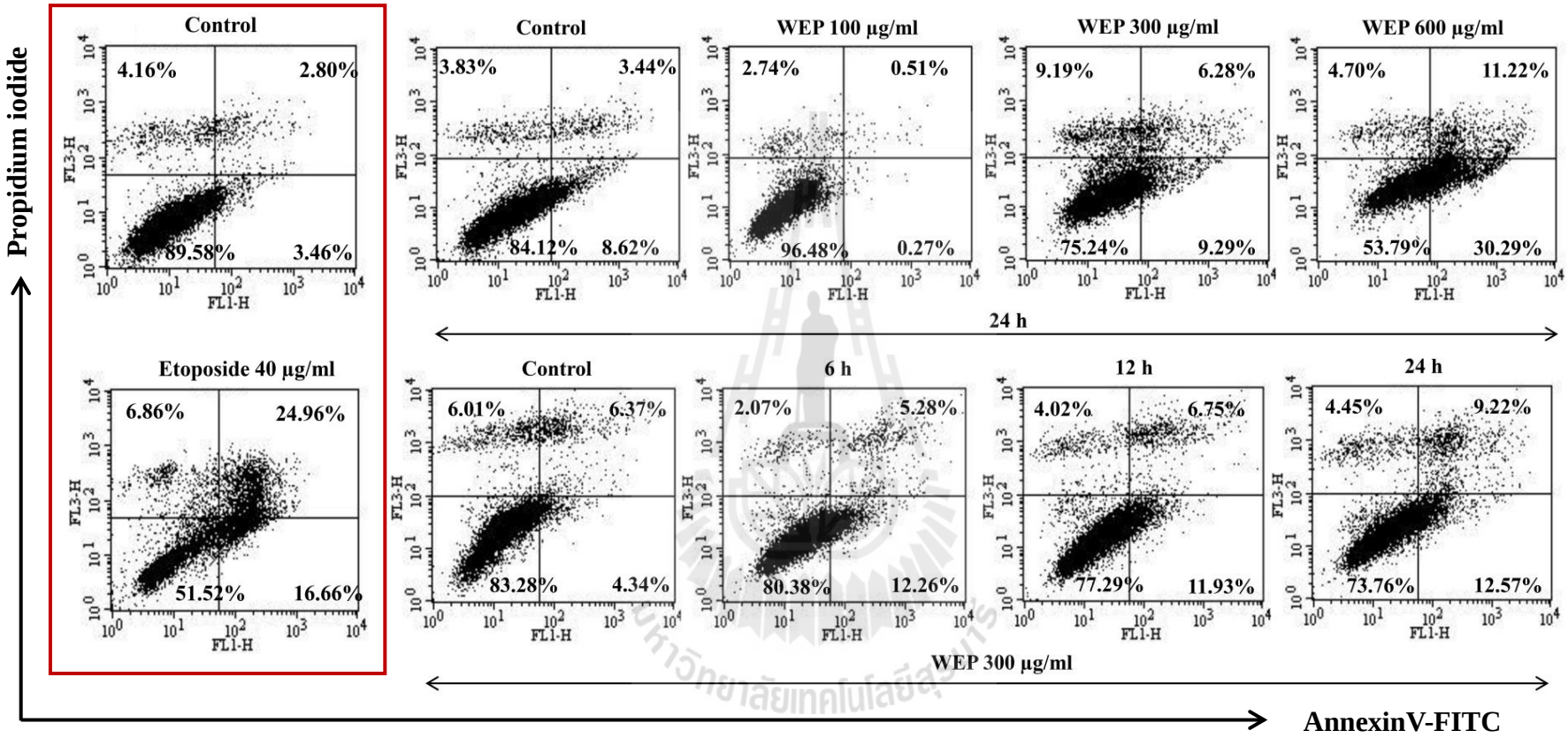

Figure 4.9 Flow cytometric analysis of apoptosis in Jurkat cells exposed to various concentrations of WEP for 24 h and kinetics of apoptosis induction in Jurkat cells exposed to 300 µg/ml of WEP. The apoptosis of Jurkat cells was detected by flow cytometry using AnnexinV-PI staining method. Data are a representative of two independent experiments.

4.3.4 Cytochrome C release

Cytochrome C is a protein that located in the space between the inner and outer mitochondrial membranes. During apoptotic process, the mitochondrial membrane is disrupted causing the translocation of cytochrome C from mitochondria into cytosol. The levels of cytochrome c in mitochondria can be detected directly by probing with anti-cytochrome c-FITC and analyzed by flow cytometry. Therefore, the cells undergoing apoptosis demonstrated the reduction of FITC intensity in mitochondria, implicating the cytochrome C release. As shown in Figure 4.10 and 4.11, Jurkat cells after exposed to EEP and WEP induced the release of cytochrome C from mitochondria in both dose- and time-dependent manners. As suggested in Figure 4.10(A), exposure to EEP for 24 h significantly increased ($p < 0.05$) the mitochondrial cytochrome C release from the percentage of 7.21±1.42% in control cells to 71.06±3.14% and 81.87±6.03% at the treated groups of 300 and 600 μg/ml, respectively. Similarly, Jurkat cells exposed to 300 μg/ml of EEP for 12 and 24 h also significantly increased ($p < 0.05$) the cytochrome C release by 49.32±3.64% and 71.06±3.14%, respectively, when compared to controls (Figure 4.10(B)). The levels of cytochrome C release were significantly higher ($p < 0.05$) than those that induced by etoposide, the positive control group. Likewise, WEP treatment, also exhibited a significant increase ($p < 0.05$) in the percentages of cytochrome C release from 8.69±1.47% in untreated control cells to 52.89±4.49% and 80.56±10.09% in 300 and 600 μg/ml treated group, at 24 h, respectively (Figure 4.11(A)), and to 52.01±1.46% and 52.89±4.49% in 300 μg/ml WEP-treated group at 12 and 24 h (Figure 4.11(B). In addition, 600 μg/ml WEP significantly induced the cytochrome C release higher ($p < 0.05$) than the etoposide-treated group.

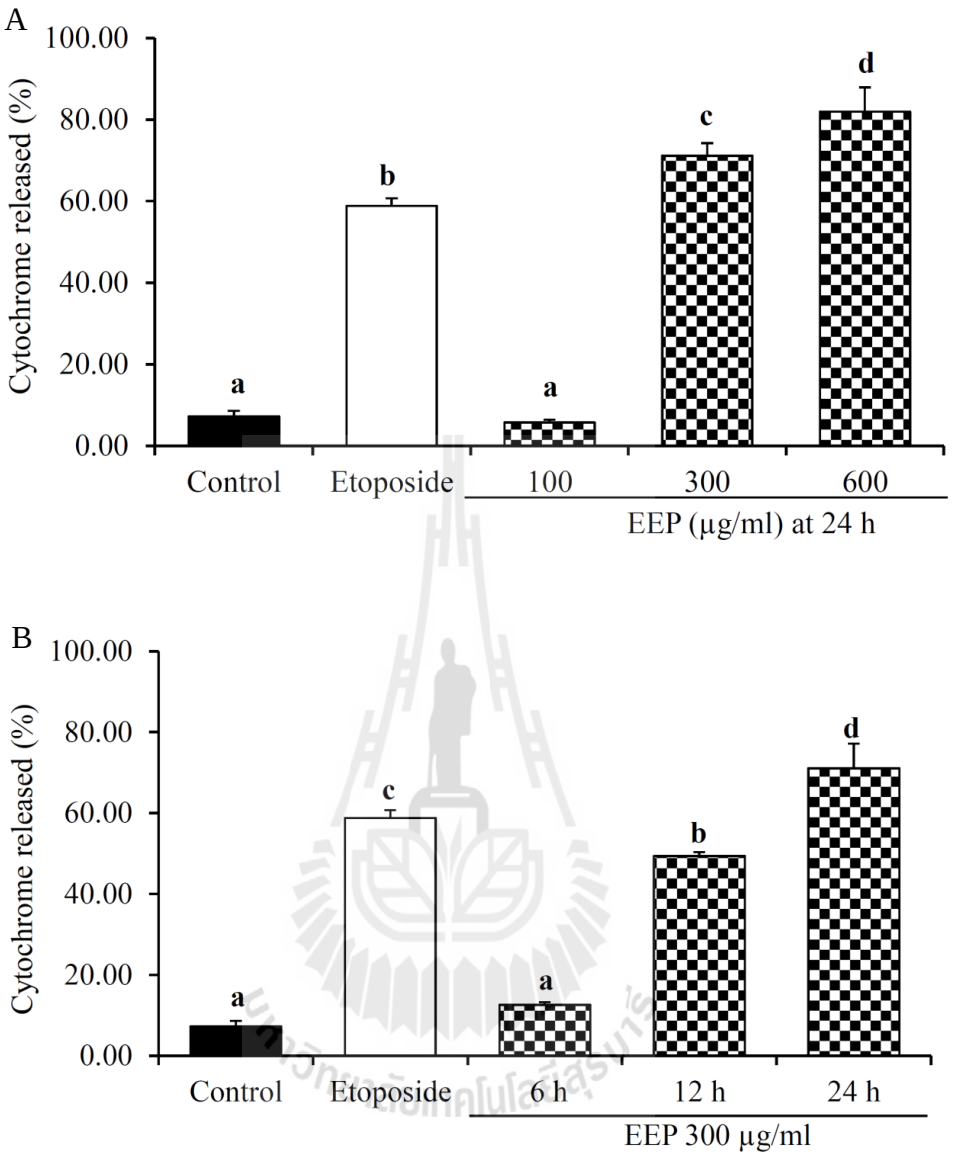

Figure 4.10 Percentages of cytochrome C release of Jurkat cells exposed to various concentrations of EEP for 24 h (A) and kinetics of apoptosis induction in Jurkat cells exposed to 300 µg/ml of EEP (B). Values are expressed as means ± SD (n = 3) and are representative of three independent experiments with similar results. Bars marked with different letters are significantly different at $p < 0.05$ as determined by one-way ANOVA.

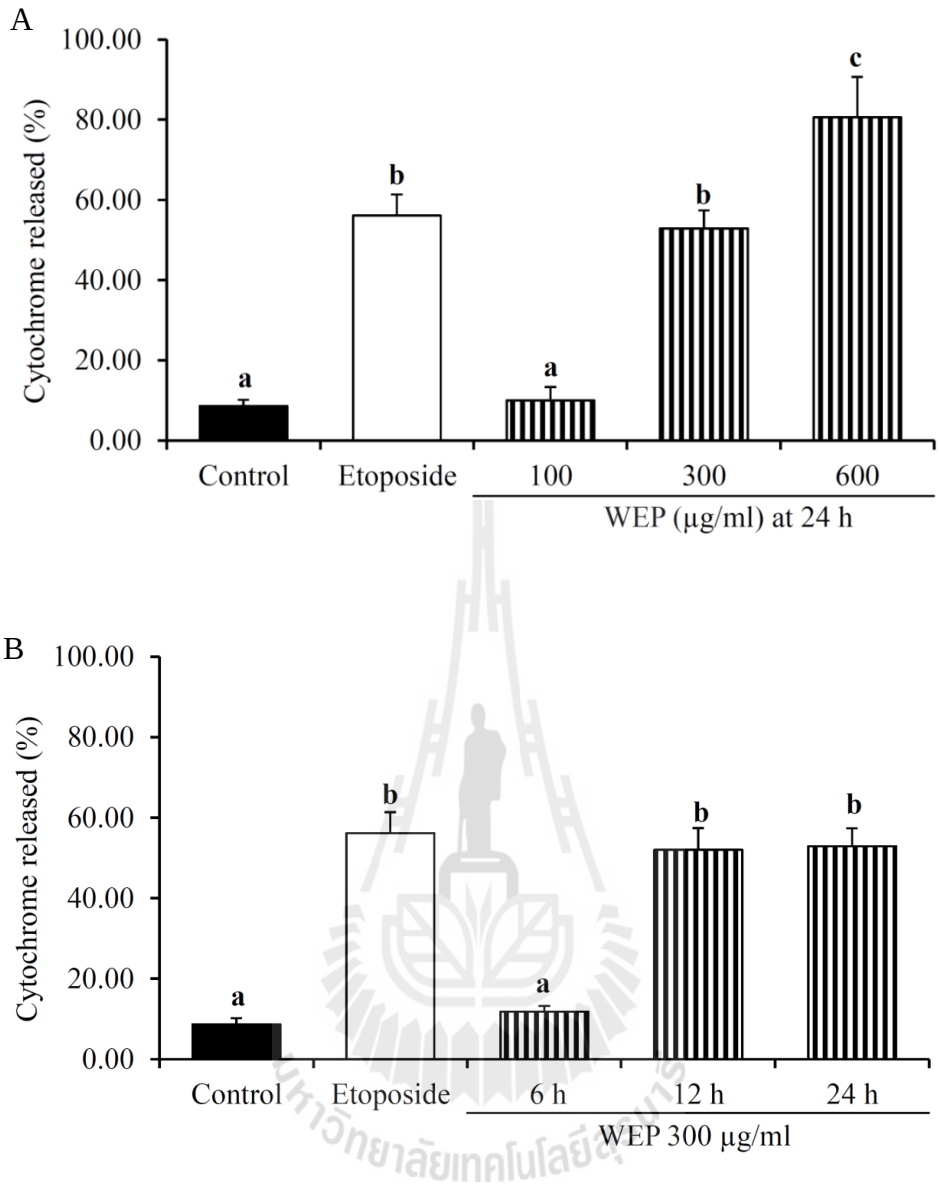

Figure 4.11 Percentages of cytochrome C release of Jurkat cells exposed to various concentrations of WEP for 24 h (A) and kinetics of apoptosis induction in Jurkat cells exposed to 300 µg/ml of WEP (B). Values are expressed as means ± SD (n = 3) and are representative of three independent experiments with similar results. Bars marked with different letters are significantly different at $p < 0.05$ as determined by one-way ANOVA.

4.3.5 FTIR microspectroscopy

FTIR microspectroscopy was used to identify bimolecular changes of apoptotic cell death in Jurkat cells induced by EEP or WEP exposure. The FTIR absorption spectrum of sample at the wavelengths between 3000-800 cm^{-1} were related to specific macromolecule as follows:

(1) The lipid region (3000-2800 cm^{-1}) is indicated to the symmetric and asymmetric stretching of the CH_2 and CH_3 groups of lipid. The absorbance centered at 1743 cm^{-1} is reflected to C=O stretching of lipid esters (Cao et al., 2013 and Lipiec, 2013).

(2) The amide I region (1700-1600 cm^{-1}) is related to protein secondary structure, which is refer to the C=O stretch vibrations of peptide linkages. The protein secondary structural elements in the amide I region including β-turn (centered at 1685 cm^{-1}), α-helix (centered at 1654 cm^{-1}), and β-pleated sheet (centered at 1635 cm^{-1}) (Kong and Yu, 2007, Cao et al., 2013, and Lipiec, 2013).

(3) The nucleic acid and carbohydrate regions or "fingerprint region" (1300-850 cm^{-1}) is referred to the vibration of the superimposed contributions of nucleic acid (DNA and RNA), phosphates and carbohydrates. The absorption band centered at 1238 cm^{-1} and 1080 cm^{-1} are assigned to P=O symmetrical stretching of PO_2 phosphodiester groups from phosphorylated molecules, and glycogen. The absorbance band centered at 1153 cm^{-1} and 1050-1022 cm^{-1} are refered to C–O vibrations from glycogen and other carbohydrates. The absorbance band centered at 995 cm^{-1} is related to C–O stretch from RNA ribose chain and other carbohydrates. The C–C vibration of nucleic acids is presented at 950 cm^{-1} (Cao et al., 2013 and Lipiec, 2013).

4.3.5.1 FTIR analysis of apoptosis induced by EEP in Jurkat cell

The average of FTIR original spectra of untreated control and EEP-treated Jurkat cells at 100, 300, and 600 µg/ml for 24 h at the wavelength 3000-2800 and 1300-800 cm^{-1} are shown in Figure 4.12. The absorbance spectra at wavelength 1800-1300 cm^{-1} showed the poor quality of FTIR spectra (data not shown). Therefore, it was excluded from the spectral data because the data of this spectra range could not be analyzed and interpreted.

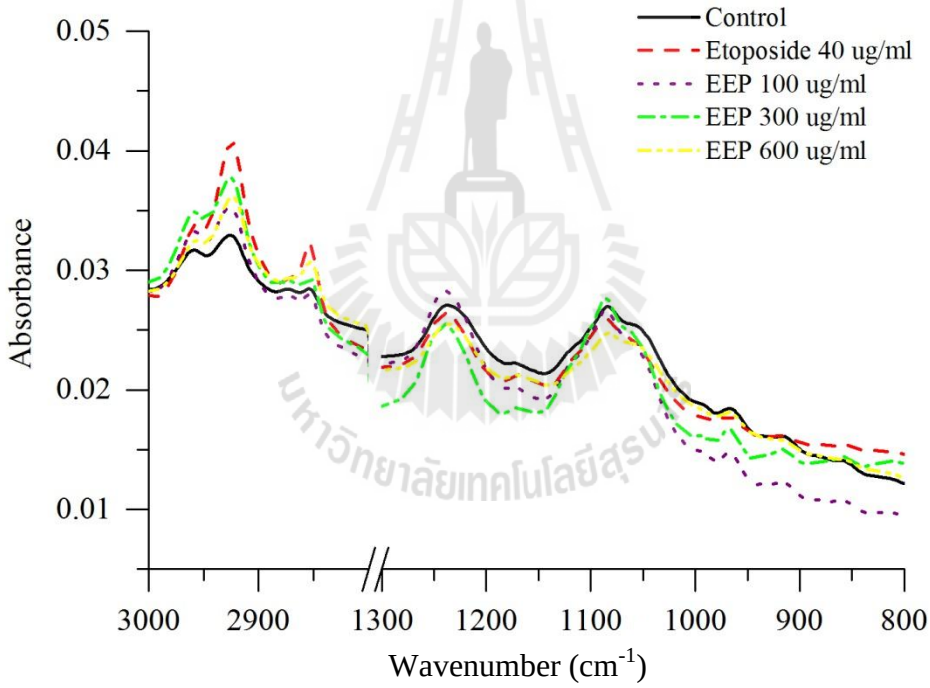

Figure 4.12 Average original FTIR spectra (n=426) obtained from Jurkat control cells (n=50) and Jurkat cells exposed to EEP at 100 µg/ml (n=86), 300 µg/ml (n=45), 600 µg/ml (n=161), or 40 µg/ml of etoposide positive control (n=84) for 24 h.

However, the original spectra between control and EEP-treated Jurkat cells were difficult to be differentiated. Therefore, the second derivative was accomplished for spectral analysis and a sharp absorption individual peak of control and treated cells was clearly identified. Figure 4.13(A) and 4.13(B) illustrated the second derivative data of the respective lipid region (3000-2800 cm^{-1}) and nucleic acid region (1300-800 cm^{-1}) of untreated control and EEP-treated Jurkat cells at 100, 300, and 600 µg/ml for 24 h. The lipid absorbance in both asymmetric stretching of CH_2 (at 2922 cm^{-1}) and symmetric stretching of CH_2 (at 2852 cm^{-1}) of EEP-treated Jurkat cells at 100, 300, and 600 µg/ml for 24 h showed difference from untreated control. They exhibited a dramatically increase of lipid absorbance in a dose-dependent manner. Especially, the highest lipid absorbance peak was shown in the positive control group (40 µg/ml etoposide) at 24 h. Moreover, The four important IR bands (at 1240 cm^{-1}, 1084 cm^{-1}, 993 cm^{-1} and 966 cm^{-1}) due to various structure groups in DNA and RNA illustrated a decrease of nucleic absorbance in EEP-treated Jurkat cells when compared with untreated cells, whereas the positive control group showed the lowest absorbance peak to assigned every important IR bands of nucleic acid regions. The band at 1240 cm^{-1} and 1084 cm^{-1} are related to P=O symmetrical stretching of PO_2 phosphodiester groups from phosphorylated molecules and glycogen. The band at 993 cm^{-1} is marked to C–O stretch from RNA ribose chain and other carbohydrates. The C–C vibration of nucleic acids is presented at 950 cm^{-1}.

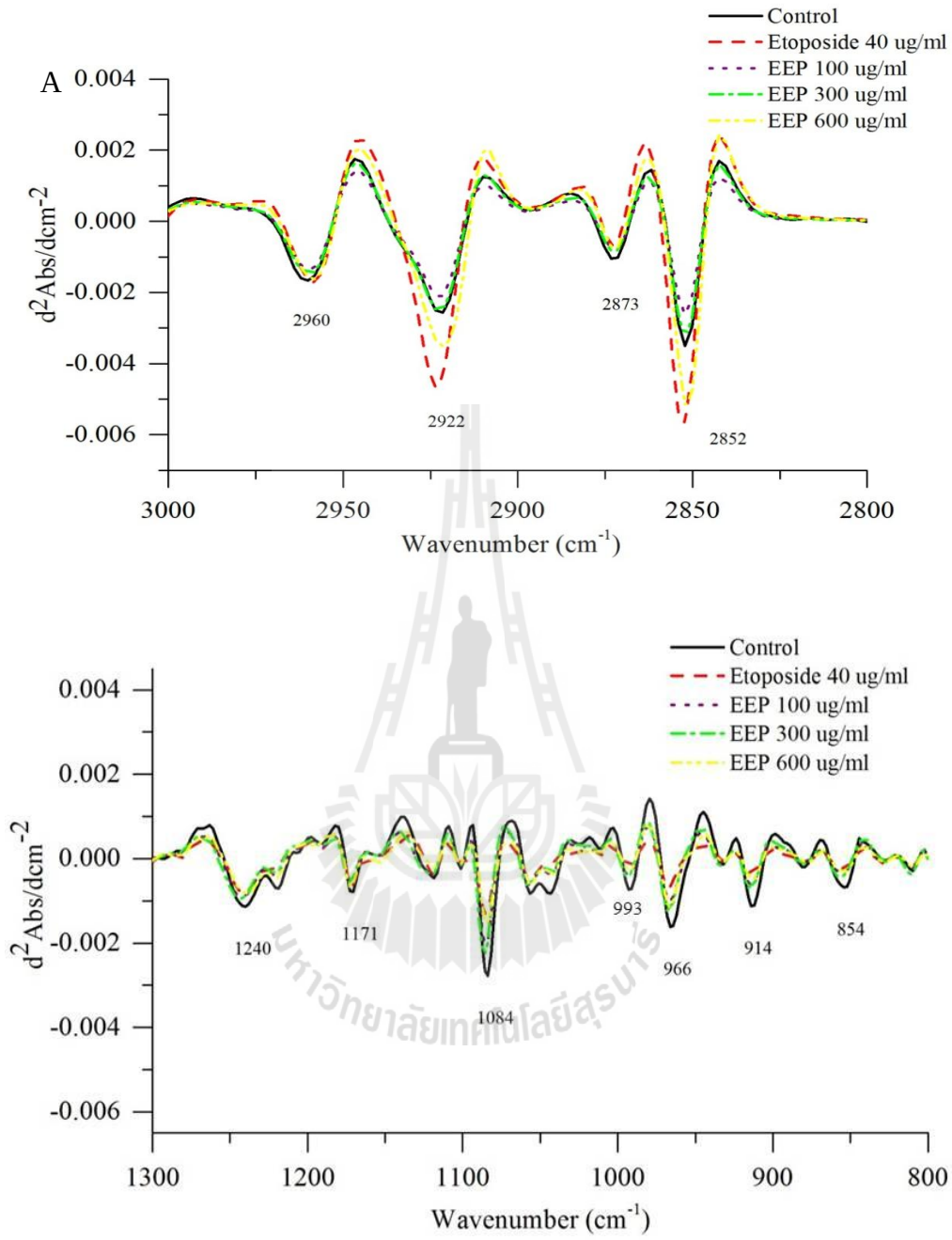

Figure 4.13 Average 2nd derivative spectra of Jurkat control cells and Jurkat exposed to EEP at 100, 300, 600 µg/ml , and 40 µg/ml of etoposide positive control at 24 h after baseline and normalized with extended multiplicative signal correction (EMSC).The data were represented in two regions: (A) lipid regions (3000-2800 cm^{-1}) and (B) nucleic acid regions (1300-800 cm^{-1}).

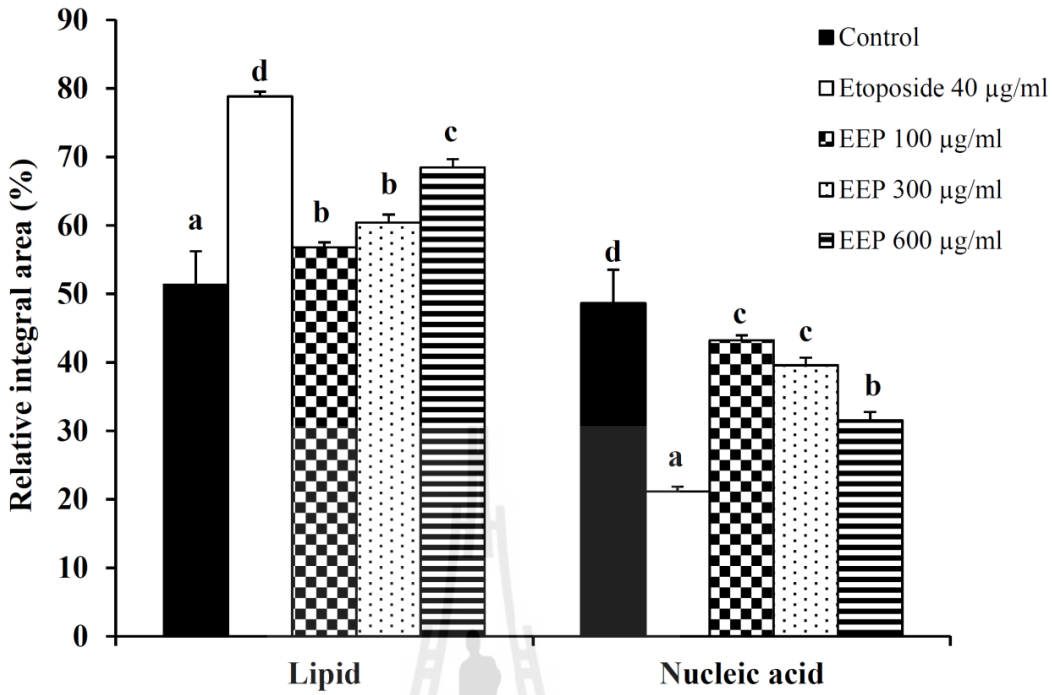

Figure 4.14 The percentages of integrated areas for remarkable lipid and nucleic acid regions of Jurkat control cells and Jurkat exposed to EEP at 100, 300, 600 µg/ml, and 40 µg/ml of etoposide positive control at 24 h. Data were calculated from normalized second derivative spectra. The differences between means of the percentages of integrated areas were significantly difference among five groups by one-way ANOVA ($p < 0.05$). Data are represented as means ± SD. Error bars indicate standard errors of means.

Figure 4.14 illustrated the average of integrated areas of lipid regions (2971-2950 cm^{-1}, 2936-2913 cm^{-1}, 2878-2867 cm^{-1}, 2860-2845 cm^{-1}, 1748-1733 cm^{-1}) and nucleic acid regions (1060-1033 cm^{-1}, 996-988 cm^{-1}, 973-955 cm^{-1}, 919-950 cm^{-1},and 1864-847 cm^{-1}) of untreated and EEP-treated Jurkat cells. The percentages of integrated areas of lipid and nucleic acid of untreated control cells (51.35±4.88%) showed significantly different ($p > 0.05$) from cells treated with EEP

at 100, 300, and 600 µg/ml for 24 h. The percentages of integrated areas of lipid in Jurkat cells after exposure to EEP at 100, 300, and 600 µg/ml for 24 h were significantly increased in a dose-dependent manner (56.79±0.74%, 60.43±1.13%, and 68.46±1.19%, respectively). In contrast, the same exposure levels of EEP exhibited a significant in a dose-dependent effect on decreasing percentages of integrated areas of nucleic acid (43.21±0.74%, 39.57±1.13%, and 31.54±1.19% when treated with EEP at 100, 300, and 600 µg/ml for 24 h, respectively). Notably, the Jurkat cells when treated with etoposide 40 µg/ml (positive control) at 24 h demonstrated integrated areas of lipid and nucleic acid as 78.83±0.69% and 21.17±0.69%, respectively.

The second derivative spectra of untreated and EEP-treated Jurkat cells were further analyzed by principle component analysis (PCA). The PCA two dimensional score plot was used to examined significant spectral differences of untreated and EEP-treated in Jurkat cells (Figure 4.15(A)). The most shape changes control and EEP-treated cells were contribute to clustering in the PCA loading plot (Figure 4.15(B)). Therefore, the PCA could identify the most significant spectral changes between untreated and EEP-treated Jurkat cells.

The PCA score plots demonstrate that the clusters of untreated control cells were separated from the clusters of 600 µg/ml EEP-treated cells and 40 µg/ml etoposide treated positive control at 24 h along PC1 (55%). The spectra of 100 and 300 µg/ml EEP-treated cells were distinguished from untreated control cells at 24 h along PC2 by 16% (Figure 4.15(A)).

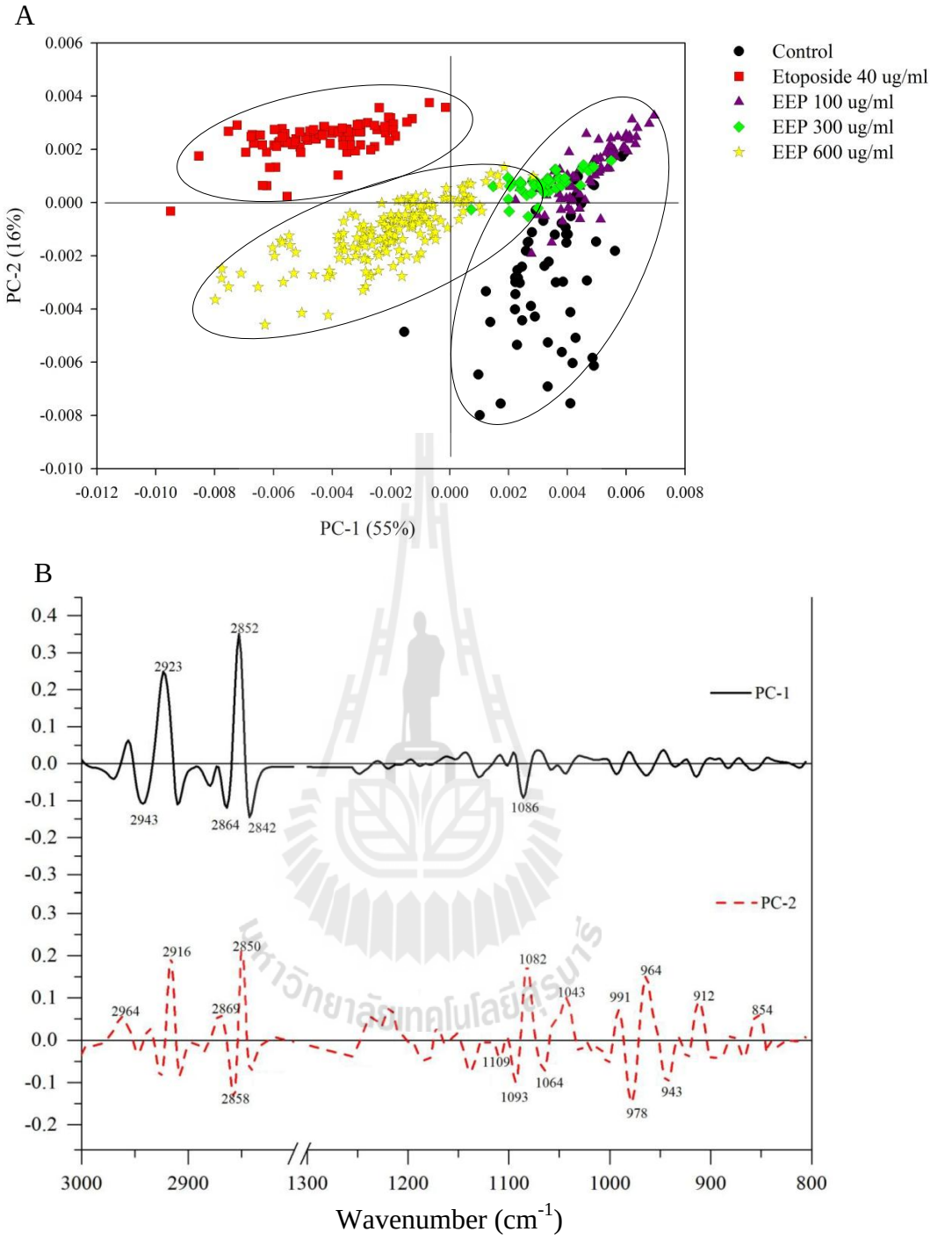

Figure 4.15 PCA analysis of FTIR spectral range 3000-800 cm^{-1} giving PCA score plot (A) and PCA loading plot (B). PCA score plots showed distinct clustering between Jurkat control cells and Jurkat exposed to EEP at 100, 300, 600 µg/ml, and 40 µg/ml of etoposide positive control at 24 h. PCA loading plots identify biomarker difference over spectral range of samples.

The spectral changes in PCA loading plots were occurred apoptotic cell death in untreated and EEP-treated Jurkat cells at 24 h in Figure 4.15(B). The C-H stretching region (centered at 2923 cm^{-1} and 2852 cm^{-1}) was strongly positive for PC1 loading, which separated the positive score plot of the spectra of untreated control cells and EEP-treated cells at 100 and 300 µg/ml from the negative score plot of the spectra of Jurkat cells treated with 600 µg/ml EEP and 40 µg/ml etoposide. Moreover, the negative PC1 loadings at 1086 cm^{-1} indicated that the nucleic acid (phosphodiester groups) could be used to discriminate untreated control cells and EEP-treated cells at 100 and 300 µg/ml from Jurkat cells exposed to 600 µg/ml EEP or 40 µg/ml etoposide. Likewise, the discrimination along PC2 could be explained by the positive loading of PC2 in the C-H stretching region (centered at 2916 cm^{-1} and 2850 cm^{-1}) and the nucleic acid region (centered at 1082 cm^{-1}, 991 cm^{-1} 964 cm^{-1}, and 912 cm^{-1}), which separated the negative score plot of the spectra of untreated control cells from the positive score plot of the spectra of Jurkat cells treated with 100 and 300 µg/ml EEP at 24 h.

4.3.5.2 FTIR analysis of apoptosis induced by WEP in Jurkat cell

The average of original FTIR spectra of Jurkat control cells and WEP-treated Jurkat cells at 24 h at the wavelength 3000-2800 and 1800-800 cm^{-1} are shown in Figure 4.16. The second derivative of spectral data of untreated control cells and WEP-treated Jurkat cells at 100, 300, and 600 µg/ml for 24 h in the lipid region (3000-2800 cm^{-1}) and protein and nucleic acid region (1800-800 cm^{-1}) was shown in Figure 4.17(A) and 4.17(B), respectively.

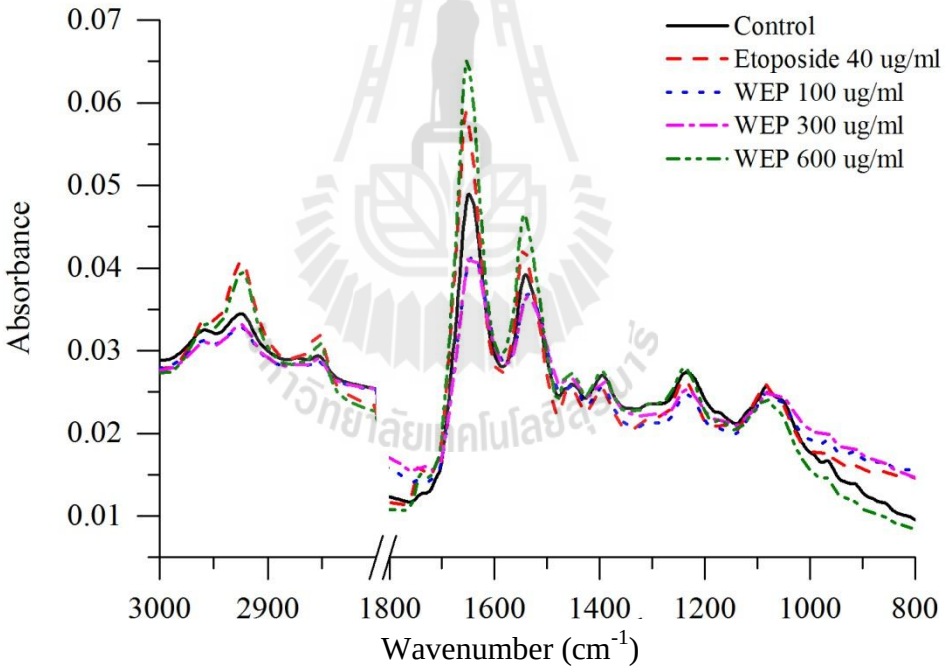

Figure 4.16 Average original FTIR spectra (n=424) obtained from Jurkat control cells (n=90) and exposed cells to WEP at 100 µg/ml (n=56), 300 µg/ml (n=58), 600 µg/ml (n=136), and 40 µg/ml of etoposide positive control (n=84) for 24 h.

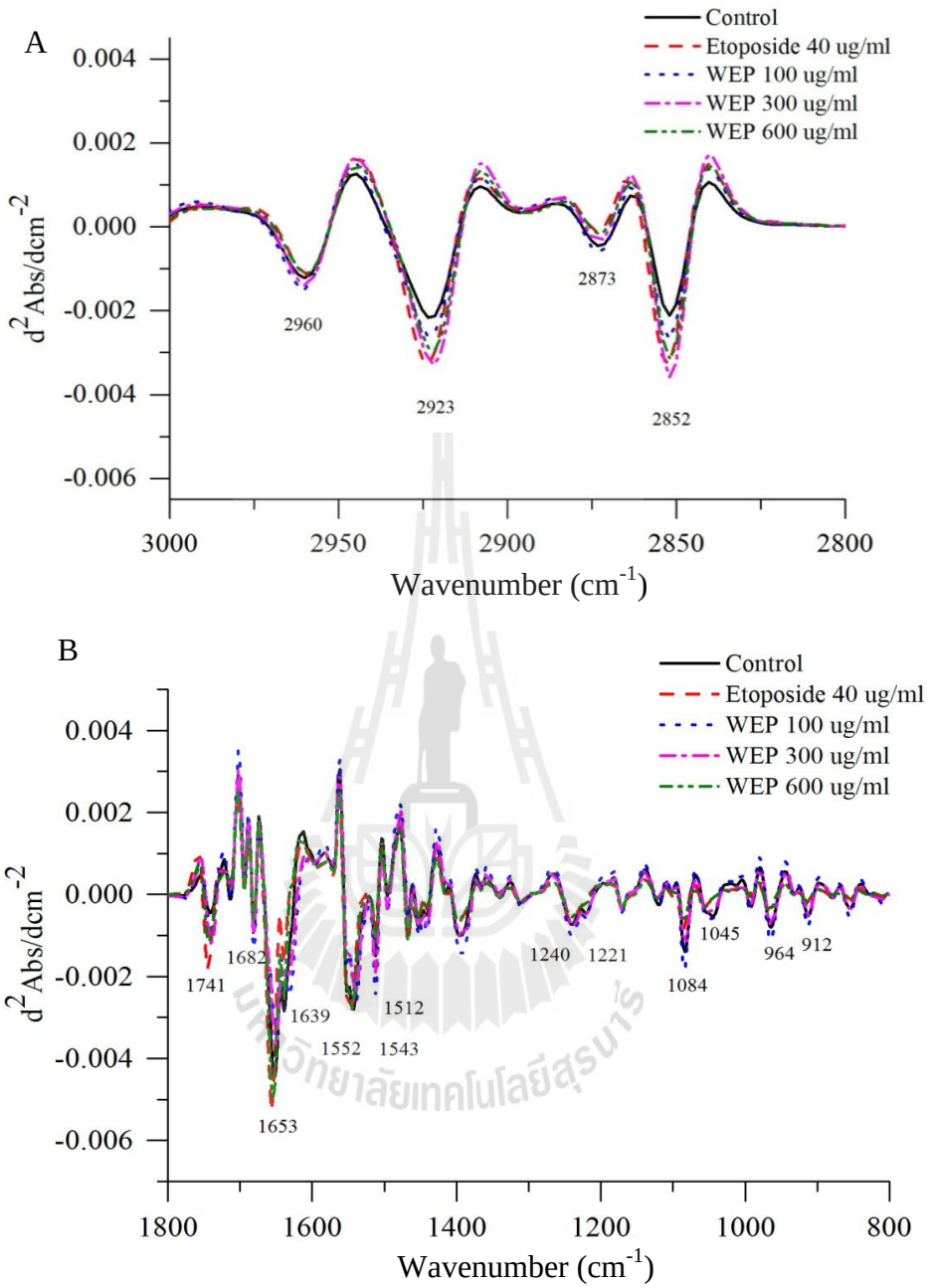

Figure 4.17 Average 2nd derivative spectra of Jurkat control cells and exposed cells to WEP at 100, 300, 600 µg/ml, or 40 µg/ml of etoposide positive control at 24 h. The baseline of data were normalized with extended multiplicative signal correction (EMSC) and are represented in two regions: (A) lipid regions (3000-2800 cm^{-1}) and (B) amide I protein and nucleic acid regions (1800-800 cm^{-1}).

The lipid absorbance in asymmetric stretching of CH_2 (at 2922 cm^{-1}), symmetric stretching of CH_2 (at 2852 cm^{-1}), and C=O stretching of lipid esters (at 1741 cm^{-1}) showed increases in the intensity when Jurkat cells were treated with 40 µg/ml etoposide or WEP at 100, 300, 600 µg/ml for 24 h. The amide I region between 1700-1590 cm^{-1} represented three secondary protein structure that including β-turn, α-helix, and β-pleated sheet components. Exposure of Jurkat cells to WEP at 100 and 300 µg/ml showed an increasing in the β-turn band (centered at 1682 cm^{-1}) from untreated control cells. The most dramatic increase in intensity at 1682 cm^{-1} was observed in Jurkat cells exposed to WEP at 100 µg/ml for 24 h. The α-helix band (centered at 1653 cm^{-1}) in the untreated control cells had higher intensity than the Jurkat cells exposed to WEP at 100 and 300 µg/ml, but the value gradually decreased when the cells were treated with 600 µg/ml WEP and 40 µg/ml etoposide. In addition, the β-pleated sheet band (centered at 1639 cm^{-1}) in Jurkat cells exposed to various concentrations of WEP or 40 µg/ml of etoposide was clearly decreased compared to the untreated Jurkat cells.

Furthermore, the absorption band of WEP-treated Jurkat cells were observed at 1240 cm^{-1} and 1084 cm^{-1} (which was assigned to asymmetrical and symmetrical stretching of PO_2 phosphodiester groups from phosphorylated molecules, respectively), at 1045 cm^{-1} (which was assigned to C–O vibrations from glycogen and other carbohydrates), and at 964 cm^{-1} (which was assigned to C–C vibrations from nucleic acids). Four second derivative spectra of nucleic acid regions in Jurkat cells exposed to WEP at 600 µg/ml or 40 µg/ml of etoposide for 24 h illustrated a decrease of nucleic absorbance when compared with untreated cells. In contrast, Jurkat cells treated with WEP at 100 µg/ml for 24 h showed an increase of nucleic acid

absorbance. However, the spectra of WEP-treated Jurkat cells at 300 µg/ml for 24 h only showed slightly different from untreated control cells.

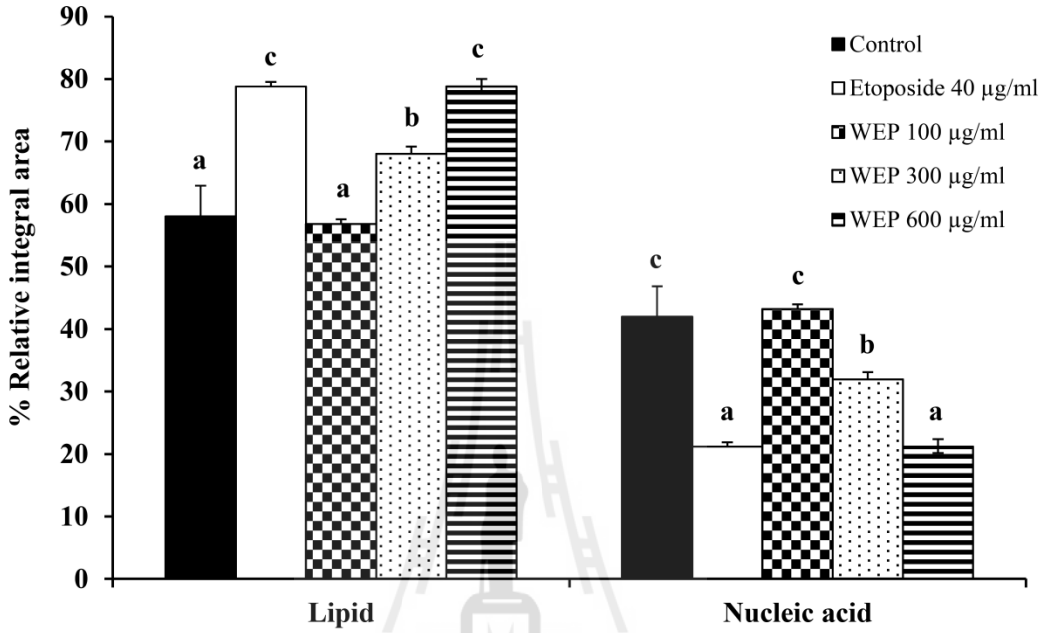

Figure 4.18 The percentages of integrated areas for remarkable lipid and nucleic acid regions of Jurkat control cells and Jurkat exposed to WEP at 100, 300, 600 µg/ml, or 40 µg/ml of etoposide positive control at 24 h. Data were obtained from normalized second derivative spectra. The differences between means of the percentages of integrated areas were significantly different among five groups by one-way ANOVA ($p < 0.05$). Data are represented as means ± SD. Error bars indicate standard errors of means.

Figure 4.18 illustrated the average of integrated areas of lipid regions (2971-2950 cm^{-1}, 2936-2913 cm^{-1}, 2878-2867 cm^{-1}, 2860-2845 cm^{-1}, 1748-1733 cm^{-1}) and nucleic acid regions (1060-1033 cm^{-1}, 996-988 cm^{-1}, 973-955 cm^{-1}, 919-950 cm^{-1},and 1864-847 cm-1) of untreated and WEP-treated Jurkat cells. The percentages of integrated areas of lipid in Jurkat cells showed dramatically increase in dose-dependent manners with 56.81±1.63%, 68.06±1.35%, and 78.82±2.27% after exposure with WEP at 100, 300, and 600 µg/ml for 24 h, respectively. In contrast, the percentages of integrated areas of nucleic acid in Jurkat cells showed dramatically decrease in dose-dependent manners with 43.19±1.63%, 31.94±1.35%, and 21.18±2.27% after exposure with WEP at 100, 300, and 600 µg/ml for 24 h, respectively. Nevertheless, the Jurkat cells after exposure with WEP at 300 and 600 µg/ml only exhibited significant difference ($p < 0.05$) in integrated areas of lipid and nucleic acid from untreated control cells. Furthermore, the integrated areas of lipid and nucleic acid of Jurkat cells treated with 40 µg/ml of etoposide for 24 h were 78.83±0.69% and 21.18±2.27%, respectively.

The quantitative contribution of the protein secondary structure (amide I) of untreated and treated Jurkat cells was obtained by band curve-fitting of the original spectra of amide I (1700-1590 cm^{-1}). The amide I band shape of untreated and treated Jurkat cells was divided into seven components (figure 4.19); the 1st, 2nd, and 3rd components with a respective peak range of between 1608-1615 cm^{-1}, 1623-1628 cm^{-1}, and 1635-1639 cm^{-1} were assigned to the β-pleated sheet; the 4th and 5th components with a respective peak range of between 1649-1654 cm^{-1} and 1664-1669 cm^{-1} were indicated to the α-helix structure; although, the 6th and 7th peak position were associated to β-turn and antiparallel β-sheet with a respective peak

range of between 1677-1682 cm^{-1} and 1689-1693 cm^{-1}, respectively. The corresponding parameters, band position, percentage of integral area, assignment of each spectral component are shown in Table 4.2. The results exhibited that the percentages of integrated areas of β-pleated sheet structure (1635-1639 cm^{-1}) of WEP-treated cells at 100 µg/ml (20.97±0.89%), 300 µg/ml (22.91±2.06%), and 600 µg/ml (18.52±1.92%) showed higher intensity than untreated control cells (18.40±0.44%). Although, the percentages of integrated areas of β-pleated sheet structure of 300 µg/ml WEP-treated only exhibited significantly increased compared to control. In contrast, the percentages of integrated areas of α-helix structure (1649-1654 cm^{-1}) of WEP-treated cells at 100 µg/ml (26.58±4.96%) and 300 µg/ml (26.20±0.80%) was decreased slightly but not significant compared to untreated control cells (32.74±1.18%). However, the percentage of integrated area of spectra from other position in WEP-treated cells was not significantly different compared with untreated control cells.

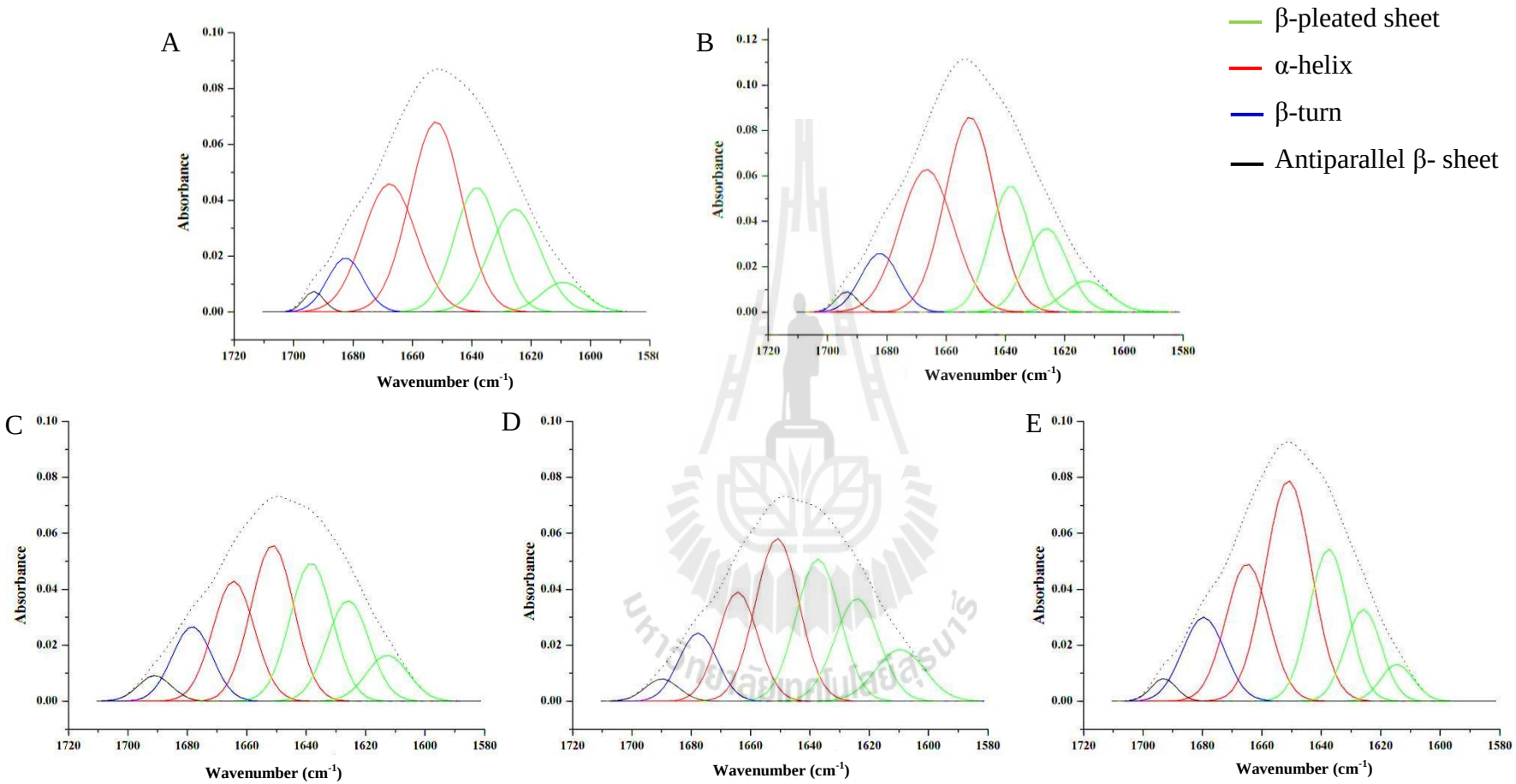

Figure 4.19 Absorbance of amide I band contour with best-fit 50% Loentzian/Gaussian individual component bands for (A) Jurkat control cells (RMS error is 0.000339), (B) Jurkat-treated with 40 µg/ml etoposide (RMS error is 0.000443), (C) WEP at 100 µg/ml (RMS error is 0.000422), (D) WEP at 300 µg/ml (RMS error is 0.000483), and (E)WEP at 600 µg/ml (RMS error is 0.002013).

Table 4.3 The positions and integral areas of Jurkat cells unexpended on exposed to 100, 300, or 600 µg/ml WEP or 40 µg/ml etoposide positive control for 24 h.

Assignment	β-pleated sheet (1608-1615 cm^{-1})		β-pleated sheet (1623-1628 cm^{-1})		β-pleated sheet (1635-1639 cm^{-1})	
	Position (cm^{-1})	Integral area (%)	Position (cm^{-1})	Integral area (%)	Position (cm^{-1})	Integral area (%)
Control	1608-1611	4.03±1.24	1624-1625	14.84±2.23	1636-1638	18.40±0.44^{ab}
Etoposide 40 µg/ml	1612-1613	3.90±1.02	1626	13.13±1.18	1638	16.68±1.19^{a}
WEP 100 µg/ml	1610-1613	6.24±1.96	1623-1625	14.83±2.70	1635-1638	20.97±0.89^{bc}
WEP 300 µg/ml	1609-1614	8.90±3.18	1624-1625	14.30±1.72	1637	22.91±2.06^{c}
WEP 600 µg/ml	1611-1615	4.21±0.94	1625-1628	11.94±1.48	1637-1639	18.52±1.92^{ab}

Assignment	α-helix (1649-1654 cm^{-1})		α-helix (1664-1669 cm^{-1})		β-turn (1677-1682 cm^{-1})		Antiparallel β-sheet (1689-1693 cm^{-1})	
	Position (cm^{-1})	Integral area (%)	Position (cm^{-1})	Integral area (%)	Position (cm^{-1})	Integral area (%)	Position (cm^{-1})	Integral area (%)
Control	1650-1652	32.74±1.18^{ab}	1666-1667	22.42±0.77	1682	5.98±0.67	1693	1.58±0.28
Etoposide 40 µg/ml	1651-1654	34.68±3.99^{b}	1666-1669	22.36±2.88	1682	7.57±0.55	1693	1.70±0.23
WEP 100 µg/ml	1649-1651	26.58±4.96^{ab}	1664-1665	19.58±2.93	1678-1681	9.34±1.53	1690-1693	2.47±1.09
WEP 300 µg/ml	1651	26.20±0.80^{a}	1664-1666	17.48±1.84	1677-1681	8.65±2.62	1689-1693	1.49±1.02
WEP 600 µg/ml	1651-1652	32.22±1.36^{ab}	1664-1666	22.09±2.44	1679-1682	9.44±2.04	1693	1.58±0.28

Values are mean ± SD (n = 3). Different letters within the same column are significantly different at $p < 0.05$ as determined by one-way ANOVA.

Then, the second derivative spectra of untreated and WEP-treated Jurkat cells were further analyzed by principle component analysis (PCA). The PCA score plot demonstrates that the clusters of untreated cells and WEP-treated cells at 100 and 300 µg/ml were separated from the clusters of the Jurkat cells treated with 600 µg/ml WEP or 40 µg/ml etoposide positive control at 24 h along PC1 (56%). The spectra of the untreated control cells were also distinguished from Jurkat cells treated with WEP at 100 and 300 µg/ml at 24 h along PC2 (17%) (Figure 4.20 (A)).

The PCA loading plots due to untreated and WEP-treated cells exhibited the spectral changes in apoptotic cell death (Figure 4.20(B)). The positive score plot of spectra of untreated control cells and 100 or 300 µg/ml WEP-exposed group could be separated from negative score plot of spectra of 600 µg/ml WEP or 40 µg/ml etoposide exposed group by having negative PC1 loadings at 1647 cm^{-1}, 1631 cm^{-1} and 1082 cm^{-1} which represented the β-pleated sheet component and nucleic acid (phosphodiester groups), respectively. Moreover, the positive PC1 loadings at 1656 cm^{-1} indicated that the α-helix component could be used to discriminate the negative score plot of spectra of 600 µg/ml WEP or 40 µg/ml etoposide exposed group from the positive score plot of untreated control cells and 100 or 300 µg/ml WEP-exposed groups. The discrimination along PC2 between the negative score plot of spectra of Jurkat control cells and the positive score plot of spectra of WEP exposed cells at 100, 300 µg/ml could be explained by positive loading PC2 at 1639 cm^{-1} which indicating β-pleated sheet components. On the other hand, the discrimination along PC2 of the positive score plots of spectra of WEP exposed cells at 100, 300 µg/ml could be distinguished from the negative score plots of spectra of Jurkat control cells by having negative loading PC2 in the C-H stretching

region (centered at 2923 cm^{-1} and 2852 cm^{-1}), which was correlated with the C=O stretching of lipid esters band loading at 1745 cm^{-1}.

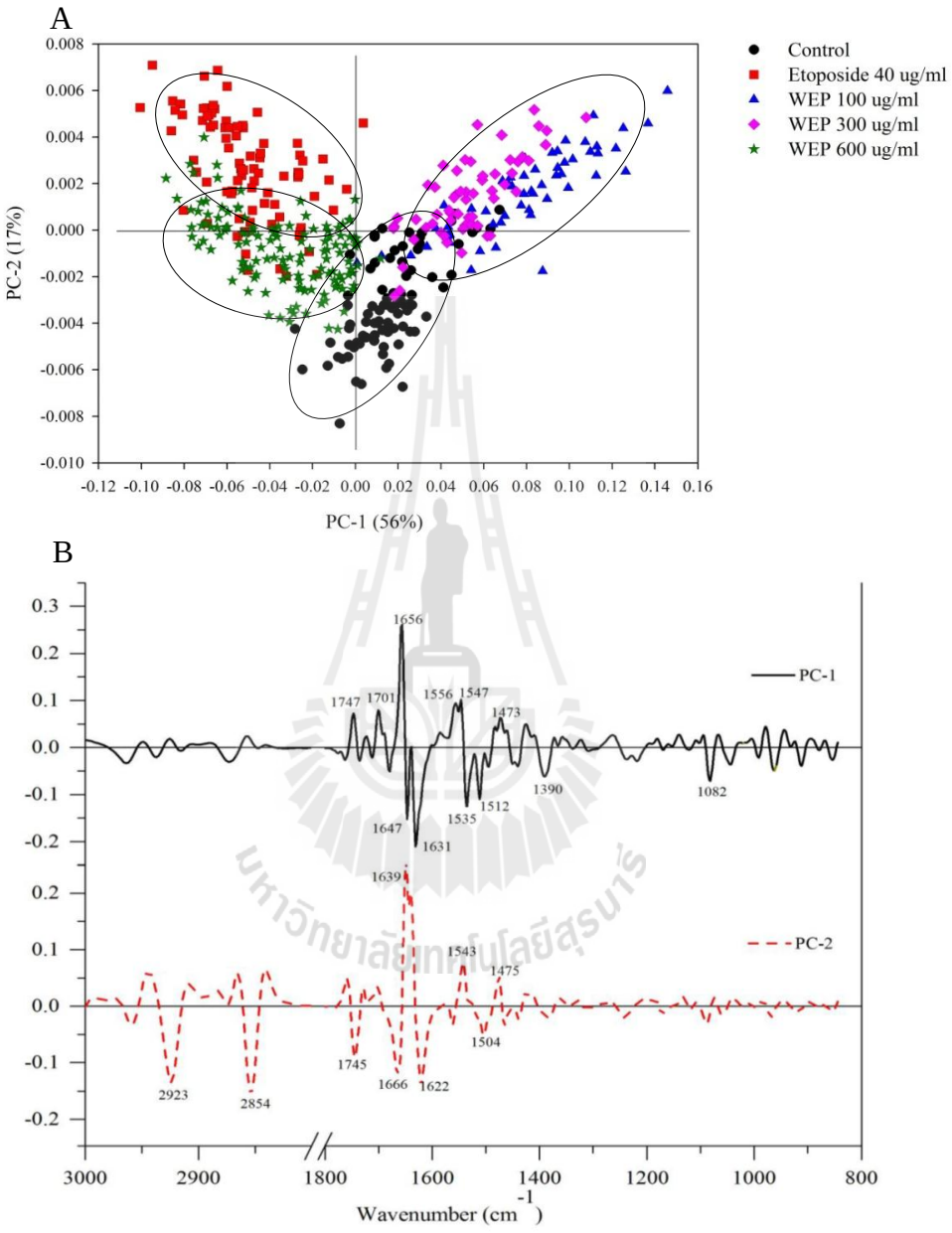

Figure 4.20 PCA analysis of FTIR spectral range 3000-800 cm^{-1} giving PCA score plot (A) and PCA loading plot (B). PCA score plots showed distinct clustering between Jurkat control cells and Jurkat exposed to WEP at 100, 300, 600 µg/ml, and 40 µg/ml of etoposide positive control at 24 h. PCA loading plots identify biomarker difference over spectral range of samples.

4.4 Mutagenic activity (Ames test)

The mutagenicity of EEP or WEP was evaluated by the Ames test using *S. typhimurium* strains TA98 and TA100 with pre-incubation procedure. The assays were performed in both absence and presence of S9 mix. Prior to conducting the assay, the toxicities of EEP or WEP towards *S. typhimurium* strains TA98 and TA100 were evaluated (data not shown). The data showed that EEP or WEP ranging from 150 µg/plates up to 600 µg/plates had no toxicity towards *S. typhimurium* strains TA98 and TA100 in both absence and presence of S9 mix. A compound tested with a mutagenic index of 2.0 or more is regarded as a potent mutagen. EEP or WEP ranging from 150 µg/plates up to 600 µg/plates had the mutagenic index of less than 2.0 on both tested strains, regardless the presence or absence of S9 mix (Table 4.2). The results showed that both EEP and WEP in the range of 150 - 600 µg/plates had no mutagenic activity, whereas all positive controls consistently induced a clear mutagenic response with high values of mutagenic indexes ranged from 13.6-50.6.

Table 4.4 Mutagenic effects of EEP on the *Salmonella typhimurium* strains TA98 and TA100 in the absence and presence of S9 mix.

Sample	Number of revertants/plate (Mean±S.D.), (MI=Mutagenic Index)			
	TA98		TA100	
	Absence of S9 mix	Presence of S9 mix	Absence of S9 mix	Presence of S9 mix
2-NF(10 µg/plate)[PC]	1,012±225,(50.6)	-	-	-
Sodium azide(10 µg/plate)[PC]	-	-	1,587±7,(13.56)	-
2-AA(2.5 µg/plate)[PC]	-	903±28,(34.74)	-	4,691±473,(41.88)
Control (1.4%DMSO)[NC]	20±5	26±8	121±10	112±9
EEP (150 µg/plate)	24±2, (1.20)	25±5, (0.96)	131±29, (1.08)	115±11, (1.03)
EEP (300 µg/plate)	20±4, (1.00)	26±4, (1.00)	105±10, (0.87)	92±7, (0.82)
EEP (600 µg/plate)	20±3, (1.00)	22±1, (0.85)	108±23, (0.89)	82±20, (0.73)
Control (Buffer alone)[NC]	22±2	24±5	117±6	111±5
WEP (150 µg/plate)	18±3, (0.82)	25±3, (1.04)	86±16, (0.74)	98±16, (0.88)
WEP (300 µg/plate)	20±4, (0.90)	20±3, (0.83)	111.00±30.05, (0.95)	117±8, (1.05)
WEP (600 µg/plate)	21±4, (0.95)	24±4, (1.00)	134.67±43.82, (1.15)	126±30, (1.14)

PC = positive control; NC = negative control

CHAPTER V

DISUSSION

Pseuderanthemum palatiferum (Nees) Radlk. or Hoan-Ngoc is a new medicinal plant that widely used in both Vietnamese and Thais as a medicinal and ornamental plant. Several studies have described the beneficial effects of *P. palatiferum* such as antioxidant, antidiabetic, anti-inflammatory, hypotensive and antiproliferative activities (Chayarop et al., 2011; Khonsung et al., 2011; Pamok et al., 2012; Sittisart and Chitsomboon, 2014). The present study aimed to investigate certain fresh leaves extracts of *P. palatiferum* as important sources of food supplement for anticancer therapeutics in the future. Moreover, this study also investigated for mutagenic effect of *P. palatiferum* to address the concerned toxicity of long-term daily consumption.

This study found phenolics and flavonoids in both 95% ethanol extract (EEP) and the water extract fractioned from 95% ethanol extract of *P. palatiferum* (WEP). As reported by Nguyen and Eun (2011), phenolics and flavonoids were found in *P. palatiferum* leaves extracted with methanol, ethanol, acetone, and water when assessed with Folin-Ciocalteu and aluminum trichloride. Dieu et al. (2008) and Chayarop et al. (2011) reported that the major chemical compositions of *P. palatiferum* leaves are flavanoids, apigenin, stigmasterol, β-sitosterol, β-sitosterol-3-0-β-glucoside, and apigenin-7-0-β-glucoside. In addition, Sittisart and Chitsomboon (2014) found high levels of phenolics and flavonoids in both 95% ethanol extract and

the water extract of *P. palatiferum*, which were correlated to DPPH radical scavenging activity.

The DPPH model was widely used in the model system to investigate the scavenging activities of various natural compounds such as phenolic compounds, anthocyanins, or crude mixtures such as ethanolic extract of plants (Panchawat and Sisodia, 2010). The results of the current study demonstrated that both EEP and WEP possessed high levels of phenolic and flavonoid contents which were correlated to high radical scavenging activities when assessed by DPPH assay. This study was also agreed with Sittisart and Chitsomboon (2014), who reported that the IC_{50} values of 95% ethanol extract and water extract fractioned from 95% ethanol extract of *P. palatiferum* were 23.45±0.12 and 21.55±0.06 μg/ml, respectively. Moreover, Nguyen and Eun (2011) reported DPPH scavenging activity of ethanol extract and water extract of *P. palatiferum* with IC_{50} values of 23.30±0.46% and 7.44±0.56%, respectively. In addition, researchers have found a correlation between total phenolic and flavonoid contents and antioxidant activity. Saeed et al. (2012) also found total phenolic and flavonoid contents activity in *Torilis leptophylla* with free radical scavenging activity. Fernandes de Oliveira et al. (2012) observed a strong correlation between total polyphenol contents and antioxidant activity of the crude extracts of *Sidastrum micranthum* and *Wissadula periplocifolia*. Bunea et al. (2011) demonstrated a high correlation between total polyphenol content and antioxidant activity in cultivated blueberry varieties from Romania. Therefore, high total phenolic and flavonoid contents in EEP or WEP could be associated to the scavenging activity against DPPH radicals.

The current study showed distinct cytotoxic effects of EEP and WEP against various human cancer cell lines, namely Jurkat, HepG2, and MCF-7. The results in this study agreed with several previous reports which showed the cytotoxic effects of *P. palatiferum* crude extracts against different cancer cell lines such as colon cancer cell lines; HCT15, SW48, SW480 (Pamok et al., 2012), colon cancer cells (Caco2), and breast cancer cell lines (MCF-7) (Phasuk and Meeratana, 2015). Moreover, several medicinal plants containing polyphenol compounds have been reported to have cytotoxicity against various types of cancer cell lines such as Jurkat cell (Musika and Indrapichate, 2014), gastric (AGS, SNU-668 and SNU-638) and breast (MDA-MB-231, MCF-7 and SK-BR-3) cancer cell lines. Interestingly, WEP possessed higher anti-proliferative effects against Jurkat cell line than that of EEP. Therefore, the antiproliferative activity of EEP and WEP towards cancer cell lines might be due to phytochemical constituents that dissolved in water fraction such as flavanoids, apigenin, catechin, gallic acid, and tannic acid (Dieu et al., 2008; Das et al., 2009; Chayarop et al., 2011). Moreover, the most selective cytotoxicity of EEP and WEP towards Jurkat cells might be due to the differences in cell properties and genetic backgrounds of various human cancer types (Thi Mai et al., 2011; Sak, 2014). Importantly, a great desired property of chemotherapeutic compounds is the selective cytotoxicity against cancer cells with less cytotoxic effect to normal cells for avoiding side effects to healthy tissues (American Cancer Society, 2013). The cytotoxic effects of both EEP and WEP at the same concentrations (50-1500 µg/ml) that were cytotoxic against jurkat cells induced less toxicity in normal human PBMCs. These data indicated the preferential toxicity of EEP and WEP to cancer. However, cell death largely occurs through either of two distinct processes: necrosis or apoptosis

(Majno and Joris, 1995). Consequently, it is necessary to distinguish apoptotic from necrotic cell death. Being the most sensitive target of EEP and WEP, the Jurkat cells were selected for further investigation whether the cytotoxic effect of EEP and WEP was mediated through the apoptotic mechanism.

Accordingly, either morphological changes or distinct biochemical events occurring during programmed cell death were analyzed by several assays, including observation of nuclear morphology changes with Hoechst 33258 staining by fluorescence microscopy, visualization of DNA fragmentation by gel electrophoresis, Annexin V-PI staining and cytochrome C release by flow cytometry, and identification of macromolecular changes by FTIR (Machana et al., 2012; Musika and Indrapichate, 2014). This study indicated that both EEP and WEP induced apoptotic cells death in Jurkat cells in both dose- and time dependent manners. Both EEP and WEP induction of apoptotic cell death in Jurkat cells had demonstrated physical hallmarks of apoptosis, including nuclear morphology changes, chromatin condensation, nuclear fragmentation, and formation of apoptotic bodies. In addition, DNA ladder formation revealed in gel electrophoresis also clearly indicated that both EEP and WEP had a potent apoptosis-inducing activity in Jurkat cells. The data from flow cytrometry revealed that both EEP- and WEP-induced apoptotic cell death with greater levels of early apoptosis which denoted by the alteration of cell surface occurring during the early apoptosis process, resulting in phosphatidylserine externalization which are recognized by macrophages for engulfment. Moreover, this study found that both EEP- and WEP-treated cells induced the release of cytochrome C from the mitochondria into cytosol suggesting that the extracts inducer apoptosis via the intracellular pathway. During apoptosis,

pro-apoptotic Bcl-2 family (Bax, Bad, and Bid) induced the permeabilization of outer mitochondrial membrane and led to the formation of pores in the mitochondria and then cytochrome C and pro-apoptotic molecules were released into cytosol. Cytochrome C binded to Apaf-1 and instigated the assembly of the apoptosome and induced caspase-dependent apoptotic pathway (Von Ahsen et al., 2000; Donovan and Cotter, 2004; Garrido et al., 2006). The results in this study were in accordance with previous reports which showed apoptotic effects of β-sitosterol in a variety of other human cancer cell lines, including LNCaP human prostate cancer cells (Fink and Awad, 1998), HT116 human colon cancer cells (Choi et al., 2003), Human leukemic U937 cells (Park et al., 2007), and MDA-MB-231 human breast cancer cells (Awad, Roy, and Fink, 2003; Park et al., 2008).

FTIR microspectroscopy was used to identify biomolecular changes of apoptotic cell death in Jurkat cells induced by EEP or WEP exposure. The results suggested that EEP or WEP induced apoptosis cells death in Jurkat cells, which was correlated with the changing of macromolecules (lipid, protein secondary structure (amide I), and nucleic acid) in Jurkat cells. Exposure of EEP or WEP at 100-600 µg/ml raised the intensity of lipid content higher than the untreated control cells. An increase in lipid absorbance of apoptotic cells was related to membrane changes during apoptosis process (Liu and Mantsch, 2001, Lamberti, Sanges, and Arcari, 2010, Lipiec, 2013) such as the collapse of lipid membrane asymmetry causing the inside out exposure of phosphatidylserine to the outer leaflet of membrane, cell shrinkage, membrane blebbing, and apoptotic body formation. Moreover, the lipid absorbance was found to decrease in necrotic cell death due to the membrane changing during necrosis including cells swelling and loss of plasma membrane

integrity. Exposure to 100, 300, and 600 μg/ml of WEP induced apoptotic cell death and showed slightly increased of β-pleated sheet component compared to the untreated control cells. In addition, the α-helix component of Jurkat cells exposed to WEP at 100, 300, and 600 μg/ml exhibited slightly decreased from untreated control cells. These results suggested the conformation change of the protein during apoptosis process. The protein structural change in apoptotic cell death was previously reported to correlate with the production of new proteins and some enzymes such as pro-apoptotic protein (Bax), anti-apoptotic protein (Bcl-2) family, and caspase family proteases (Adams and Cory, 1998). The C-terminal domain of Bak indicated the predominance of an extended β-structure (centered at 1636 cm^{-1}) which was able to insert itself into membranes resulting to different amide I band spectrum and indicating a predominantly α-helical structure (centered at 1658 cm^{-1}) (Matínez-Senac, Corbalán-García, and Gómez-Fernández, 2002). Bak-Bax interaction was also an important function of the mitochondrial outer membrane permeabilization, resulting to releases of cytochrome C and pro-apoptotic molecules into cytosol (Dewson, G. and Kluck, R. M., 2009). In contrast, the nucleic acid content of EEP-treated or WEP-treated Jurkat cells showed a dramatic decrease in a dose-dependent manner. The absorbance of nucleic acid region was reported to decrease in apoptotic cell death and by contrast, to increase in necrotic cells (Liu et al., 2001, Zelig et al., 2009, Machana et al., 2012). The apoptotic DNA absorbed less IR due to the opaqueness of DNA (non-Beer-Lambert absorption) caused by condensation of DNA during apoptosis (Mohlenhoff et al., 2005). Importantly, the opaque nature of apoptotic chromatin was likely due to its tight association with high-mobility group protein B1 (HMGB-1), which masks the chromatin from neighboring cells and

prevents activation of the inflammatory response. In contrast, during necrosis, the DNA is completely unwound; therefore, the necrotic DNA absorbs more IR. In addition, the decreasing of DNA content may correlated with the progress of internucleosomal DNA cleavage during apoptosis process (Verrier et al., 2004)

For a safety concern of long-term use, the mutagenic effect of EEP and WEP was investigated by the Ames assay. This study clearly showed that both EEP and WEP ranging from 150 µg/plates up to 600 µg/plates had no toxicity and mutagenicity in *S. typhimurium* strains TA98 (frameshift mutation) and TA100 (base-pair substitution), regardless the presence or absence of S9 mix (Table 4.2). Whereas, all positive controls always induced a clear mutagenic response with high values of mutagenic indexes (13.6-50.6). Concordantly, Pamok et al. (2012) recently reported that aqueous and ethanol extracts from *P. palatiferum* leaves at 25 to 100 µg/plate had no mutagenic effect on *S. typhimurium* TA98 and TA100.

Overall, the results suggested that both EEP and WEP contained phenolics and flavonoids which exhibited DPPH radical scavenging activities. Moreover, both EEP and WEP exerted the most potent antiproliferative effect on Jurkat cells, and its cytotoxicity was mediated through apoptosis via mitochondrial pathway. The antiproliferative effect against Jurkat cells of the extracts was mediated via apoptosis which was indicated by nuclear morphological changes, chromatin condensation, DNA fragmentation, externalization of phosphatidylserine, and distribution of cytochrome C from mitochondria to cytosol. Moreover, FTIR microspectroscopy suggested the changing of macromolecules (lipid, nucleic acid, and secondary protein) in EEP- or WEP-treated cells which may be related to the changing of plasma membrane, conformation change of apoptotic proteins (Bcl-2, Bax),

caspase family proteases and internucleosomal DNA cleavage during apoptosis process. In addition, both extracts in the range of 150 to 600 µg/plate had no mutagenicity in the Ames assay.

CHAPTER VI

CONCLUSION

The TPC and TFC of EEP and WEP determined by Folin-Ciocalteu method and aluminium trichloride colorimetric assay, respectively, revealed that extracts contained the comparable levels of TPC. However, WEP contained higher TFC than EEP ($p < 0.05$). The extracts exhibited different extents of antioxidant activity as estimated by the DPPH assay. The WEP possessed higher DPPH radical scavenging activity than EEP ($p < 0.05$). The TPC and TFC in both extracts were correlated to DPPH radical scavenging activity.

In vitro cytotoxicity studies revealed that the sensitivity of cancer cells to EEP and WEP extracts were ranged in the descending order of Jurkat > HepG2 > MCF-7 > PC-3. Importantly, both extracts exhibited the preferential cytotoxicity towards cancer cells as less toxicity was obtained in normal PBMCs cells exposed to the same concentration of both extracts that killed cancerous Jurkat cells ($P < 0.05$). In addition this study showed that the cytotoxicity against Jurkat cells by EEP and WEP was dose- and time-dependent, and the mechanism of cell death was occurred via apoptosis.

The apoptosis induction by EEP and WEP on Jurkat cells was confirmed by morphological changes under microscope, DNA ladder formation, annexin-V FITC binding and the distribution of cytochrome C from mitochondria to cytosol. Therefore, the apoptosis induction by EEP and WEP was mediated through the mitochondrial

pathway. Moreover, FTIR microspectroscopy also showed the changing of macromolecules (lipid, nucleic acid, and secondary structure of proteins) in EEP- or WEP-treated cells which can be related to changes of plasma membrane, apoptotic proteins, and internucleosomal DNA cleavage during apoptosis process. Moreover, the extract in the range of 150 to 600 µg/plate had no mutagenicity in the Ames assay.

REFERENCES

REFERENCES

Adams, J. M., and Cory, S. (1998). The Bcl-2 Protein Family: Arbiters of Cell Survival. **Apoptosis**. 281: 1322-1326.

American Cancer Society. (2013). **Chemotherapy Principles**. [On-line]. Available: http://www.cccsa.ca/modrinke.html.

AuntieV. (2012). **Hoan-Ngoc**. [On-line] Available: http://www.bloggang.com/viewdiary.php.

Awad, A. B., Roy, R., and Fink, C. S. (2003). β-sitosterol, a plant sterol, induces apoptosis and activates key caspases in MDA-MB-231 human breast cancer cells. **Oncology Reports**. 10(2): 497-500.

Awad, A.B., Chinnam, M., Fink, C.S., and Bradford, P.G. (2007). β-sitosterol activates Fas signaling in human breast cancer cells. **Phytomedicine**. 14(11): 747-754.

Bell, P. (2002). Apoptosis: cell'death' reveals creation. **Journal of Creation**. 16(1): 91-102.

Bennani, H., Drissi, A., Giton, F., Kheuang, L., Fiet, J., and Adlouni, A. (2007). Antiproliferative effect of polyphenols and sterols of virgin argan oil on human prostate cancer cell lines. **Cancer Detection and Prevention**. 31(1): 64-69.

Boatright, K. M., and Salvesen, G. S. (2003). Mechanisms of caspase activation. **Current Opinion in Cell Biology**. 15: 725–731.

Boehringer Mannheim GmbH, (1998). **Apoptosis and Cell Proliferation** (2nd ed.). Mannheim: Germany.

Bold, R. J., Termuhlen, P. M., and McConkey, D. J. (1997). Apoptosis, cancer and cancer therapy. **Surgical Oncology**. 6(3): 133-142.

Bras, M., Queenan, B., and Susin, S. A. (2005). Programmed cell death via mitochondria: Different modes of dying. **Biochemistry (Moscow)**. 70(2): 231-239.

Bröker, L. E., Kruyt, F. A., and Giaccone, G. (2005). Cell death independent of caspases: A review. **Clinical Cancer Research**. 11(9): 3155-3162.

Brudnak, M. (2000). Cancer-preventing properties of essential oil monoterpenes D-limonene and perillyl alcohol [19 paragraphs]. **Positive health online**. [On-line serial] 53: Available: http://www.positivehealth.com/article/cancer/cancer-preventing-properties-of-essential-oil-monoterpenes-d-limonene-and-perillyl-alcohol.

Bunea, A., Rugina, O. D., Pintea, A. M., Sconta, Z., Bunea, C. I., and Socaciu, C. (2011). Comparative polyphenolic content and antioxidant activities of some wild and cultivated blueberries from romania. **Notulae Botanicae Horti Agrobotanici Cluj-Napoca**. 39(2): 70-76.

Calvino-Fernández, M., and Parra-Cid, T. (2010). *H. pylori* and mitochondrial changes in epithelial cells. The role of oxidative stress. **Revista Española de Enfermedades Digestivas**. 102: 41-50.

Candé, C., Cecconi, F., Dessen, P., and Kroemer, G. (2002). Apoptosis-inducing factor (AIF): key to the conserved caspase-independent pathways of cell death?. **Journal of Cell Science**. 115: 4727-4734.

Cao, J., Ng, E. S., McNaughton, D., Stanley, E. G., Elefanty, A. G., Tobin, M. J., and Heraud, P. (2013). The characterisation of pluripotent and multipotent stem cells using fourier transform infrared microspectroscopy. **International Journal of Molecular Sciences**. 14: 17453-17476.

Chaabane, W., User, S. D., El-Gazzah., M., Jaksik, R., Sajjadi, E., Rzeszowska-Wolny, J., and J.Łos, M. (2013). Autophagy, apoptosis, mitoptosis and necrosis: Interdependence between those pathways and effects on cancer. **Archivum Immunologiae et Therapia Experimentalis**. 61: 43-58.

Chai, J.W., Kuppusamy, U.R., and Kanthimathi, M.S. (2008). Beta-sitosterol induces apoptosis in MCF-7 Cells. **Malaysian Journal of Biochemistry and Molecular Biology**. 16(2): 28-30.

Chayarop, K., Peungvicha, P., Wongkrajang, Y., Chuakul, W., Amnuoypol, S., and Temsiririrkkul, R. (2011). Pharmacognostic and Phytochemical Investigations of *Pseuderanthemum palatiferum* (Nees) Radlk. ex Lindau Leaves. **Pharmacognosy Journal**. 3(23): 18-23.

Choi, E. J., and Kim, G. H. (2009). Apigenin induces apoptosis through a mitochondria/caspase-pathway in human breast cancer MDA-MB-453 cells. **Journal of Clinical Biochemistry and Nutrition**. 44: 260-265.

Choi, Y. H., Kong, K. R., Kim, Y. A., Jung, K. O., Kil, J. H., Rhee, S. H., and Park, K. Y. (2003). Induction of Bax and activation of caspases during β-sitosterol-mediated apoptosis in human colon cancer cells. **International Journal of Oncology**. 23(6): 1657-1662.

Chuakul, W., and Arunya, S. (2008). Hoan-Ngoc. **Medicinal Plant Newletters**. 25(3): 3-6.

Chun, S.-C., Jee, S. Y., Lee, S. G., Park, S. J., Lee, J. R., and Kim, S. C. (2007). Anti-inflammatory activity of the methanol extract of Moutan Cortex in LPS-activated Raw264.7 cells. **Evidence-Based Complementary and Alternative Medicine**. 4(3): 327-333.

Cohausz, O., Blenn, C., Malanga, M., and Althaus, F. R. (2008). The roles of poly(ADP-ribose)-metabolizing enzymes in alkylation-induced cell death. **Cellular and Molecular Life Sciences**. 65(4): 644-655.

Constanta, S., and Rodica S. (2010). Analytical study of the determination of flavonoids in Black Sea algae. **Ovidius University Annals of Chemistry**. 21(1): 29-34.

Crosta, P. (2013). **What is cancer?**. [On-line]. Available: http://www.cancer.org/cancer/cancerbasics/what-is-cancer.

Damo. (2010). **DPPH assay**. [On-line]. Available:http://www.damocos.co.kr/damo/language/english/lab_paper3.php.

Das, A., Banik, N. L., and Ray, S. K. (2009). Flavonoids activated caspases for apoptosis in human glioblastoma T98G and U87MG cells but not in human normal astrocytes. **Cancer**. 116(1): 164-176.

Devi, U. P. (2005). Basics of carcinogenesis. **Health Administrator**. 17(1):16-24.

Dewson, G., and Kluck, R. M. (2009). Mechanisms by which Bak and Bax permeabilise mitochondria during poptosis**. Journal of Cell Science**. 122: 2801-2808.

Dieu, H. K. (2008). KHẢO SÁT THÀNH PHẦN HÓA HỌC CỦA LÁ XUÂN HOA *(Pseuderanthemum palatiferum).* **Tạp chí Khoa học**. 9: 232-240.

Dieu, H. K., Loc, C. B., Yamasaki, S., and Hirata, Y. (2005). The ethnobotanical and botanical study on *Pseuderanthemum palatiferum* as a new medicinal plant in the Mekong Delta of Vietnam. **Japan Agricultural Research Quarterly**. 39(3): 191-196.

Donovan, M., and Cotter, T. G. (2004). Control of mitochondrial integrity by Bcl-2 family members and caspase-independent cell death. **Biochimica et Biophysica Acta**. 1644: 133-147.

Eguchi, Y., Shimizu, S., and Tsujimoto, Y. (1997). Intracellular ATP levels determine cell death fate by apoptosis or necrosis. **Cancer Research**. (57): 1835-1840.

Evan, G. I. and Vousden, K. H. (2001). Proliferation, cell cycle and apoptosis in cancer. **Nature Reviews Cancer**. 411: 342-348.

Fan, T-J., Han, L-H., Cong, R-S., and Liang, J. (2005). Caspase family proteases and apoptosis. **Acta Biochimica et Biophysica Sinica**. 37(11): 719-727.

Favaloro, B., Allocati, N., Graziano, V., Di Ilio, C., and De Laurenzi, V. (2012). Role of apoptosis in disease. **Aging**. 4: 5.

Ferlay, J., Soerjomataram, I., Dikshit, R., Eser, S., Mathers, C., Rebelo, M., Parkin, D. M., Forman, D., and Bray, F. (2015). Cancer incidence and mortality worldwide: Sources, methods and major patterns in GLOBOCAN 2012. **International Journal of Cancer**. 136: E359-E386.

Fernandes de Oliveira, A. M., Pinheiro, L. S., Souto Pereira, C. K., Matias, W. N., Gomes, R. A., Chaves, O. S., Vanderlei de Souza, M. D .F., Nóbrega de Almeida, R., and Simões de Assis, T. (2012). Total phenolic content and antioxidant activity of some Malvaceae family species. **Antioxidants**. 1: 33-43.

Fink, S., and Awad, A. B. (1998). β-sitosterol activates the sphingomyelin cycle and induces apoptosis in LNCaP human prostate cancer cells. **Nutrition and Cancer**. 32(1): 8-12

Garrido, C., Galluzzi, L., Brunet, M., Puig, P. E., Didelot, C., and Kroemer, G. (2006). Mechanisms of cytochrome *c* release from mitochondria. **Cell Death and Differentiation**. 13: 1423-1433.

Gasparri, F. and Muzio, M. (2003). Monitoring of apoptosis of HL60 cells by Fourier-transform infrared spectroscopy. **Biochemical Society**. 369: 239-248.

Gavrilescu, L. C., and Denkers, E. Y. (2003). Apoptosis and the balance of homeostatic and pathologic responses to protozoan infection**. Infection and Immunity**. 71(11): 6109-6115.

Goldman, R., and Shields, P. G. (2003). Biomarkers of nutritional exposure and nutritional status. Food Mutagens**. American Society for Nutritional Sciences**. 133: 965S-973S.

Granado-Serrano, A. B. n., Martı´n, M. a. A., Bravo, L., Goya, L., and Ramos, S. (2006). Quercetin induces apoptosis via caspase activation, regulation of Bcl-2, and inhibition of PI-3-Kinase/Akt and ERK pathways in a human hepatoma cell line (HepG2). **The Journal of Nutritional**. 136: 2715-2721.

Hakura, A., Shimada, H., Nakajima, M., Sui, H., Kitamoto, S., Suzuki, S., and Satoh, T. (2005). Salmonella/human S9 mutagenicity test: a collaborative study with 58 compounds. **Mutagenesis**. 20(3): 217-228.

Health Information System Development Office. (2005). Cancer in Thailand. **Thai journal of Thai Health**. 1(5): 1-6.

Hongmei, Z. (2012). **Extrinsic and intrinsic apoptosis signal pathway review**. [Online]. Available: http://www.intechopen.com/books/apoptosis-and-medicine/extrinsic-and-intrinsic-apoptosis-signal-pathway-review.

Janmejai, K. S., and Gupta, S. (2009). Extraction, characterization, stability and biological activity of flavonoids isolated from Chamomile flowers. **Molecular and Cellular Pharmacology**. 1(3): 138-147.

Kang, Y. H., Yi, M. J., Kim, M. J., Park, M. T., Bae, S., Kang, C. M., Cho, C. K., Park, I. C., Park, M.J., Rhee, C.H., Hong, S. I., Chung, H. Y., Lee, Y. S., and Lee, S. J. (2004). Caspase-independent cell death by arsenic trioxide in human cervical cancer cells: reactive oxygen species-mediated poly (ADP-ribose) polymerase-1 activation signals apoptosis-inducing factor release from mitochondria. **Cancer Research**. 64: 8960-8967.

Khonsung, A., Panthong, A., Chiranthanut, N., and Intahphuak, S. (2011). Hypotensive effect of the water extract of the leaves of *Pseuderanthemum palatiferum*. **The Japanese Society of Pharmacognosy and Springer**. 65(3-4): 551-558.

Kim, J. H., Jung, C. H., Jang, B. H., Go, H. Y., Park, J. H., Choi, Y. K., Hong, S. I., Shin, Y. C., and Ko, S. G. (2009). Selective cytotoxic effects on human cancer cell lines of phenolic-rich ethyl-acetate.**World Scientific Publishing Company**. 37(3): 609-620.

Kim, R., Emi, M., and Tanabe, K. (2006). Role of mitochondria as the gardens of cell death. **Cancer Chemother Pharmacology**. 57:545–553.

Kong, J., and Yu, S. (2007). Fourier transform infrared spectroscopic analysis of protein secondary structures. **Institute of Biochemistry and Cell Biology**. 39(8): 549-559.

Kusherb. (2012). **Herb Kung**. [On-line]. Available: http://kusherb.exteen.com/page/3.

Lamberti, A., Sanges, C., and Arcari, P. (2010). FT-IR spectromicroscopy of mammalian cell cultures during necrosis and apoptosis induced by drugs. **Spectroscopy**. 24: 535-546.

Lee, S. H., Meng, X. W., Flatten, K. S., Loegering, D. A., and Kaufmann, S. H. (2013). Phosphatidylserine exposure during apoptosis reflects bidirectional trafficking between plasma membrane and cytoplasm. **Cell Death and Differentiation**. 20: 64-76.

Li, Z., and Sheng, M. (2012). Caspases in synaptic plasticity. **Molecular Brain**. 5(15): 1-6.

Li, Z., Li, J., Mo, B., Hu, C., Liu, H., Qi, H., Wang, X., and Xu, J. (2008). Genistein induces cell apoptosis in MDA-MB-231 breast cancer cells via the mitogen-activated protein kinase pathway. **Toxicology in Vitro**. 22(7): 1749-1753.

Lieberman, J., and Fan, Z. (2003). Nuclear war: the granzyme A-bomb. **Current Opinion in Immunology**. 15: 553-559.

Ling, W. H., and Jones, P. J. H. (1995). Dietary phytosterols: a review of metabolism, benefits and side effects. **Life Sciences**. 57(3): 195-206.

Lipiec, E. W. (2013). **Research into radiation damage in single cells using molecular spectroscopic techniques**. Ph.D. Dissertation, Polish Academy of Sciences.

Liu, K. Z., and Mantsch, H. H. (2001). Apoptosis-induced structural changes in leukemia cells identied by IR spectroscopy. **Journal of Molecular Structure**. 565-566: 299-304

Liu, K. Z, Jia, L., Kelsey, S. M., Newland, A. C., and Mantsch, H. H. (2001). Quantitative determination of apoptosis on leukemia cells by infrared spectroscopy. **Apoptosis**. 6: 269-278

Liu, M., Li, X. Q., Weber, C., Lee., C. Y., Brown, J., and Liu, R. H. (2002). Antioxidant and antiproliferative activities of raspberries. **Journal of Agricultural and Food Chemistry**. 50(10): 2926-2930.

Lorenzoa, H. K. and Susin, S. A. (2004). Mitochondrial effectors in caspase-independent cell death. **Federation of European Biochemical Societies**. 557: 14-20.

Lowe, S. W., and Lin, A.W. (2000). Apoptosis in cancer. **Carcinogenesis**. 21(3): 485-495.

MacFarlane M. and Williams, A. C. (2004). Apoptosis and disease: a life or death decision. **EMBO Reports**. 5: 674-8.

Machana, S., Weerapreeyakul, N., Barusrux, S., Thumanu, K., and Tanthanuch, W. (2012). FTIR microspectroscopy discriminates anticancer action on humanleukemic cells by extracts of *Pinus kesiya*: *Cratoxylum formosum* ssp. *pruniflorum* and melphalan. **Talanta**. 93: 371-382.

Majno, G., and Joris, I. (1995). Apoptosis, oncosis, and necrosis. **American Journal of Pathology**. 146(10): 3-15.

Marinković1, N., Pašalić, D., and Potočki, S. (2013). Polymorphisms of genes involved in polycyclic aromatic hydrocarbons'biotransformation and atherosclerosis. **Biochemia Medica**. 23(3): 255-265.

Maron, D. M., and Ames, B. N. (1983). Revised methods for the Salmonella mutagenicity test, **Mutation Research**. 113: 173-215.

Matínez-Senac, M. D. M., Corbalán-García, S., and Gómez-Fernández, J. C. (2002). The Structure of the C-Terminal domain of the pro-apoptotic protein Bak and its interaction with model membranes. **Biophysical Journal**. 81: 233-243.

McIlwain, D. R., Berger, T., and Mak, T. W. (2013). Caspase functions in cell death and disease. **Cold Spring Harbor Laboratory Press**. 5: a008656.

Mohlenhoff, B., Romeo, M., Diem, M., and Wood, B. R. (2005). Mie-type scattering and Non-Beer-Lambert absorption behavior of human cells in infrared microspectroscopy. **Biophysical Journal**. 88: 3635-3640.

Moon, D. O., Lee, K-J., Choi, Y. H., and Kim, G-Y. (2007). β-Sitosterol-induced-apoptosis is mediated by the activation of ERK and the downregulation of Akt in MCA-102 murine fibrosarcoma cells. **International Immunopharmacology**. 7(8): 1044-1053.

Mortelmans, K. and Zeiger, E. (2000). The Ames Salmonella/microsome mutagenicity assay. **Mutation Research**. 455: 29-60.

Mosmann, T. (1983). Rapid colorimetric assay for cellular growth and survival: application to proliferation and cytotoxicity assays. **Journal of lmmunological Methods**. 65: 55-63.

Musika, S., and Indrapichate, K. (2014). Cytotoxicity and apoptosis induction of Mintweed (*Hyptis suaveolens* L. Poit) leaf extracts on human T-leukemia cell line, Jurkat cells. **World Journal of Pharmacy and Pharmaceutical Sciences**. 3(3): 304-317.

Nascimento, A. K. L., Melo-Silveira, R. F., Dantas-Santos, N., Fernandes, J. M., Zucolotto, S. V., Rocha, H. A. O., and Scortecci, K. C. (2013). Antioxidant and antiproliferative activities of leaf extracts from *Plukenetia volubilis* Linneo (Euphorbiaceae). **Evidence-Based Complementary and Alternative Medicine**. 2013, Article ID 950272, 10 pages.

Nguyen, Q. V., and Jong-Bang Eun, J. B. (2011). Antioxidant activity of solvent extracts from Vietnamese medicinal plants. **Journal of Medicinal Plants Research**. 5(13): 2798-2811.

Norbury, C. J., and Hickson, I. D. (2001). Cellular responds to DNA damage. **Annual Review of Pharmacology and Toxicology**. 41:367-401.

Padee, P., Nualkaew, S., Talubmook, C., and Sakuljaitrong, S. (2010). Hypoglycemic effect of a leaf extract of *Pseuderanthemum palatiferum* (Nees) Radlk. in normal and streptozotocin-induced diabetic rats. **Journal of Ethnopharmacology**. 132(2): 491-496.

Pamok, S., Saenphet, S., Vinitketkumnuen, U., and Saenphet, K. (2012). Antiproliferative effect of *Moringa oleifera* Lam. and *Pseuderanthemum palatiferum* (Nees) Radlk extracts on the colon cancer cells. **Journal of Medicinal Plants Research**. 6(1): 139-145.

Panchawat, S., and Sisodia, S. S. (2010). *In vitro* antioxidant activity of *Saraca asoca* Roxb. De Wilde stem bark extracts from various extraction process. **Asian Journal of Pharmaceutical and Clinical Research**. 3(3): 231-233.

Park, C., Moon, D. O., Rhu, Chung-H., Choi, B. T., Lee, W. H., Kim, G. Y., and Choi, Y. H. (2007). β-Sitosterol induces anti-proliferation and apoptosis in human leukemic U937 cells through activation of caspase-3 and induction of Bax/Bcl-2 ratio. **Pharmaceutical Society of Japan**. 30(7): 1317-1323.

Park, C., Moon, D. O., Rhu, Chung-H., Choi, B. T., Lee, W. H., Kim, G. Y., and Choi, Y. H. (2008). β-Sitosterol sensitizes MDA-MB-231 cells to TRAIL-induced apoptosis. **Acta Pharmacologica Sinica**. 29 (3): 341-348.

Pathology Department of Shantou University Medical College. (2006). **Defination of apoptosis**. [On-line]. Available: http://pathol.med.stu.edu.cn/pathol/english /index.htm.

Patil, J. R., Jayaprakasha, G. K., Murthy, K. N. C., Chetti, M. B., and Patil, B. S. (2010). Characterization of *Citrus aurantifolia* bioactive compounds and their inhibition of human pancreatic cancer cells through apoptosis. **Microchemical Journal**. 94(2): 108-117.

Peng, J., Fan, G., and Wu, Y. (2006). Preparative isolation of four new and two known flavonoids from the leaf of *Patrinia villosa* Juss. by counter-current chromatography and evaluation of their anticancer activities in vitro. **Journal of Chromatography A**. 1115(1-2): 103-111.

Phasuk, S., and Meeratana, P. (2014). Cytotoxicity activity of *Pseuderanthemum palatiferum* crude extracts against breast and colon cancer cells. **Thai Journal of Science and Technology**. 22 (6); 848-860.

Proskuryakov, S. Y., Konoplyannikov, A. G., and Gabai, V. L. (2003). Necrosis: a specific form of programmed cell death?. **Experimental Cell Research**. 283: 1-16.

Ramos, S. (2007). Effects of dietary flavonoids on apoptotic pathways related to cancer chemoprevention. **The Journal of Nutritional Biochemistry**. 18(7): 427-442.

Sadowski-Debbing, K., Coy, J. F., Mier, W., Hug, H., and Los, M. (2002). Caspases - their role in apoptosis and other physiological processes as revealed by knock-out studies. **Archivum Immunologiae et Therapiae Experimentalis**. 50: 19-34.

Saeed, N., Khan, M. R., and Shabbir, M. (2012). Antioxidant activity, total phenolic and total flavonoid contents of whole plant extracts *Torilis leptophylla.* **BMC Complementary and Alternative Medicine**. 12(221): 12 page.

Sak, K. (2014). Cytotoxicity of dietary flavonoids on different human cancer types. **Pharmacognosy Review**. 8(16): 122-146

Sánchez-Moreno, C., Larrauri, J. A., and Saura-Calixto, F. (1999). Free radical scavenging capacity and inhibition of lipid oxidation of wines, grape juices and related polyphenolic constituents. **Food Research International**. 32(6): 407-412.

Sarastea, A., and Pulkkic, K. (2000). Morphologic and biochemical hallmarks of apoptosis. **Cardiovascular Research**. 45: 528-537.

Singleton, V. L., Orthofer, R., and Lamuela-Ravent´os, R. M. (1998). Analysis of total phenols and other oxidation substrates and antioxidants by means of folin-ciocalteu reagent. **Methods in Enzymology**. 299: 152-178.

Sittisart, P., and Chitsomboon, B. (2014). Intracellular ROS scavenging activity and downregulation of inflammatory mediators in RAW264.7 Macrophage by fresh leaf extracts of *Pseuderanthemum palatiferum*. **Evidence-Based Complementary and Alternative Medicine**. 2014, Article ID 309095, 11 pages.

Slee, E. A., Adrain, C., and Martin, S. J. (2001). Executioner caspase-3, -6, and -7 perform distinct, non-redundant roles during the demolition phase of apoptosis. **The Journal of Biological Chemistry**. 276(10): 7320-7326.

Tan, C. P., Lu, Y. Y., Jia, L.N., and Mao, Z. W. (2014). Metallomics insights into the programmed cell death induced by metal-based anticancer compound. **Metallomics**. 6: 978-995.

Taylor, R. C., Cullen, S. P., and Martin, S. J. (2008). Apoptosis: controlled demolition at the cellular level. **Molecular Cell Biology**. 9: 231-241.

Thi Mai, H. D., Thi Minh, H. N., Pham, V. C., Bui, K. N., Nguyen, V. H., and Chau, V. M. (2011). Lignans and Other Constituents from the Roots of the Vietnamese Medicinal Plant *Pseuderanthemum palatiferum*. **Planta Med**. 77: 951-954.

Tsagarakis, N. J., Drygiannakis, I., Batistakis, A. G., Kolios, G., and Kouroumalis, E. A. (2010). A concentration-dependent effect of ursodeoxycholate on apoptosis and caspases activities of HepG2 hepatocellular carcinoma cells. **European Journal of Pharmacology**. 640(1-3): 1-7.

Tsao, A. S., Kim, E. S., and Hong, W. K. (2004). Chemoprevention of Cancer. **A Cancer Journal for Clinicians**. 54(3): 150-180.

Verrier, S., Notingher, I., Polak, J. M., and Hench, L. L. (2004). In Situ monitoring of cell death using Raman microspectroscopy. **Biopolymers**. 74: 157-162.

Von Ahsen, O., Waterhouse, N. J., Kuwana, T., Newmeyer, D. D., and Green, D. R. (2000). The harmless release of cytochrome *c*. **Cell Death and Differentiation**. 7: 1192-1199.

Wang, Z. B., Liu. Y. Q., and Cui, Y. F. (2005). Pathways to caspase activation. **Cell Biology International**. 29: 489-496.

Wikipedia. (2015a). **Mutagen** [On-line]. Available: http://en.wikipedia.org/wiki/Mutagen.

Wikipedia. (2015b). **Mutagenesis** [On-line]. Available: http://en.wikipedia.org/wiki/Mutagenesis.

Yin, Y., Chen, W., Tang, C., Ding, H., Jang, J., Weng, M., Cai, Y., and Zou, G. (2011). NF-κB, JNK and p53 pathways are involved in tubeimoside-1-induced apoptosis in HepG2 cells with oxidative stress and G2/M cell cycle arrest. **Food and Chemical Toxicology**. 49(12): 3046-3054.

Zelig, U., Kapelushnik, J., Moreh, R., Mordechai, S., and Nathan, I. (2009). Diagnosis of cell death by means of infrared spectroscopy. **Biophysical Journal**. 97: 2107-2114.

Zhao Hongmei, Z. (2012). **Extrinsic and intrinsic apoptosis signal pathway review**. [On-line]. Available: http://www.intechopen.com/books/apoptosis-and-medicine/extrinsic-and-intrinsic-apoptosis-signal-pathway-review.

Zong, W. X. and Thompson C. B. (2006). Necrotic death as a cell fate. **Genes & Development**. 20:1-15.

APPENDICES

APPENDIX A

PREPARATION OF REAGENTS FOR CHEMICAL ANALYSIS

A.1 Folin-Ciocalteu method

- Gallic acid stoCk solution (1mg/ml)
  - Gallic acid 0.011 g
  - 10% Ethanol 10 ml
- 2% Na_2CO_3
  - Na_2CO_3 2 g
  - DI water 100 ml
- 50% Folin-Ciocalteu reagent
  - Folin-Ciocalteu reagent 1 ml
  - Methanol 1 ml

A.2 Aluminium trichloride method

- 10% $AlCl_3.6H_2O$
  - $AlCl_3.6H_2O$ 1 g
  - DI water 10 ml
- 5% $NaNO_2$
  - $NaNO_2$ 0.5 g
  - DI water 10 ml

1 N NaOH

- NaOH 4 g
- DI water 100 ml

A.3 DPPH assay

- DPPH solution (63 mM)
  - DPPH 0.004 g
  - DI water 10 ml

A.4 Hoechst 33258 staining

- Fixing solution (4% *p*-formaldehyde)
  - 37% formaldehyde 2.2 ml
  - PBS, 1X 17.8 ml
- Hoechst staining solution
  - Hoechst 33258 (1 mg/ml) 40 µl
  - 1% TritonX-100 400 µl
  - DI water 3,560 µl

  (Store at -20 °C)

A.5 DNA fragmentation

- TBE buffer 10X solution
  - Boric acid 55 g
  - Tris base 108 g
  - 0.5 M EDTA, pH 8.0 40 ml
  - DI water 800 ml

  Adjust volume to 1000 ml (store at 4 °C)

- TBE buffer 1X solution
  - TBE buffer 10 X solution 100 ml
  - DI water 900 ml
- 1.5% agarose gel
  - Agarose gel 0.75 g
  - TBE buffer 1X solution 50 ml

  (Freshly prepared)
- RNase A 100 mg/ml
  - RNaseA 0.05 g
  - DI water 500 µl
- Ethidium bromide staining (0.5 µg/ml)
  - Ethidium bromide 0.05 g
  - DI water 100 ml

A.6 Ames test

- Vogel-Bonner medium E stock salt solution (VB salt)
  - $MgSO_4.7H_2O$ 10 g
  - $C_6H_{10}O_8$ 100 g
  - K_2HPO_4 500 g
  - $NaNH_4HPO_4.4H_2O$ 175 g

  Adjust volume to 1000 ml with DI water and autoclave for 20 min at 121 °C.
- 40% glucose
  - $C_6H_{12}O_6$ 40 g

  Adjust volume to 100 ml with DI water and autoclave for 20 min at 121 °C.

- Minimal glucose agar plate
  - Bacto agar 5.25 g
  - VB salt 7 ml
  - 40% glucose 17.5 ml

  Adjust volume to 350 ml with DI water and autoclave for 20 min at 121 °C. Then, add 7 ml of sterile VB salts and 17.5 ml of a sterile 40% glucose solution and swirl thoroughly. Dispense the agar medium in 100 mm petri dishes.
- Oxiod nutrient broth no.2
  - Nutrient broth no.2 2.5 ml

  Adjust volume to 100 ml with DI water. Then, distribute in 12 ml aliquots and autovlave for 20 min at 121 °C.
- 0.1 M L-histidine HCl stock
  - L-histidine HCl 2.096 g

  Adjust volume to 100 ml with DI water and autovclave for 20 min at 121 °C.
- 1 mM L-histidine HCl
  - 0.1 M L-histidine HCl 1 ml

  Adjust volume to 100 ml with DI water and autoclave for 20 min at 121 °C.
- 1 mM biotin stock
  - 0.1 M L-histidine HCl 0.02443 g

  Adjust volume to 100 ml with DI water and autoclave for 20 min at 121 °C.
- 0.5 mM L-histidine HCl-0.5 mM biotin
  - 1 mM L-histidine HCl 100 ml
  - 1 mM biotin stock 100 ml

- Top agar
  - Agar 0.6 g
  - NaCl 0.5 g

  Adjust volume to 100 ml with DI water and autoclave for 20 min at 121 °C. Then, add 0.5 mM L-histidine HCl-0.5 mM biotin and swirl thoroughly.
- 0.2 M NaH_2PO_4
  - $NaH_2PO_4.2H_2O$ 14.2 g

  Adjust volume to 500 ml with DI water.
- 0.2 M Na_2HPO_4
  - $Na_2HPO_4.2H_2O$ 13.8 g

  Adjust volume to 500 ml with DI water.
- 0.2 M $NaPO_4$, pH 7.4 (Use: for S9 mutagenic assay)
  - 0.2 M NaH_2PO_4 60 ml
  - 0.2 M Na_2HPO_4 440 ml

  After mixing the two ingredients, mix well. Adjust pH to 7.4 using 0.1 M NaH_2PO_4 and autoclave for 20 min at 121 °C.
- 1 M KCl
  - KCl 7.5 g

  Adjust volume to 100 ml with DI water and autoclave for 20 min at 121 °C.
- $NaPO_4$-KCl buffer
  - 0.5 M $NaPO_4$, pH 7.4 100 ml
  - 1 M KCl 16.5 ml

  Adjust volume to 330 ml with DI water and autoclave for 20 min at 121 °C.

- $MgCl_2$-KCl salts (Use: for S9 mutagenic assay)
  - $MgCl_2.6H_2O$ 61.5 g
  - KCl 40.7 g

  Adjust volume to 500 ml with DI water and autoclave for 20 min at 121 °C.
- 1 M glucose-6-phosphate (Use: for S9 mutagenic assay)
  - Glucose-6-phosphate 2.82 g
  - Distilled water 10 ml
- 0.1 Nicotinamide adenine dinucleotide phosphate (NADP) (Use: for S9 mutagenic assay)
  - NADP 0.383 g
  - Distilled water 5 ml
- Co-factors for standard S-9 mix, total volume 50 ml (Use: to provide the NADH regenerating system)
  - S9 (4%) 2 ml
  - $MgCl_2$-KCl salts 1 ml
  - 1 M glucose-6-phosphate 0.25 ml
  - 0.1 NADP 2 ml
  - 0.2 M $NaPO_4$, pH 7.4 25 ml
  - Distilled water 19.75 ml

  The solution must be prepared fresh and kept on ice.

APPENDIX B

PREPARATION OF REAGENTS FOR CELL CULTURE

B.1 Phosphate buffer saline (PBS), 1X, pH 7.4

- KH_2PO_4 0.144 g
- $Na_2HPO_4.7H_2O$ 0.795 g
- NaCl 9.0 g
- DI water 1 L

Adjust pH to 7.2 ± 0.1 and filter sterile (store at 4 °C).

B.2 Trypsin/EDTA preparation

- Trypsin 0.25 g
- EDTA 0.04 g
- PBS, 1X 100 ml

Filter sterile and aliquot (store at 4 °C).

B.3 Culture media preparation

- FBS (heat inactivated)
  - Slowly thaw the frozen FBS in a beaker filled with water.
  - Put in water bath at 37 °C till completely thaw.
  - Heat inactivate (56 °C, 20 min), gentle mix every 10 min.
  - Aliquot 45 ml into conical tubes.

    (store at -20 °C).

- HEPES buffer, 1M
  - HEPES 23.83 g
  - DI water 100 ml

  Filter sterile and aliquot (store at -20 °C).
- Penicillin/Streptomycin, 100X
  - Penicillin 0.6 g
  - Streptomycin 1.34 g
  - PBS, 1X 100 ml

  Filter sterile and aliquot (store at -20 °C).
- RPMI 1640, 1X (incomplete medium)
  - RPMI 1640, 1X with L-glutamine and phenol red 1 pack
  - $NaHCO_3$ 2 g
  - DI water 1 L

  Adjust pH to 7.2-7.4 and filter sterile (Store at 4 °C).
- RPMI 1640, 1X (complete medium)
  - Inactivated FBS 20 ml
  - Penicillin/Streptomycin 2 ml
  - HEPES buffer, 1M 3 ml

  Adjust volume to 200 ml with RPMI 1640, 1X (incomplete medium) (store at 4 °C).

- DMEM, high glucose, 1X (incomplete medium)
  - DMEM, high glucose, 1X with L-glutamine and phenol red 1 pack
  - $NaHCO_3$ 3.7 g
  - DI water 1 L

  Adjust pH to 7.2-7.4 and filter sterile (store at 4 °C).
- DMEM, high glucose, 1X (complete medium)
  - Inactivated FBS 20 ml
  - Penicillin/Streptomycin 2 ml
  - HEPES buffer, 1M 3 ml

  Adjust volume to 200 ml with DMEM, high glucose, 1X (incomplete medium). (store at 4 °C).

APPENDIX C

DETECTION KITS

C.1 DNA mini kit manufacturer's instructions

1. Pipet 200 µl sample to the microcentrifuge tube.
2. Add 20 µl Proteinase K per 200 µl lysate.
3. Add 200 µl Buffer AL per 200 µl lysate.
4. Mix immediately by pulse-vortexing for 15 s.
5. Incubate at 56 °C for 10 min
6. Add 200 µl ethanol (96-100%) per 200 µl lysate, and mix again by pulse-vortexing for 15 s. Then, centrifuge at 6000 × *g* for 1 min. Place the QIAamp spin column in a clean 2 ml collection tube and discard the tube containing the filtrate.
7. Add 500 µl Buffer AW1 without wetting the rim. Close the cap and centrifuge at 6000 ×*g* for 1 min. Place the QIAamp spin column in a clean 2 ml collection tube and discard the collection tube containing the filtrate.
8. Add 500 µl Buffer AW2 without wetting the rim. Close the cap and centrifuge at full speed (20,000 × *g*) for 3 min.
9. Place the QIAamp spin column in a clean 1.5 ml microcentrifuge tube, and discard the collection tube containing the filtrate.
10. Add 50 µl Buffer AE. Incubate at room temperature for 15 min and then centrifuge at 6000 × *g* for 1 min.

11. Repeat step 10 again.
12. Five microgram of DNA sample in AE buffer was mixed with 100 µg/ml of RNase A (final concentration) and incubated at 37 °C for 30 min.
13. The DNA sample was loaded in 1.5% agarose gel and the gel was run at 70 volts for 1.50 h.

C.2 FlowCellectTM CytoChrome c Kit manufacturer's instructions

1. Add 200 µl of cell suspension (1x106 cells) to tube.
2. Centrifuge cells at 400× g for 5 min.
3. Aspirate off the supernatant and add 200 µl of 1X PBS to each well or tube. Mix each sample thoroughly.
4. Centrifuge cells at 400 × g for 5 to 7 minutes and aspirate off supernatant.
5. Add 100 µl of Permeabilzation Buffer Working Solution to each well or tube and mix thoroughly
6. Cover the plate with a plate sealer or cap each tube and incubate for 10 minutes on ice.
7. After permeabilzation incubation add 100µl of the Fixation buffer Working Solution prepared to each sample and mix each sample thoroughly.
8. Incubate at room temperature for 20 min.
9. After incubation, centrifuge cells for 5 to 7 min at 300 × g.
10. Aspirate off the supernatant and add 150 µl of 1X Blocking Buffer to each sample.
11. Centrifuge cells for at least 5 to 7 min at 400 × g.

12. Aspirate off the supernatant and add 100 µl of 1X Blocking Buffer to each sample and mix thoroughly.
13. Incubate the plate for 30 min at room temperature.
14. After incubation add 10 µl of either the Anti-IgG1-FITC Isotype Control or Anti-CytoChrome c-FITC Antibody to each sample and mix thoroughly.
15. Incubate the plate at room temperature for 30 min in the dark.
16. After incubation, add 100 µl of 1X Blocking Buffer to each sample.
17. Centrifuge sample for at 5 to 7 min at 300 × g.
18. Aspirate off the supernatant, and add 200 µl of 1X Blocking Buffer to each well.
19. Samples are now ready for acquisition on a flow cytometer.
20. Read within 4 h.

APPENDIX D

DATA ANALYSIS

D.1 Standard curves

- **Total phenolic content**

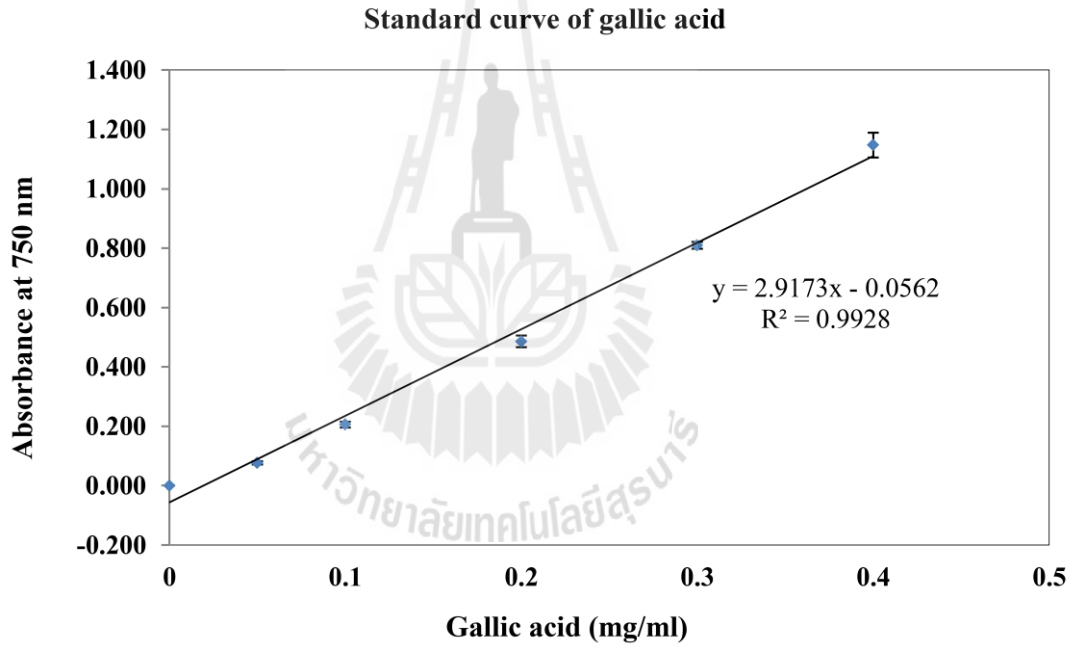

- **Total flavonoid content**

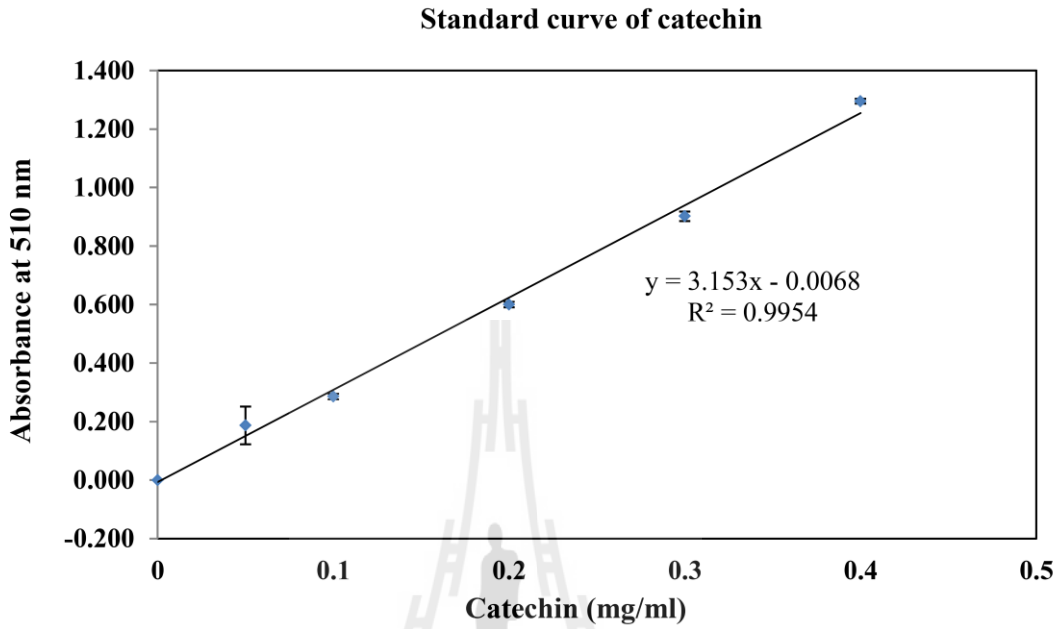

- **DPPH radical scavenging activity of *P. palatiferum* leaf extracts (EEP and WEP) and positive controls (ascorbic acid and trolox)**

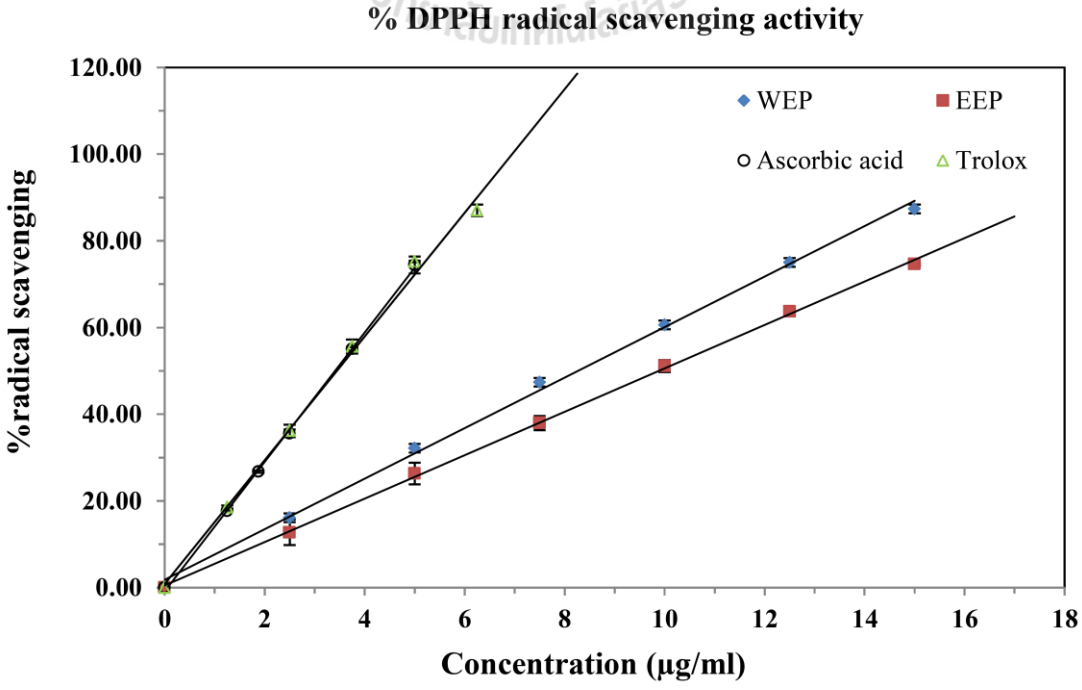

D.2 Representative flow cytrometric histrograms of immunolabeled cytochrome C

- **The dose-dependent effect of EEP on cytochrome C release in Jurkat cells.**

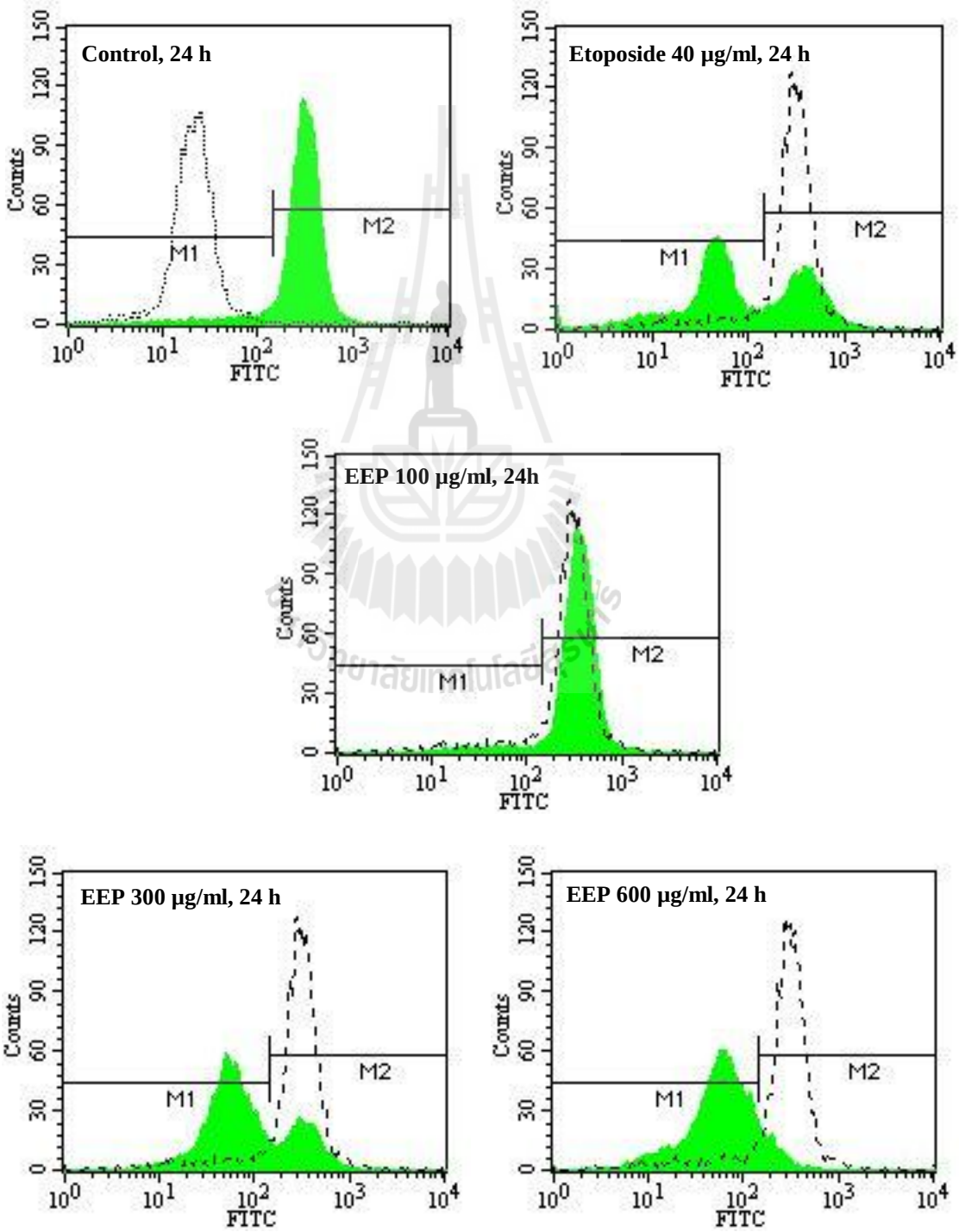

- **The time-course study of cytochrome C release in EEP-exposed Jurkat cells.**

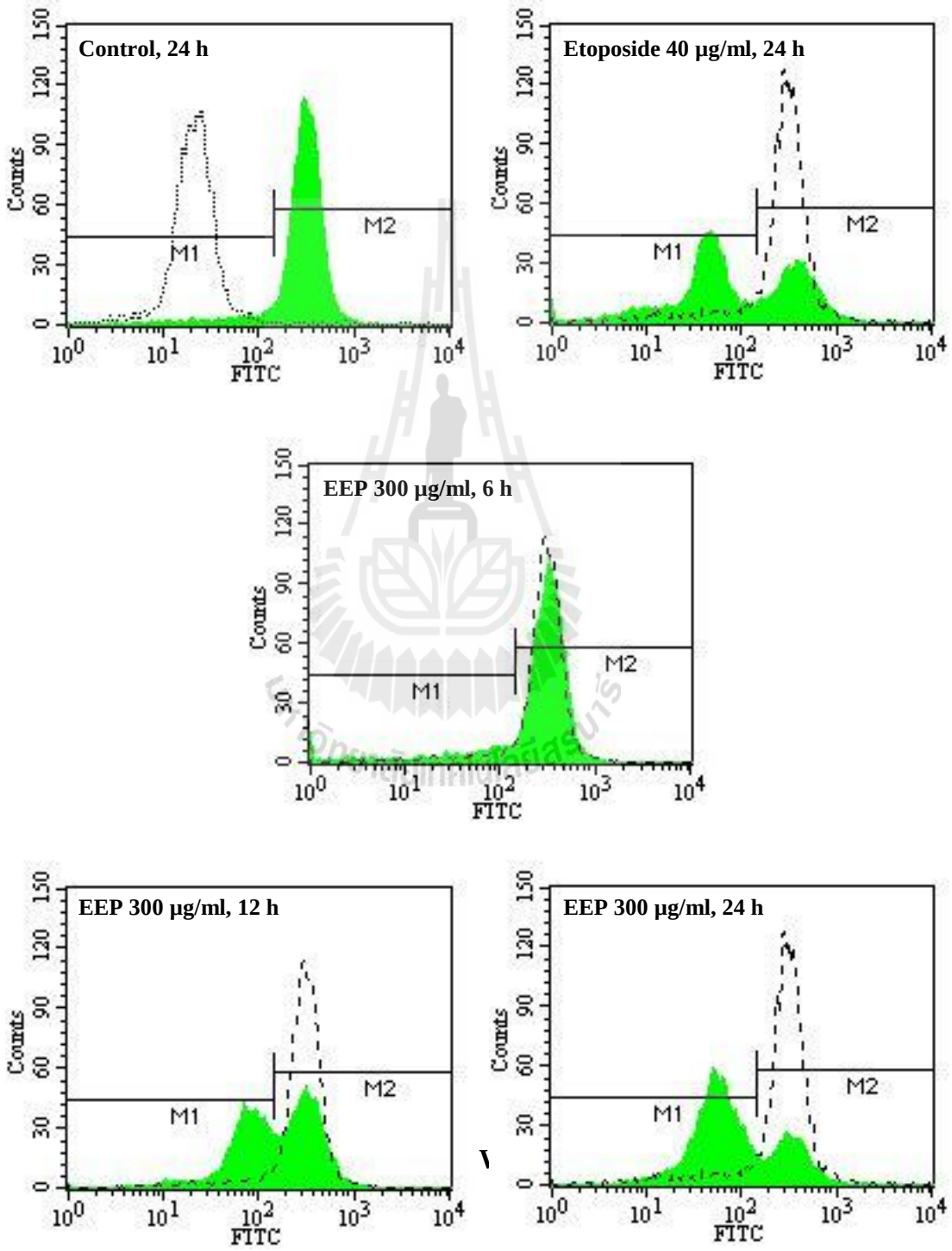

- **The dose-dependent effect of WEP on cytochrome C release in Jurkat cells.**

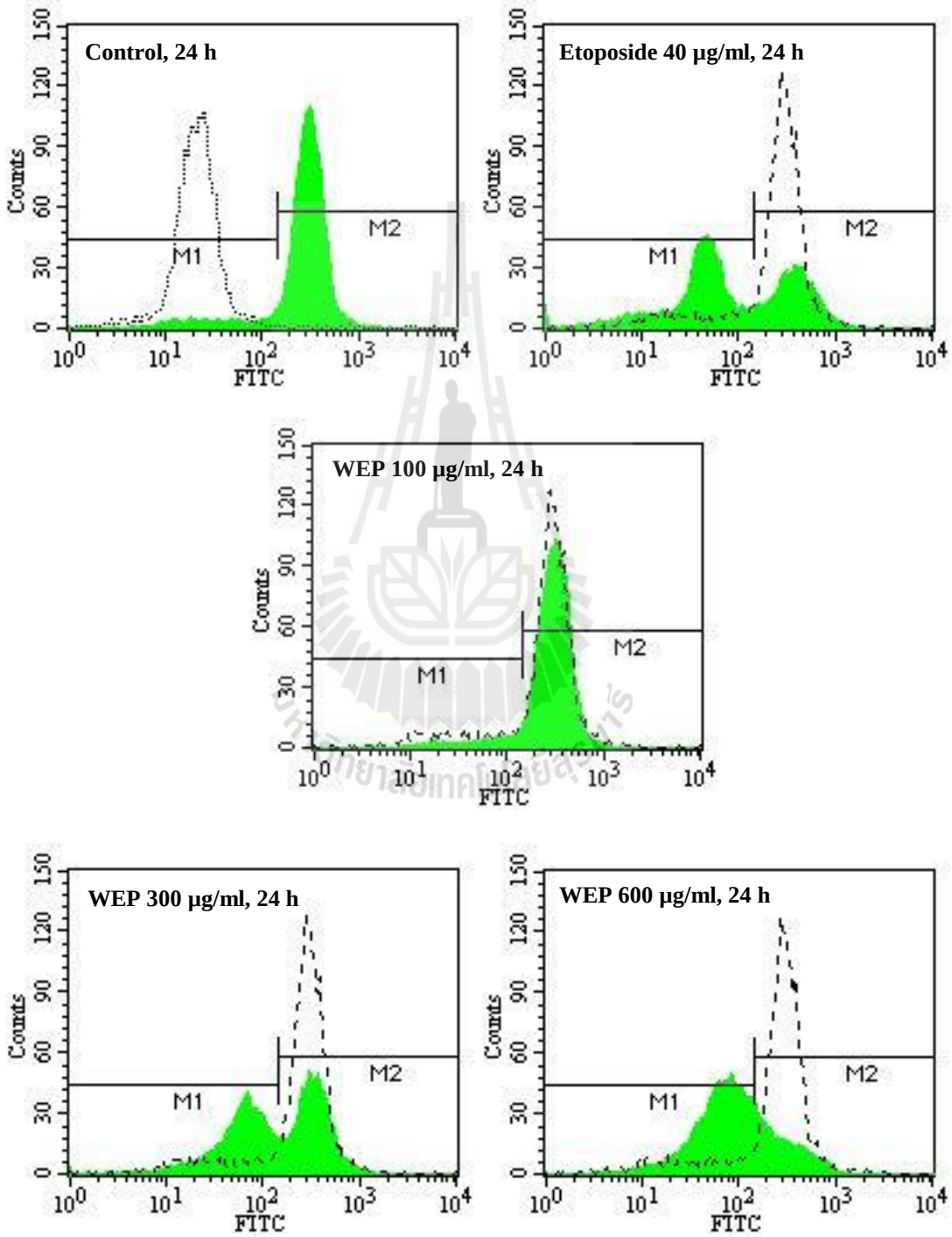

- **The time-course study of cytochrome C release in WEP-exposed Jurkat cells.**

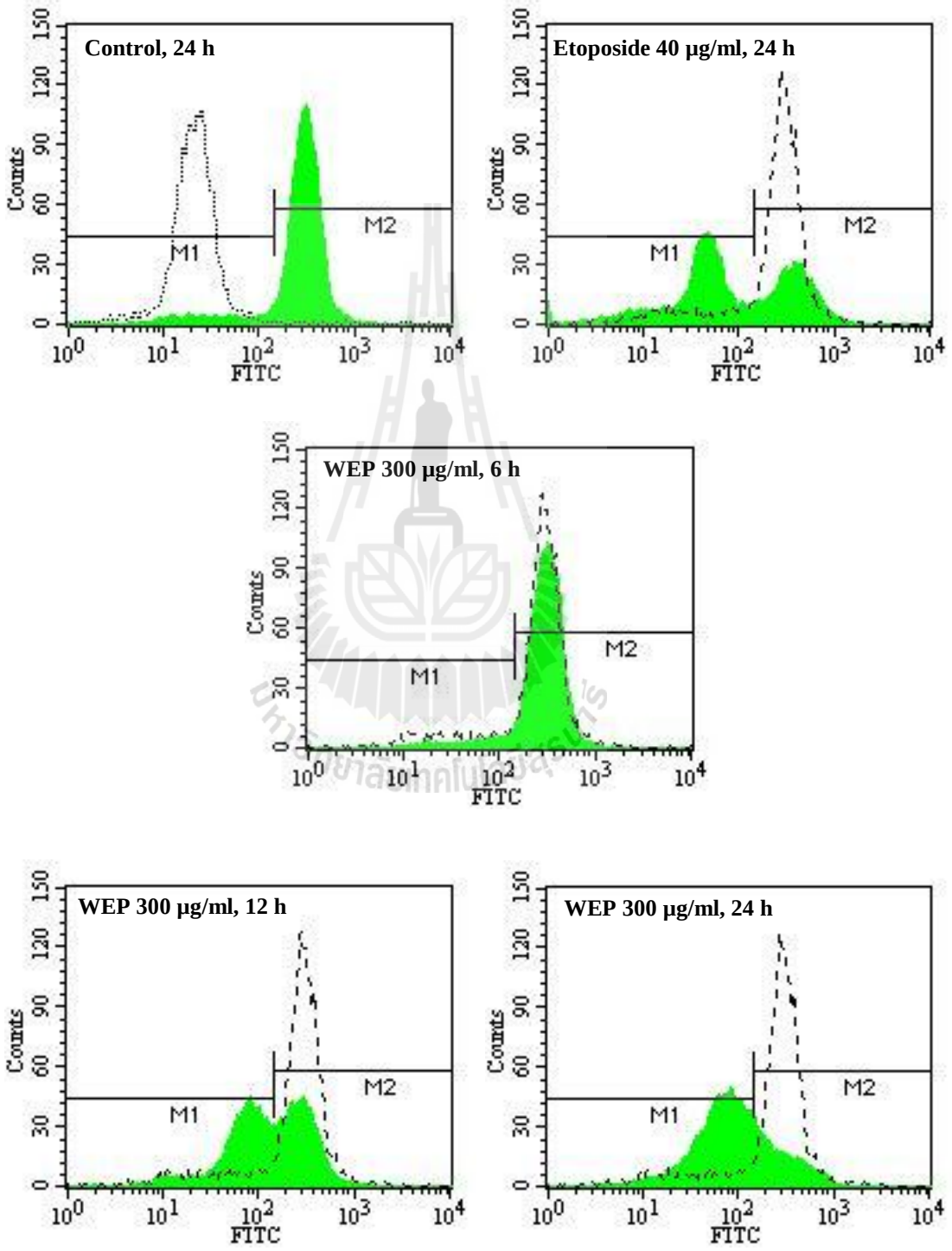

CURRICULUM VITAE

Name Miss Benjawan Dunkhunthod

Date of Birth December, 20 1987

Place of Birth Nakhon Ratchasima, Thailand

Education

2006-2009: Bachelor of Science (Environmental Health) (First Class Honors), Suranaree University of technology, Nakhon Ratchasima, Thailand

Oral presentation and proceeding

1. Dunkhunthod, B., Chitsomboon, B. (2014). Antiproliferative effect on cancer cells and mutagenic activity of *Pseuderanthemum palatiferum* (Nees) Radlk. The 5th International Conference on Natural Products for Health and Beauty (NATPRO5). 6th to 8th May. Moevenpick Resort & Spa Karon Beach, Phuket, Thailand.